

Durham E-Theses

*Environmental and relative sea-level reconstruction
from isolation basins in NW Scotland using
geochemical techniques*

Elizabeth Anne Victoria Mackie

How to cite:

Mackie, Elizabeth Anne Victoria (2004) Environmental and relative sea-level reconstruction from isolation basins in NW Scotland using geochemical techniques. Doctoral thesis, Durham University.

Use policy

The full-text may be used and/or reproduced, and given to third parties in any format or medium, without prior permission or charge, for personal research or study, educational, or not-for-profit purposes provided that:

- a full bibliographic reference is made to the original source
- a <https://etheses.durham.ac.uk/id/eprint/3033/> is made to the metadata record in Durham E-Theses
- the full-text is not changed in any way

The full-text must not be sold in any format or medium without the formal permission of the copyright holders.

Please consult the [full Durham E-Theses policy](#) for further details.

**ENVIRONMENTAL AND RELATIVE SEA-LEVEL
RECONSTRUCTION FROM ISOLATION BASINS IN NW
SCOTLAND USING GEOCHEMICAL TECHNIQUES**

Volume Two:
Figures and Tables

Elizabeth Anne Victoria Mackie

**A copyright of this thesis rests
with the author. No quotation
from it should be published
without his prior written consent
and information derived from it
should be acknowledged.**



Thesis submitted for the degree of Doctor of Philosophy.
University of Durham, Department of Geography
2004

20 APR 2005

LIST OF FIGURES- Volume two

Chapter 1

- Figure 1.1:** Schematic representation of an isolation basin during a RSL fall.....1
- Figure 1.2:** Schematic representation of the hydrological conditions in an isolation basin during an RSL fall.....2
- Figure 1.3:** A conceptual model of the biological assemblage change during a RSL fall.....3
- Figure 1.4:** Relative sea level (RSL) observations from the Arisaig area.....4

Chapter 2

- Figure 2.1:** Schematic representation of the $\delta^{13}\text{C}$ inputs into a freshwater (A), and the marine (B) systems.....5

Chapter 3

- Figure 3.1:** Location map of the field study region.....6
- Figure 3.2:** Map of Arisaig field area with the locations of the fossil and contemporary isolation basins analysed.....7
- Figure 3.3:** Base geology of Arisaig and the surrounding area.....10
- Figure 3.4:** Upper Alt Dail An Dubh-Asaid (UADD) - Overview of the lithostratigraphy and measurements down core.....11
- Figure 3.5:** Torr a' Bheithe (arrow) looking down towards Loch Torr a' Bheithe.....12
- Figure 3.6:** Torr A' Bheithe (TB) - overview of the lithostratigraphy and measurements down core.13
- Figure 3.7a:** Overview of Loch Torr a' Bheithe (arrow), looking west towards Loch nan Ceall.....14
- Figure 3.7b:** Loch Torr a' Bheithe marked by a black arrow and site of the new core being taken (red arrow)14

Figure 3.7c: Sill of Loch Torr a' Bheithe marked by an (arrow)	14
Figure 3.8: Loch Torr A' Bheithe (LTB) - overview of the lithostragraphy and measurements down core.	15
Figure 3.9a: Overview of Loch a' Mhuilinn looking towards Loch nan Ceall.....	16
Figure 3.9b: Loch a' Mhuilinn - view of the loch and the surrounding catchment.....	16
Figure 3.10: Loch A' Mhuilinn (LAM) lithostratigraphy and overview of the measurements down core.	17
Figure 3.11: Upper Loch Nan Eala looking towards the sill (arrow)	18
Figure 3.12: Upper Loch Nan Eala (ULNE) - Overview of the lithostratigraphy and measurements down core.....	19
Figure 3.13: Main Loch Nan Eala and the remaining shallow loch (arrow)	20
Figure 3.14: Overview of lithostragraphy and measurements down core of Main Loch Nan Eala (MLNE).....	21
Figure 3.15a: Overview of the staircase of two isolation basins (each marked with an arrow).....	22
Figure 3.15b: Rumach VI (arrow) looking east to west.....	22
Figure 3.16a: Overview of the lithostratigraphy and measurements down core of Rumach VI Lateglacial section.	23
Figure 3.16b: Overview of the lithostratigraphy and measurements down core from the Holocene core.....	24
Figure 3.17: Cross section of Rumach VI stratigraphy and morphology.	25
Figure 3.18: Rumach tidal pond site map - showing details for the site.	26
Figure 3.19a: View of Rumach Tidal Pond sill (arrow) at low tide looking west over to Eigg.....	27

Figure 3.19b: View of Rumach Tidal Pond sill (arrow) at high tide looking north to south.....	27
Figure 3.19c: View of Loch nan Ceall looking over to Eigg, taken from Rumach Tidal Pond sill.....	27
Figure 3.19d: View of Stream 1 (arrow) entering Rumach Tidal Pond.....	28
Figure 3.19e: View of Stream 1 (arrow) looking up stream to the surrounding catchment.....	28
Figure 3.19f: View of stream 2 (arrow) entering Rumach Tidal Pond.....	28
Figure 3.20a: Rumach Tidal Pond water column profiles at station 1 during Spring-tide HT and LT (11/8/02).	29
Figure 3.20b: Rumach Tidal Pond water column profiles at station 1 during mid-cycle tide tide LT and HT (7/8/02).	30
Figure 3.20c: Rumach Tidal Pond water column profiles at station 1 during neap-tide HT & LT (4/8/02).	31
Figure 3.21: Loch nan Corr, Kintail site map.....	32
Figure 3.22a: Overview of Loch Nan Corr.....	33
Figure 3.22b: New piston core from Loch nan Corr. View of the shallow freshwater loch and the aquatic vegetation	33
Figure 3.23: Loch nan Corr - overview of the lithostratigraphy and measurements down core.	34
Figure 3.24: Craiglin site map - showing details for the site.....	35
Figure 3.25a: View of Craiglin Lagoon (arrow) showing the culvert and the sill from Loch Sween.....	36
Figure 3.25b: View of sill waters entering the culvert. Sill marked with the arrow.....	36
Figure 3.25c: View of Loch Sween (arrow) and the inlet stream to the basin at high tide.....	36

Figure 3.26a: Craiglin Lagoon water column profiles at station 2 during spring-tide LT and HT (11/8/02).37

Figure 3.26b: Craiglin Lagoon water column profiles at station 2 during spring-tide LT and HT (7/10/02).38

Chapter 5

Figure 5.1: Upper Loch nan Eala (ULNE) - summary of $\delta^{13}\text{C}_{\text{org}}$ and C/N ratios data compared to the diatom palaeosalinity reconstruction40

Figure 5.2: $^{87}\text{Sr}/^{86}\text{Sr}$ vs. salinity for water and foraminiferal samples from Rumach VI (Holocene core).44

Figure 5.3: Elemental /Al ratios from ULNE compared to against the diatom reconstruction.....45 ,46

Figure 5.4: REE elements plotted from Upper Loch nan Eala.47

Chapter 6

Figure 6.1a: C/N vs. $\delta^{13}\text{C}_{\text{org}}$ plot of the contemporary samples from NW Scotland.....49

Figure 6.1a: C/N vs. $\delta^{13}\text{C}_{\text{org}}$ plot of the contemporary data from this study and values from the published literature.....49

Figure 6.2: Upper Loch nan Eala - profiles of TOC, C/N ratios and $\delta^{13}\text{C}_{\text{org}}$52

Figure 6.3: Upper Loch nan Eala C/N vs. $\delta^{13}\text{C}_{\text{org}}$53

Figure 6.4: Main Loch nan Eala - profiles of TOC, C/N ratios and $\delta^{13}\text{C}_{\text{org}}$ compared to the diatom summary.54

Figure 6.5: Main Loch nan Eala C/N vs. $\delta^{13}\text{C}_{\text{org}}$55

Figure 6.6a: Rumach VI - Lateglacial core- Profiles of TOC, C/N ratios and $\delta^{13}\text{C}_{\text{org}}$ compared to the diatom summary.....56

Figure 6.6b: Rumach VI (Holocene section) Summary of TOC, C/N and $\delta^{13}\text{C}_{\text{org}}$ against the foraminiferal salinity reconstruction.....57

Figure 6.7: Rumach VI C/N vs. $\delta^{13}\text{C}_{\text{org}}$	58
Figure 6.8: Loch nan Corr - profiles of TOC, C/N ratios and $\delta^{13}\text{C}_{\text{org}}$ compared to the foraminifera summary.	59
Figure 6.9: Loch nan Corr C/N vs. $\delta^{13}\text{C}_{\text{org}}$	60
Figure 6.10: Upper Allt Dail An Dubh-Asaid - profiles of TOC, C/N ratios and $\delta^{13}\text{C}_{\text{org}}$	61
Figure 6.11: Upper Allt Dail Dubh-Asaid - C/N vs. $\delta^{13}\text{C}_{\text{org}}$	62
Figure 6.12: Torr a' Bheithe -profiles of TOC, C/N ratios and $\delta^{13}\text{C}_{\text{org}}$ against the diatom palaeosalinity reconstruction.	63
Figure 6.13: Torr a' Bheithe C/N vs. $\delta^{13}\text{C}_{\text{org}}$	64
Figure 6.14: Loch Torr a' Bheithe -profiles of TOC, C/N ratios and $\delta^{13}\text{C}_{\text{org}}$ against the diatom summary.	65
Figure 6.15: Loch Torr a' Bheithe C/N vs. $\delta^{13}\text{C}_{\text{org}}$	66
Figure 6.16: Loch a' Muihinn - profiles of TOC, C/N ratios and $\delta^{13}\text{C}_{\text{org}}$ against the diatom palaeosalinity reconstruction.....	67
Figure 6.17: Loch a' Mhuilinn C/N vs. $\delta^{13}\text{C}_{\text{org}}$	68
Figure 6.18: Regional RSL curve showing altitude of Rumach VI, MLNE and Upper Loch Nan Eala.....	69
Figure 6.19: Biplot of $\delta^{13}\text{C}_{\text{org}}$ vs. C/N ratio from Holocene marine samples from Upper Loch Nan Eala, Main Loch Nan Eala and Rumach VI.....	70

Chapter 7

Figure 7.1a: Relationship between contemporary $\delta^{18}\text{O}_w$ vs. salinity for all samples taken from RTP, Craiglin Lagoon and Loch Nan Corr.	71
Figure 7.1b: Relationship between contemporary $\delta^{13}\text{C}_{\text{TDIC}}$ vs. salinity for all samples taken from RTP, Craiglin Lagoon and Loch Nan Corr.....	71

Figure 7.2a: Relationship between contemporary $\delta^{18}\text{O}_w$ vs. temperature for all samples taken from RTP, Craiglin Lagoon and Loch Nan Corr.....	71
Figure 7.2b: Relationship between contemporary $\delta^{13}\text{C}_w$ vs. temperature for all samples taken from RTP, Craiglin Lagoon and Loch Nan Corr.....	71
Figure 7.3a: Relationship between contemporary Rumach Tidal Pond $\delta^{18}\text{O}_w$ vs. salinity for basin, sill and stream waters.....	72
Figure 7.3b: Relationship between contemporary Rumach Tidal Pond $\delta^{18}\text{O}_w$ vs. temperature for basin, sill and stream waters.....	72
Figure 7.4a: Relationship between contemporary Rumach Tidal Pond $\delta^{13}\text{C}_{\text{TDIC}}$ vs. salinity for basin, sill and stream waters	72
Figure 7.4b: Relationship between contemporary Rumach Tidal Pond $\delta^{13}\text{C}_{\text{TDIC}}$ vs. temperature for basin, sill and stream waters.....	72
Figure 7.5a: Relationship between contemporary Craiglin Lagoon $\delta^{18}\text{O}_w$ vs. salinity for basin, stream and sill water samples.....	73
Figure 7.5b: Relationship between contemporary Craiglin Lagoon $\delta^{18}\text{O}_w$ vs. temperature for basin, stream and sill samples	73
Figure 7.6a: Relationship between contemporary Craiglin Lagoon $\delta^{13}\text{C}_{\text{TDIC}}$ vs. salinity for basin, stream and sill water samples	73
Figure 7.6b: Relationship between contemporary Craiglin Lagoon $\delta^{13}\text{C}_{\text{TDIC}}$ vs. temperature for basin, stream and sill samples	73
Figure 7.7: Loch nan Corr profiles of TOC, $\delta^{13}\text{C}_{\text{org}}$, $\delta^{18}\text{O}_{\text{foram}}$, $\delta^{13}\text{C}_{\text{foram}}$ results against foraminiferal summary.	74
Figure 7.8: Relationship between $\delta^{13}\text{C}_{\text{foram}}$ and $\delta^{18}\text{O}_{\text{foram}}$ from sediment core Loch Nan Corr.....	75
Figure 7.9: Relationship between $\delta^{13}\text{C}_{\text{org}}$ and $\delta^{13}\text{C}_{\text{foram}}$ from the sediment core Loch Nan Corr	75

Chapter 8

Figure 8.1a: Brackish water diatoms separated using an STP density of 2.2gcm^3	76
Figure 8.1b: Marine diatoms separated using an STP density of 2.2gcm^3	76
Figure 8.1c: Marine diatoms separated using an STP density of 2.3gcm^3	76
Figure 8.2: Ranges of end-member values defined from the published results.....	78
Figure 8.3: Summary of $\delta^{13}\text{C}_{\text{org}}$ and $\delta^{18}\text{O}_{\text{diatom}}$ data compared to the diatom salinity reconstruction	79
Figure 8.4: The $\delta^{18}\text{O}_{\text{diatom}}$ results from Upper Loch Nan Eala compared to the end-member ranges identified from the published literature.....	80

Chapter 9

Figure 9.1: Loch Nan Corr -Profiles of Foraminiferal summary, particle size, TOC, BSiO_2	81
Figure 9.2: Profiles of C/N ratios, TOC, BSiO_2 compared to the GRIP $\delta^{18}\text{O}$ and diatom summary diagram	82
Figure 9.3: TOC, BSiO_2 , and Age/depth model for the new core from Loch Nan Corr and the GRIP temperature record.....	85

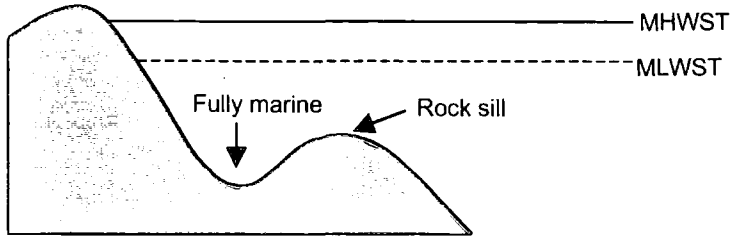
Chapter 10

Figure 10.1: Environmental synthesis for Upper Loch nan Eala (ULNE) - comparing all geochemical proxies as palaeosalinity indicators against the published diatom summary.....	86
Figure 10.2: Environmental synthesis at Loch nan Corr (LNC) - comparing all geochemical proxies as palaeosalinity indicators.	87

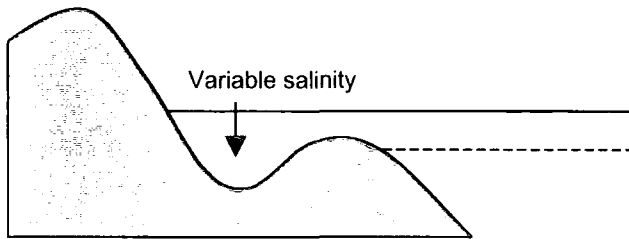
Tables – Volume two

Table 3.1: Summary data for contemporary basins.....	8
Table 3.2: Summary data for fossil basins.....	9
Table 3.3: Summary of geochemical and isotope proxies tested at each field site.....	38
Table 5.1: Summary table of the abundance of <i>H.germanica</i> foraminifera in ULNE, Rumach VI and LNC.....	41
Table 5.2: Summary table of the abundance of diatoms in Upper Loch Nan Eala.....	42
Table 5.3: Summary table of the abundance of diatoms in Main Loch Nan Eala.....	42
Table 5.4: Summary table of the abundance of diatoms from Rumach VI (Holocene core).....	42
Table 5.5: Summary of contemporary water samples from Rumach Tidal Pond and foraminifera.....	43
Table 6.1: Values of contemporary $\delta^{13}\text{C}_{\text{org}}$ and C/N ratios collected from NW Scotland.....	48
Table 6.2: Published contemporary $\delta^{13}\text{C}_{\text{org}}$ and C/N ratios from a range of sedimentary and aquatic environments.....	50 - 51
Table 8.1: Summary table of published $\delta^{18}\text{O}_{\text{diatom}}$ values from around the world.....	77
Table 9.1: A summary of climate events across Europe recorded in peat, lake, speleothem and marine records.	83-84
Table 11.1: Summary of palaeosalinity proxies.....	Vol 1- 167

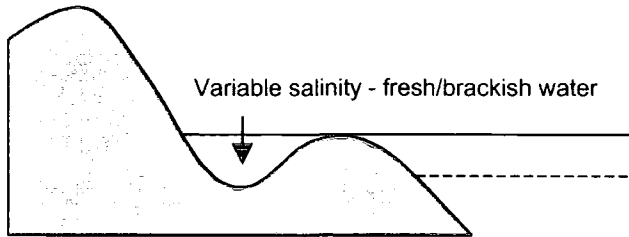
Stage 1 - Highstand



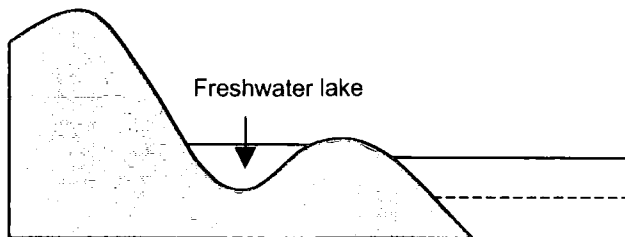
Stage 2 - Beginning of relative sea-level fall



Stage 3 - Relative sea-level fall



Stage 4 - Lowstands

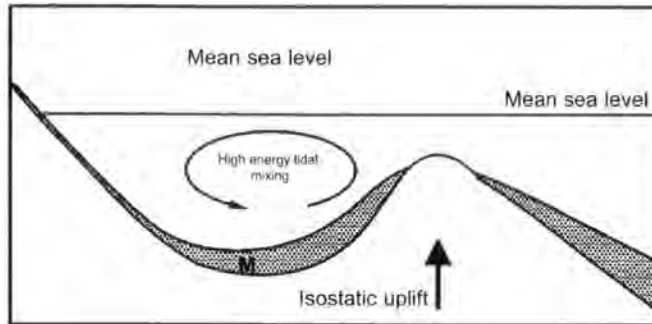


————— Mean High Water Spring Tides (MHWST)
- - - - - Mean Low Water Spring Tides (MLWST)

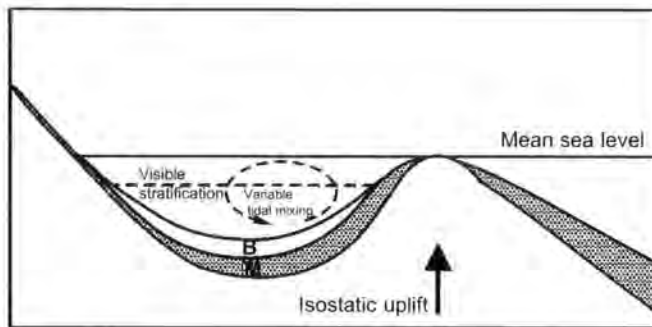
Figure 1.1: Schematic representation of an isolation basin during a RSL fall. Adapted from Kjemperund (1981b) and Shennan et al. (1996)



Stages 1



Stages 2-3



Stage 4

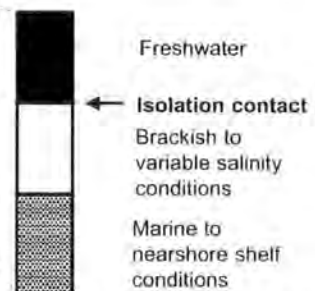
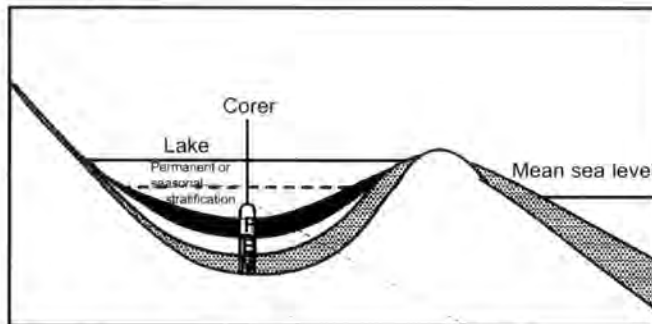


Figure 1.2: Schematic representation of the hydrological conditions in an isolation basin during an RSL fall. Stages correspond with stages in Figure 1.1. (Adapted from Kjemperund 1981b)

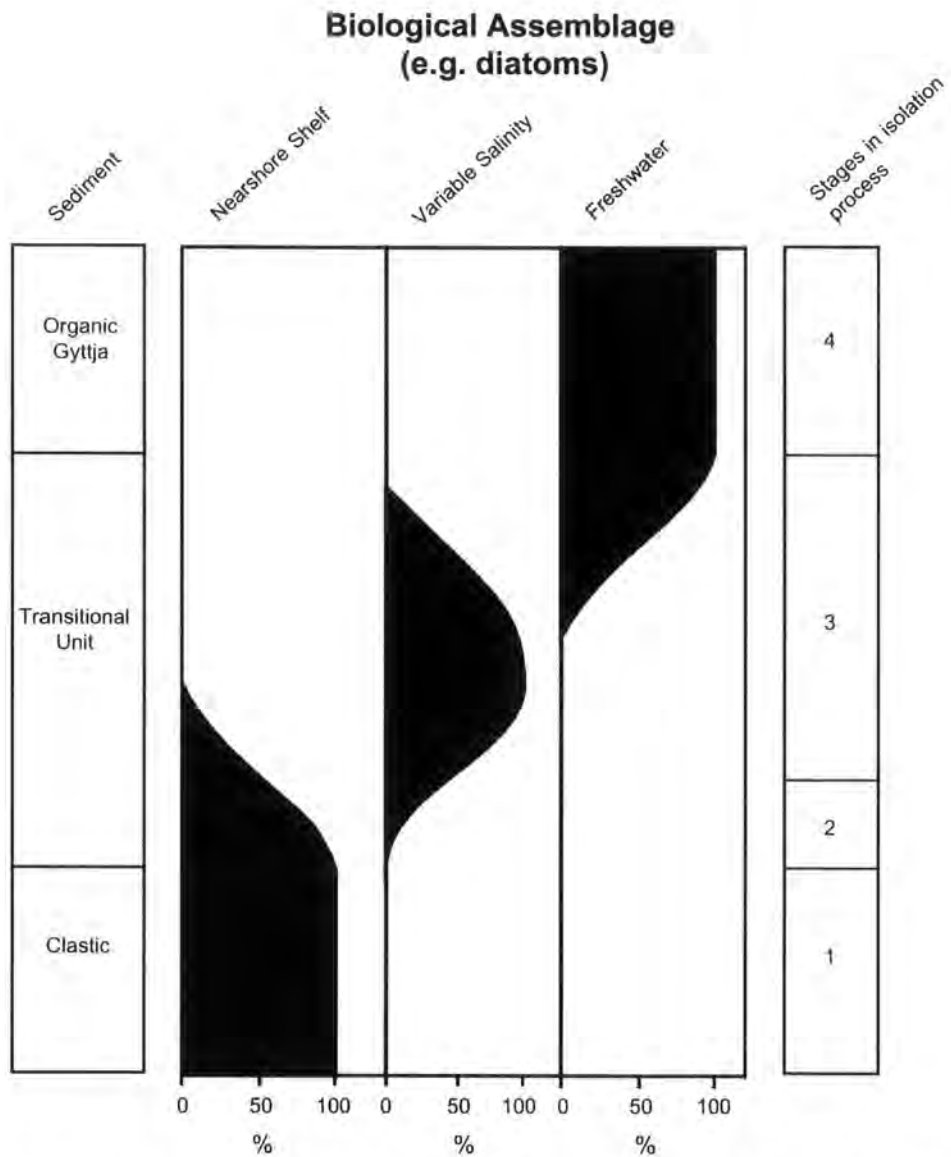


Figure 1.3: A conceptual model of the biological assemblage change during a RSL fall. The left column presents typical sediment types deposited during an isolation process. The right column relates to stages on the isolation process in Figures 1.1 and 1.2. (Diagram adapted from Laidler 2002)

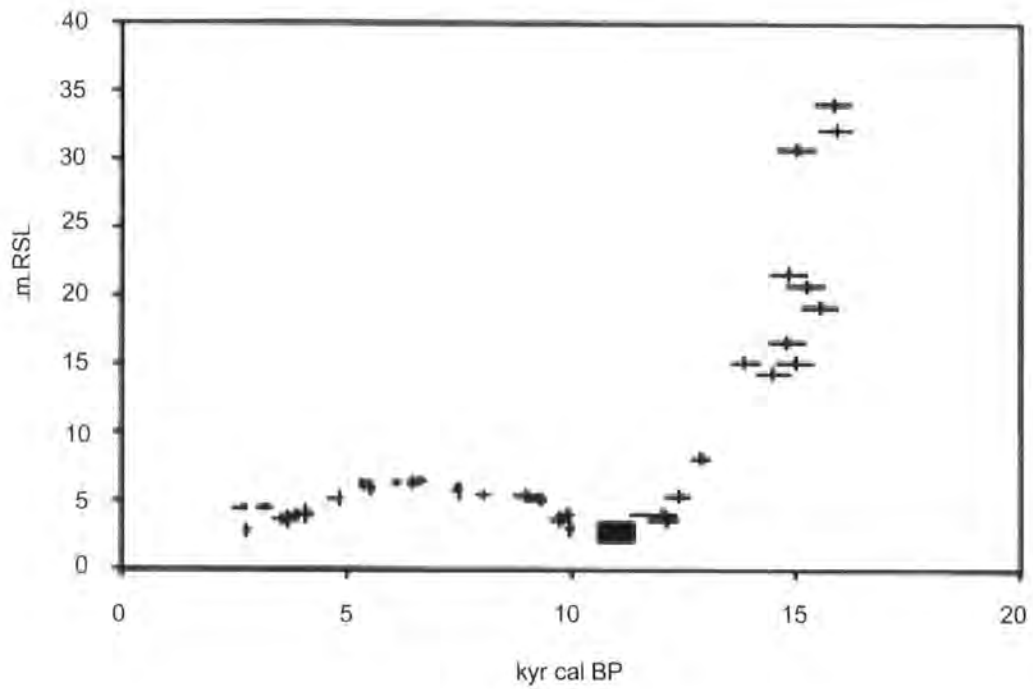
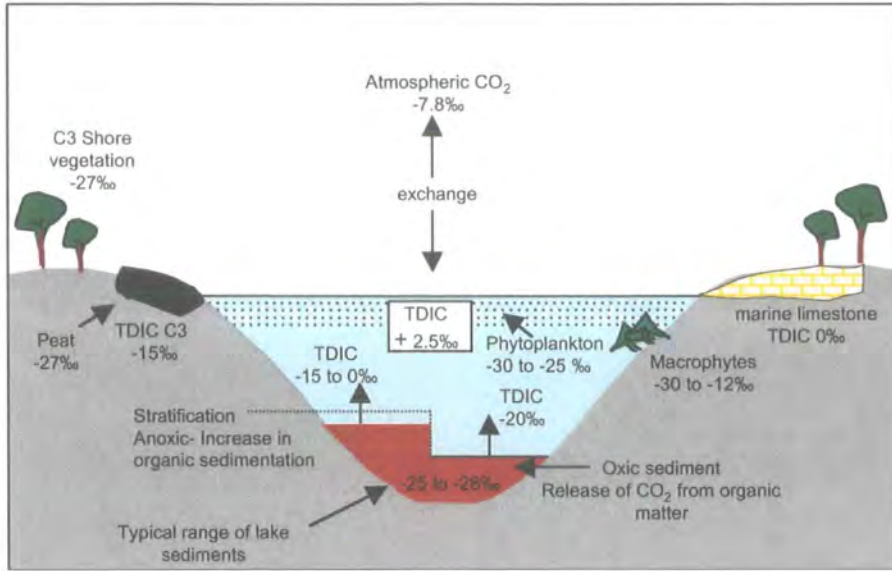


Figure 1.4: Relative sea level (RSL) observations from the Arisaig area. The ■ symbol indicates a minimum for RSL based on bio-stratigraphic evidence from the lowest isolation basin, Rumach VI (Shennan *et al.*, 1999). (Diagram from Shennan *et al.*, 2000)

A Freshwater environment



B Marine environment

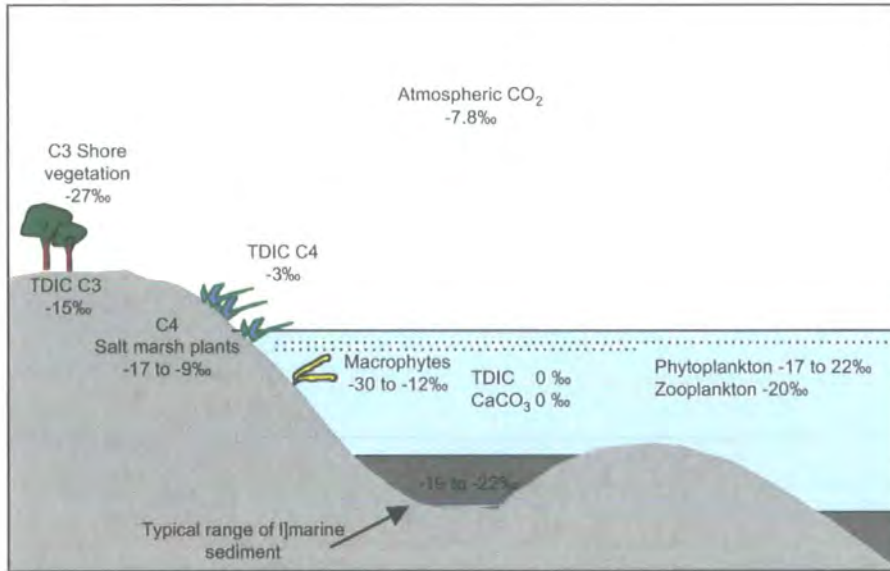


Figure 2.1: Schematic presentation of the $\delta^{13}\text{C}$ inputs into a freshwater (A), and the marine (B) systems. Equilibrium with atmospheric CO₂ only usually occurs in closed lakes. Note the 5‰ difference between the two systems (adapted from Boutton (1991) and Leng and Marshall (2004)).

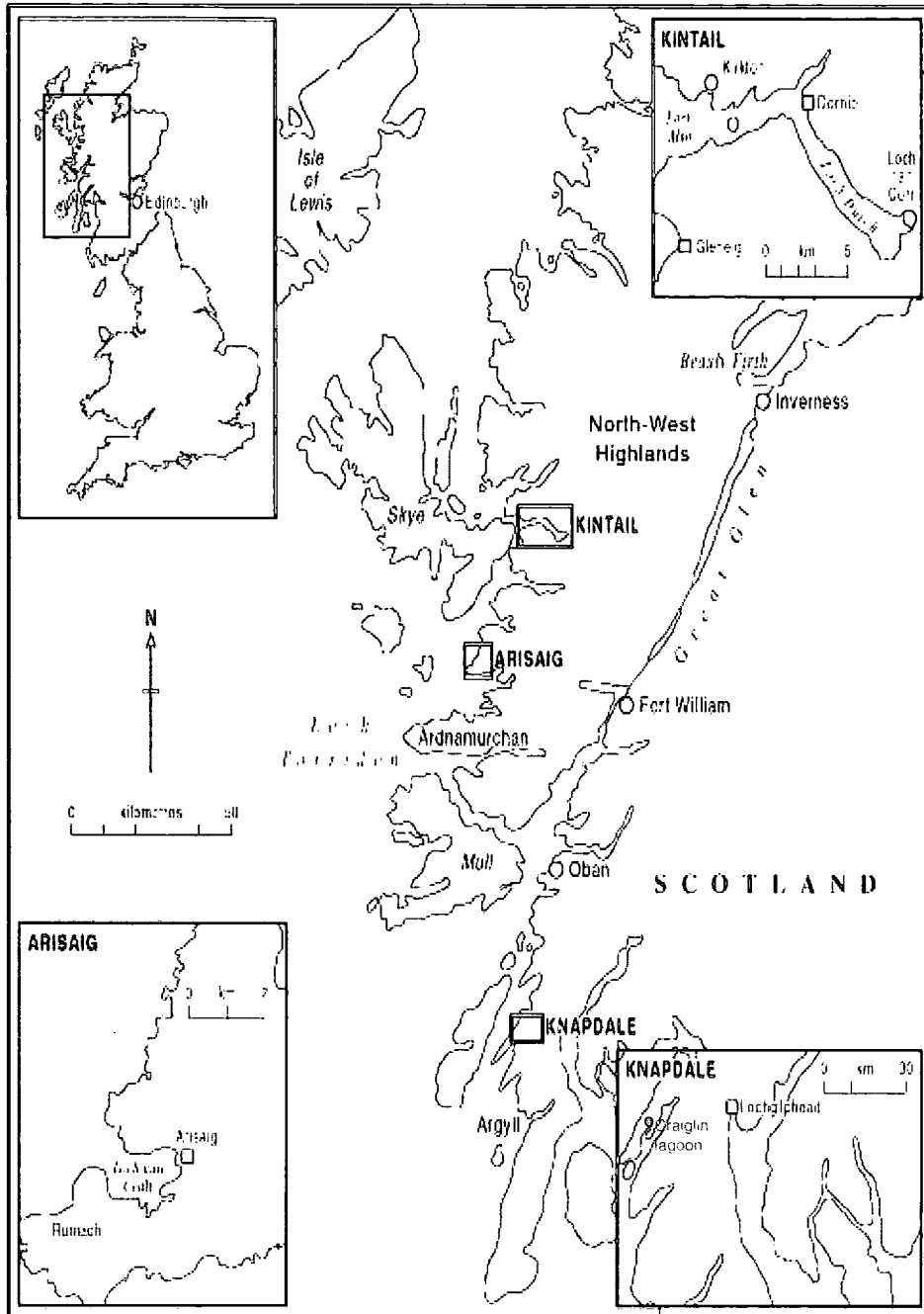


Figure 3.1: Location map of the field study region. Insets show locations of the study areas with the individual sites indicated (see Tables 3.1 and 3.2).

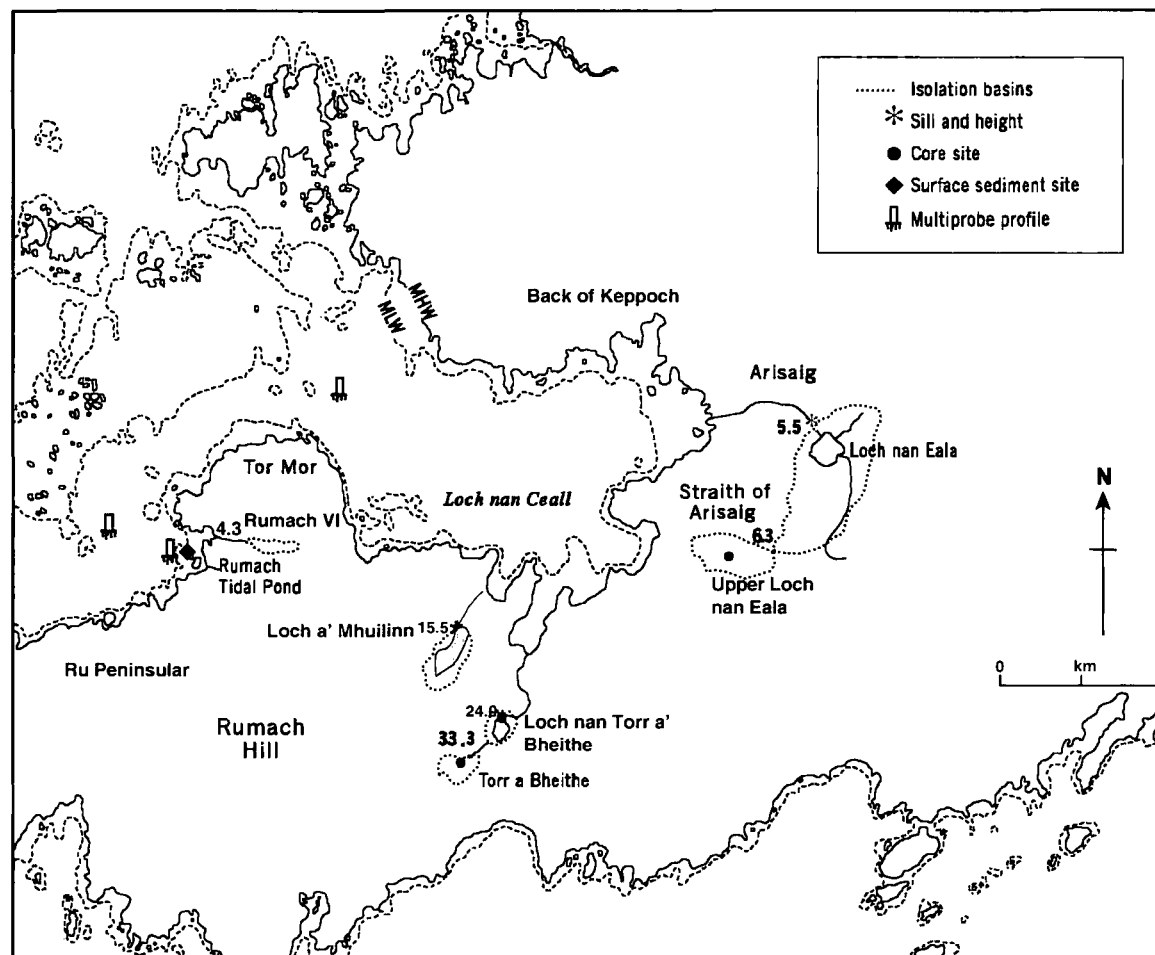


Figure 3.2: Map of Arisaig field area with the locations of the fossil and contemporary isolation basins analysed.

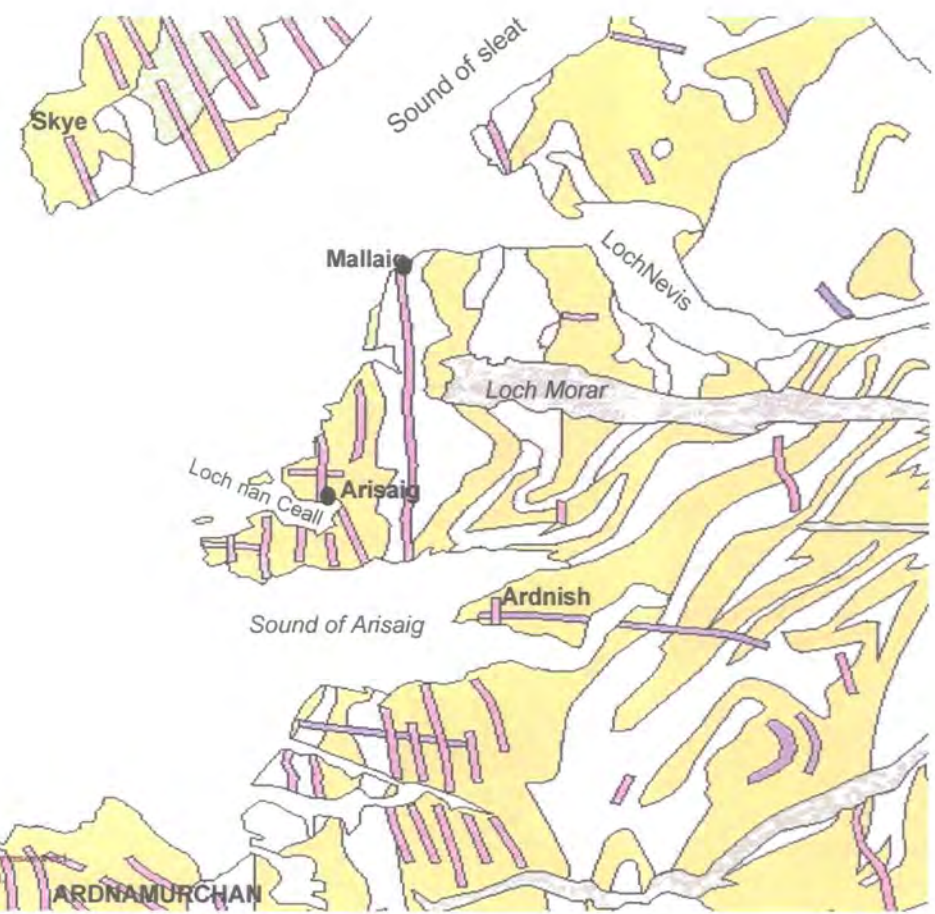
Table 3.1: Summary data for contemporary basins

Basin	Position (Latitude, Longitude)	OS Coordinate	Type of environment	Sill Altitude (m OD)	MHWST	HAT	Approximate Area (ha)		Max depth at high tide (m) (MHST)	Theoretical stage of isolation (Figure 1.1)
							<i>Mean low water</i>	<i>Mean high water</i>		
Arisaig										
Rumach tidal pond (RTP)	56°89'84N, 5°89'56W	NM6280 8530	Marine	0.27	2.38	2.96	0.2	1.2	1.9	2
Knapdale										
Craiglin Lagoon	56°03'15N, 5°57'09W	NR7754 8781	Brackish	1.417	1.29	1.64	6.8	6.9	1.6	3
Kintail										
Loch nan Corr	57°23'39N, 5°40'94W	NG9425 2103	Fresh water loch	2.7	2.62	3.24	1.7	1.7	0.6	4

Table 3.2: Summary data for fossil basins

Basin	Position (Latitude, Longitude)	OS Coordinate	Microfossil	Sill Altitude (m OD)	Relative Sea Level History	Reference for RSL history and previous analyses
Arisaig Upper Allt Dail An Dubh-Asaid	Back of Keppock	Site destroyed	Diatoms	61.88	Above marine limit	Shennan <i>et al.</i> (in prep)
Loch a' Mhuilinn	56°53'37N, 5°52'11W	NM644 846	Diatoms	15.5	Late Lateglacial RSL fall	Shennan <i>et al.</i> (2000)
Loch Torr a' Bheithe	56°53'21N, 5°51'51W	NM647 842	Diatoms	24.0	Late Lateglacial RSL fall	Shennan <i>et al.</i> (2000)
Torr a' Bheithe	56°88'90N, 5°86'34W	NM6470 8415	Diatoms	35.2	Late Lateglacial RSL fall	Shennan <i>et al.</i> (2000)
Upper Loch nan Eala	56°54'00N, 5°50'27W	NM662 853	Diatoms	6.27	Late Lateglacial RSL fall and through to Holocene RSL fall and rise	Shennan <i>et al.</i> (1994, 2000)
Main basin Loch nan Eala	56°90'63N, 5°83'14W	NM6676 8596	Diatoms	5.20	Late Lateglacial RSL fall and through to Holocene RSL fall and rise	Shennan <i>et al.</i> (1994,2000)
Rumach VI	56°53'63N, 5°53'14W	NM633853	Diatoms foraminifera dinoflagellate cysts	4.80	Late Lateglacial RSL fall and through to Holocene RSL fall and rise	Shennan <i>et al.</i> (1994,2000)
Kintail Loch nan Corr	57°23'39N, 5°40'94W	NG9425 2103	Foraminifera	2.70	Holocene RSL fall	Lloyd (2001)

- Mica-schist, semi-pelitic schist and mixed schists
- Undifferentiated gneiss
- Basalt dolerite, camptonite and allied types
- Sandstone and grit
- Quartz-feldspar-granulite
- Porphyrite, lamprophyre and allied types
- Quartzite
- Ryholite, trachyte, felsite, elvans and allied types
- Great and inferior oolite and corbrash
- Basalt and spilite
- Ryolite, trachyte and allied types
- Upper, middle and lower lias, Lower Jurassic
- Agglomerate in neck
- Gabbro and allied types
- Granite, syenite, granophyre and allied types



Geological Information Copyright © 2004
 Topography Copyright © 2004
 Ordnance Survey Licence No. GD2721812004

ARDNAMURCHAN

Figure 3.3: Base geology of Arisaig and the surrounding area. (adapted from 2004)



Figure 3.4: Upper Alt Dail An Dubh-Asaid (UADD) - Overview of the lithostratigraphy and measurements down core made. Key: Organic limus Clay, silt some sand. Data from Shennan *pers. com.* Date calibrated using Calib 4.3 (Stuvier *et al.*, 1998) radiocarbon date.



Figure 3.5: Torr a' Bheithe (arrow) looking down towards Loch Torr a' Bheithe

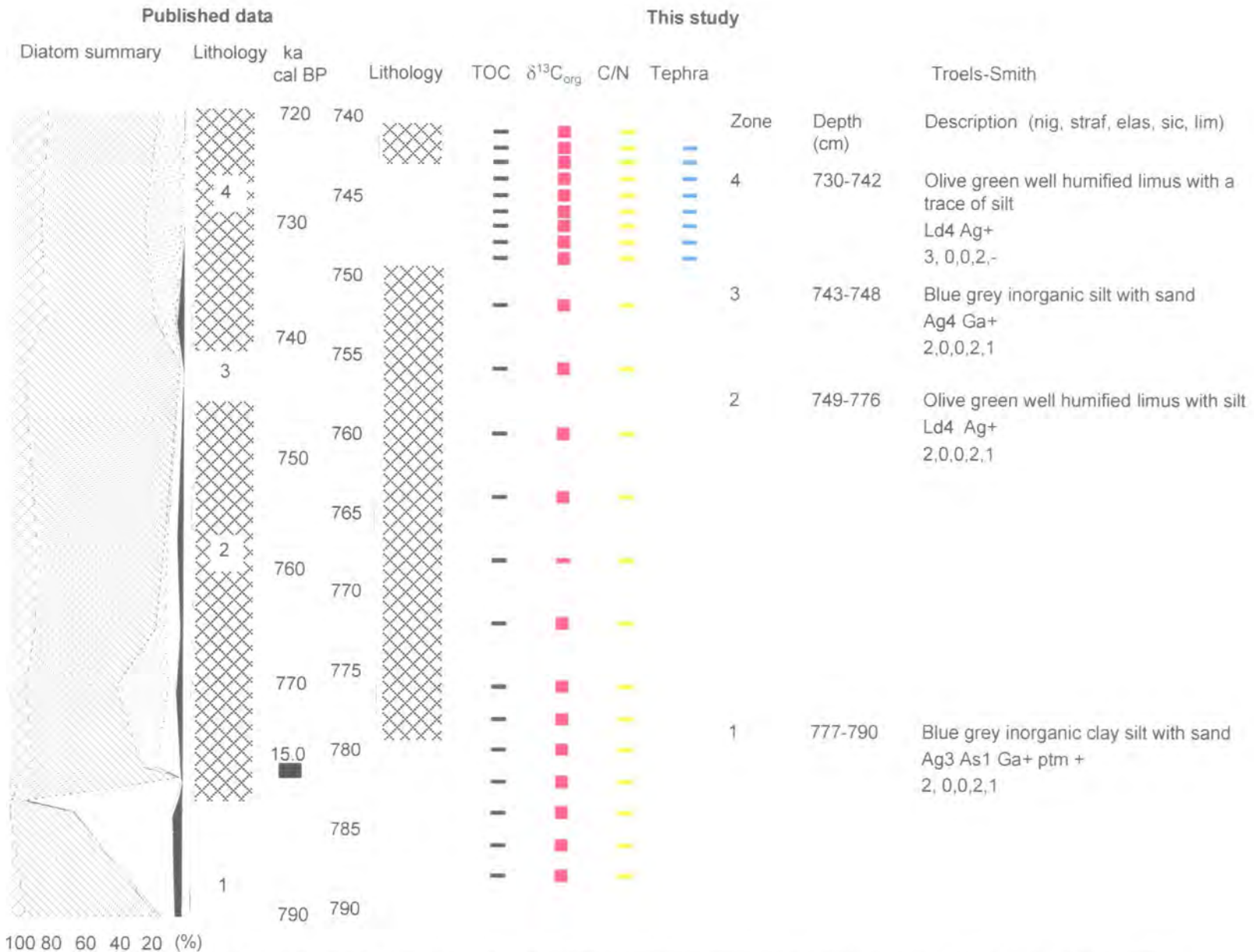


Figure 3.6: Torr A' Bheithe (TB) - overview of the lithostratigraphy and measurements down core. Published data from Shennan *et al.* (2000).

Key: Organic limus Clay, silt, some sand. Diatom classes polyhalobian, Meshohalobian oiohalobian -halophile oligohalobian - indifferent halophobe



Figure 3.7a: Overview of Loch Torr a' Bheithe (arrow), looking west towards Loch nan Ceall



Figure 3.7b: Loch Torr a' Bheithe marked by a black arrow and site of the new core being taken (red arrow)



Figure 3.7c: Sill of Loch Torr a' Bheithe marked by an (arrow)

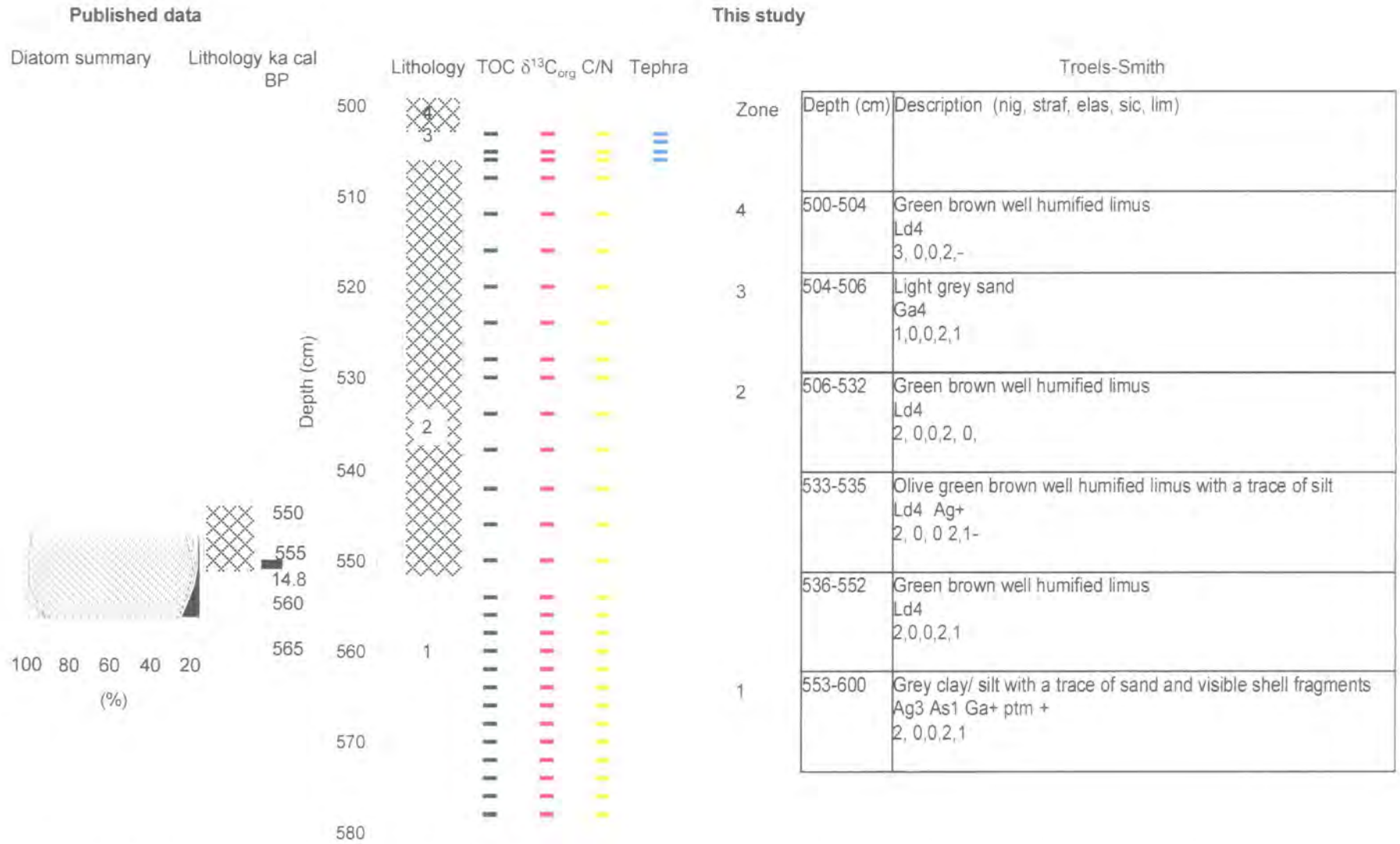


Figure 3.8: Loch Torr a' Bheithe (LTB) - overview of the lithostratigraphy and measurements down core. Published data from Shennan *et al.* (2000). Key as before.



Figure 3.9a: Overview of Loch a' Mhuilinn looking towards Loch nan Ceall



Figure 3.9b: Loch a' Mhuilinn - view of the loch and the surrounding catchment

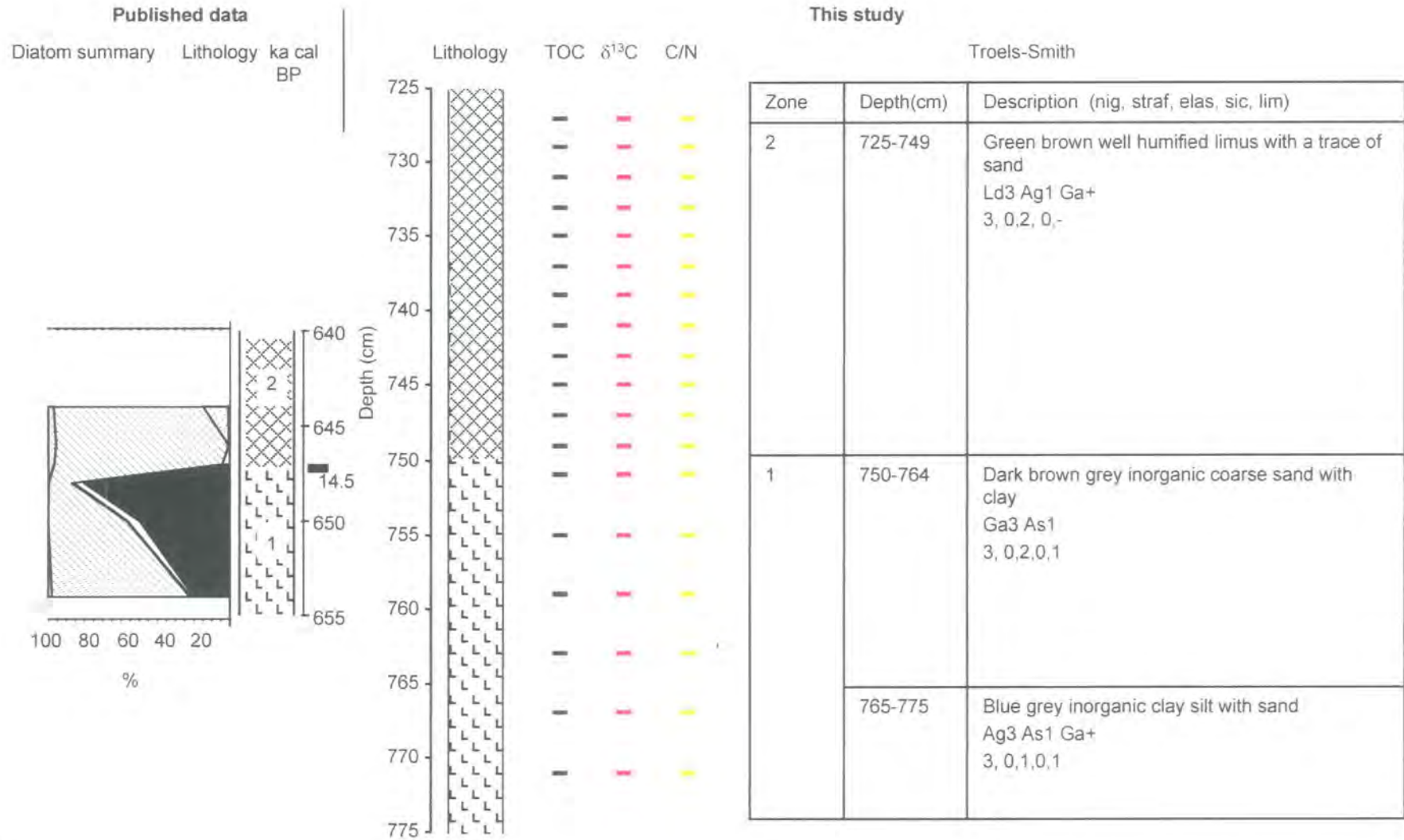


Figure 3.10: Loch a' Mhuilinn (LAM) lithostratigraphy and overview of the measurements down core. Published data from Shennan *et al.* (2000). Key: as before.



Figure 3.11: Upper Loch Nan Eala looking towards the sill (arrow)

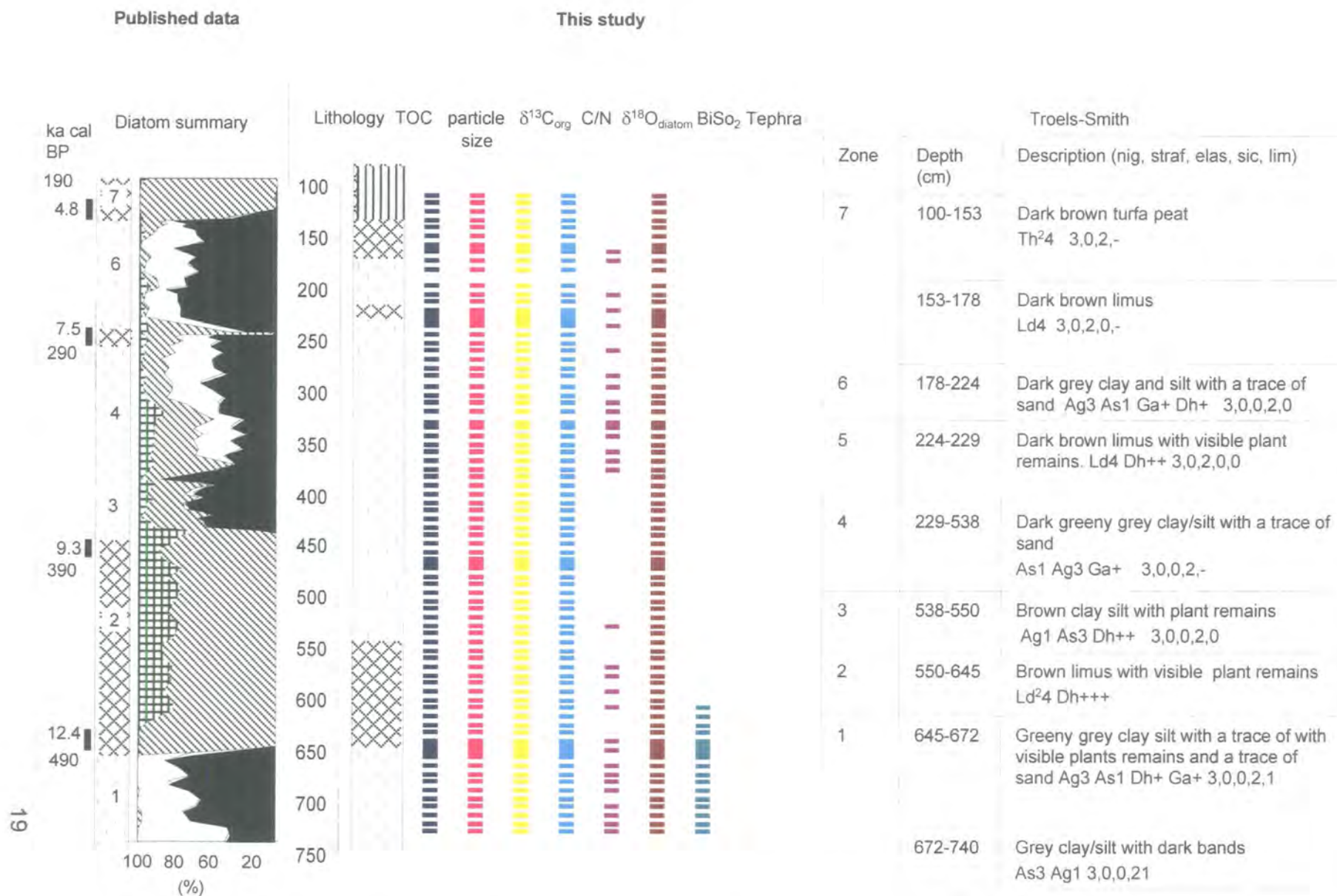


Figure 3.12: Upper Loch Nan Eala (ULNE) - Overview of the lithostratigraphy and measurements down core. Published data from Shennan *et al.* (1994, 2000). Key as before.



Figure 3.13: Main Loch Nan Eala and the remaining shallow loch (arrow)

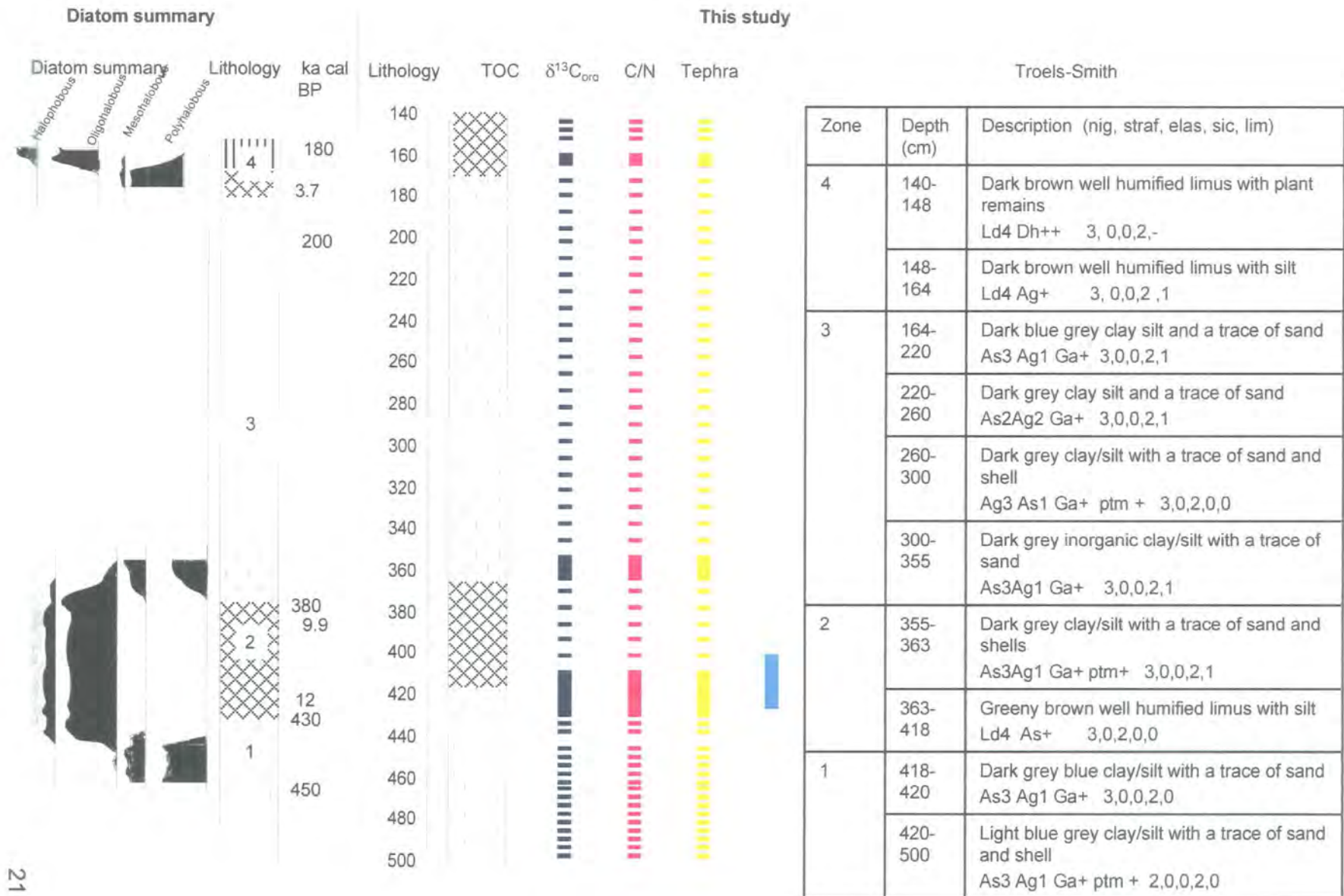


Figure 3.14: Overview of lithostratigraphy and measurements down core of Main Loch Nan Eala (MLNE). Published data from Shennna *et al.* (1994, 2000). Key as before.



Figure 3.15a: Overview of the staircase of two isolation basins (each marked with an arrow). Rumach VI is in the foreground. The picture is taken looking westwards towards Loch nan Ceall



Figure 3.15b: Rumach VI (arrow) looking east to west

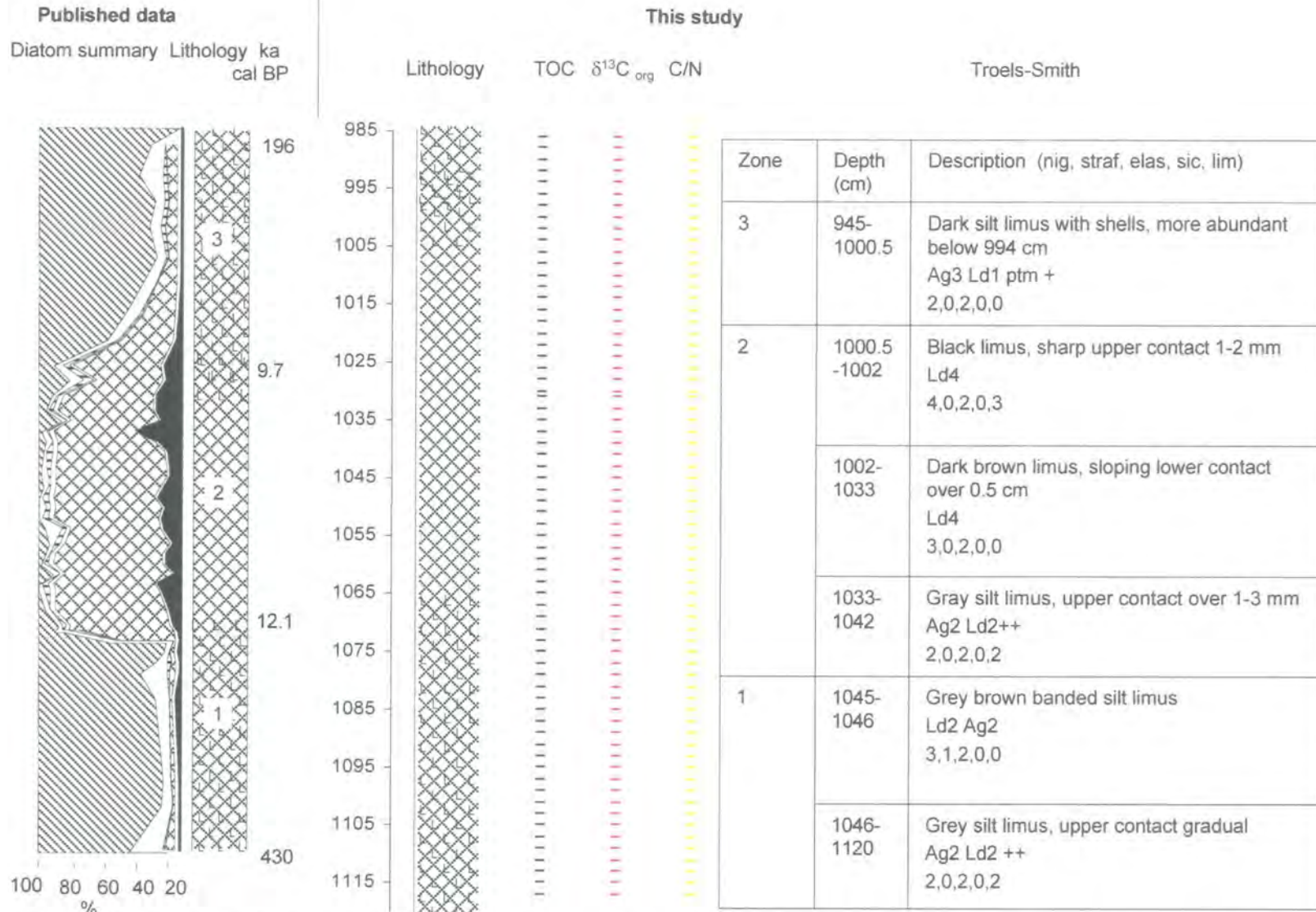


Figure 3.16a: Overview of the lithostratigraphy and measurements down core of Rumach VI Lateglacial section. Key: Figure 3.6

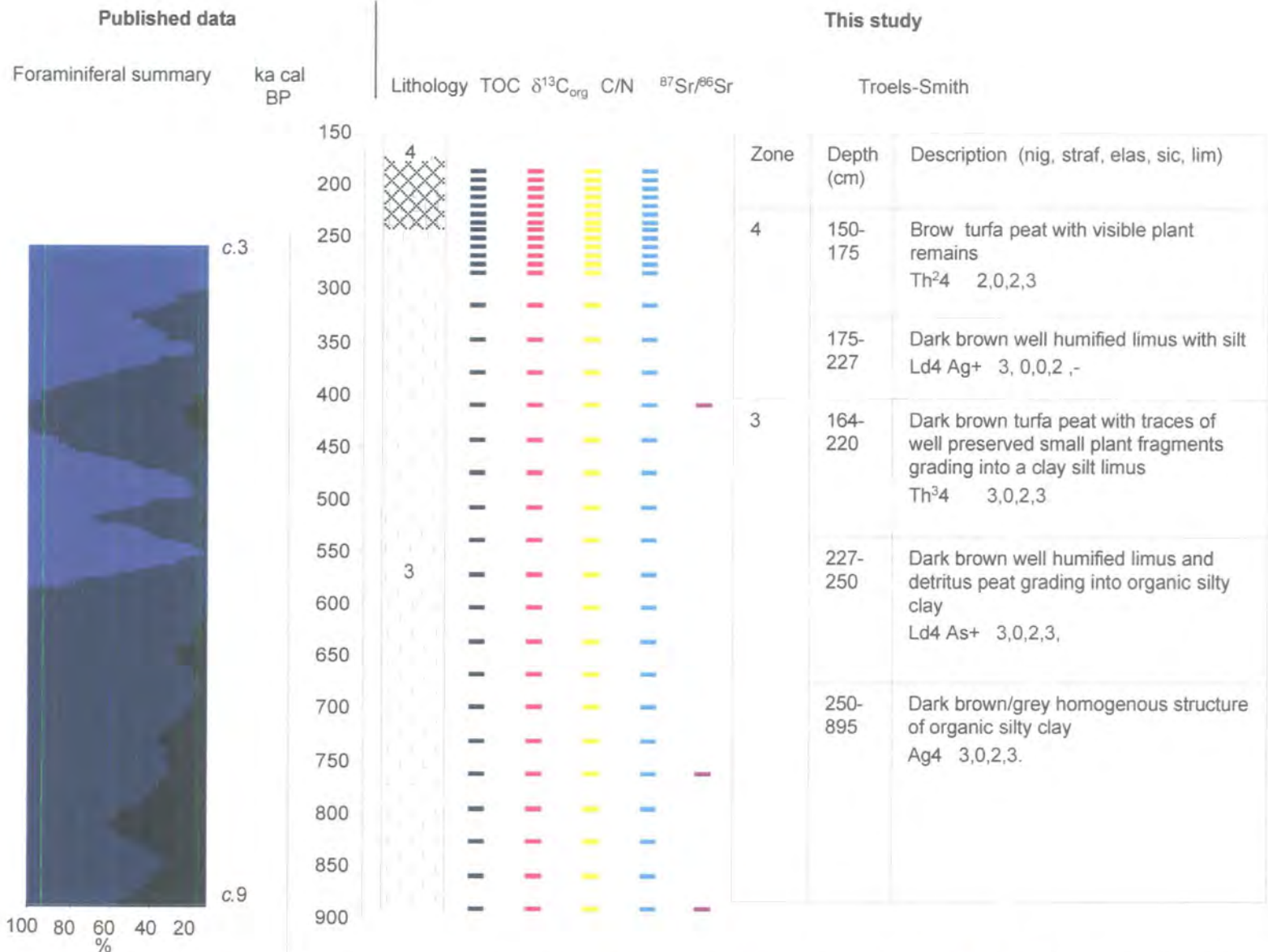


Figure 3.16b: Overview of the lithostratigraphy and measurements down core from the Holocene core. Publish data and radiocarbon dates from Lloyd and Evans (2002). Key: Lithology- Figure 3.7. Foraminifera summary: ■ Marine ■ Brackish lagoon ■ Saltmarsh

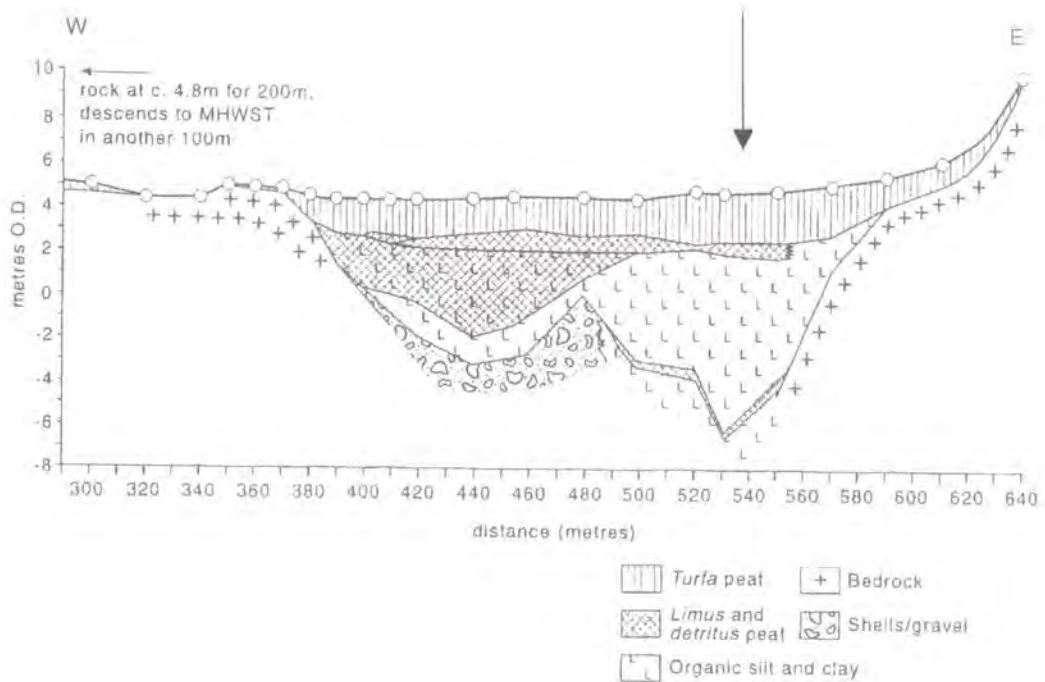


Figure 3.17: Cross section of Rumach VI stratigraphy and morphology. The west end of the basin is shallower than the eastern end. The arrow marks the section of the basin where the Holocene and Lateglacial core were taken. The open circles present the location of boreholes taken to construct the stratigraphy of the site. (Diagram adapted from Shennan *et al.*, 1999).

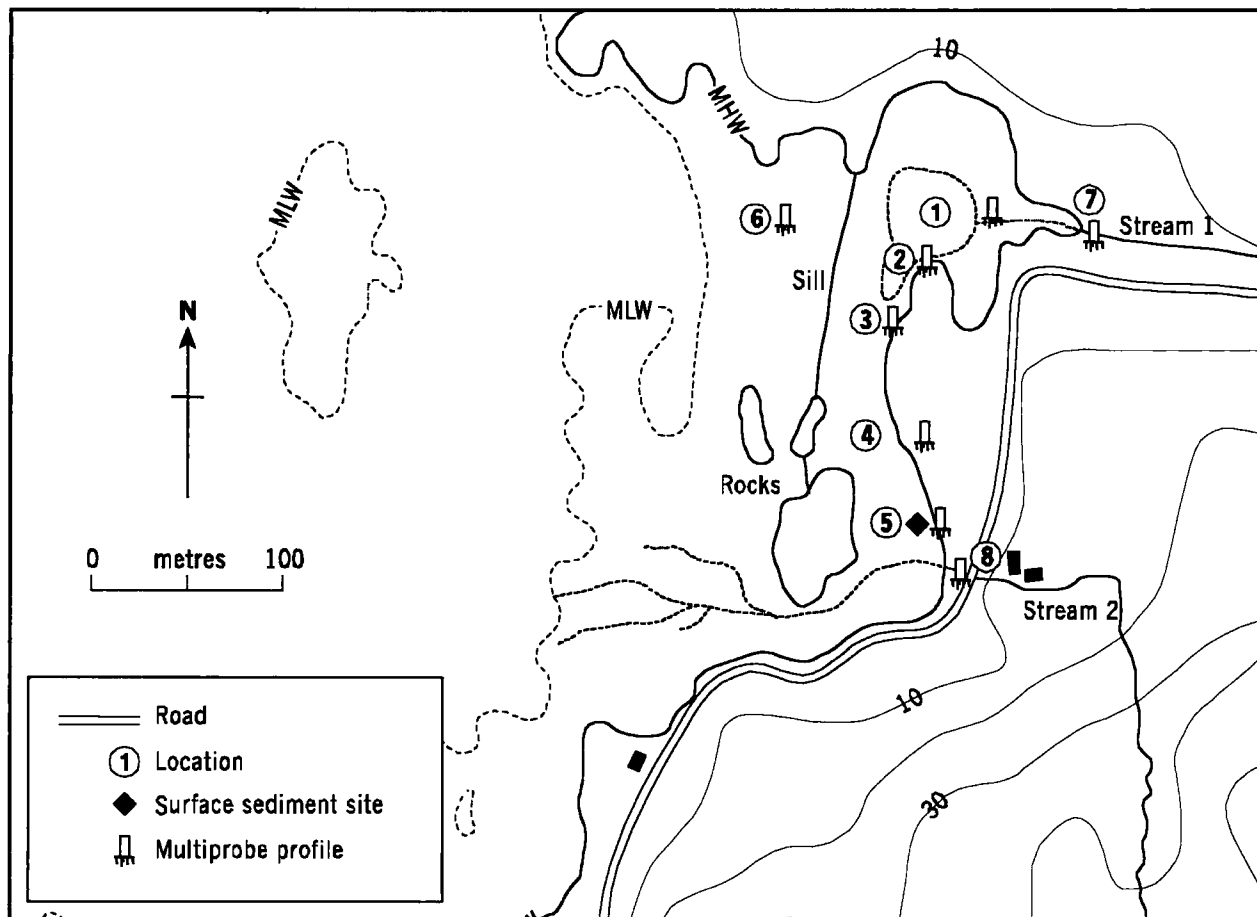


Figure 3.18: Rumach tidal pond site map - showing details for the site. Sampling stations (1-8) and type of sample or data obtained at each station is indicated. The locations of MHW, MLW and the two freshwater stream inputs are also illustrated.



Figure 3.19a: View of Rumach Tidal Pond sill (arrow) at low tide looking west over to Eigg



Figure 3.19b: View of Rumach Tidal Pond sill (arrow) at high tide looking north to south



Figure 3.19c: View of Loch nan Ceall looking over to Eigg, taken from Rumach Tidal Pond sill



Figure 3.19d: View of Stream 1 (arrow) entering Rumach Tidal Pond



Figure 3.19e: View of Stream 1 (arrow) looking up stream to the surrounding catchment



Figure 3.19f: View of stream 2 (arrow) entering Rumach Tidal Pond

Figure 3.20a: Rumach Tidal Pond water column profiles at station 1 during Spring-tide HT and LT (11/8/02).

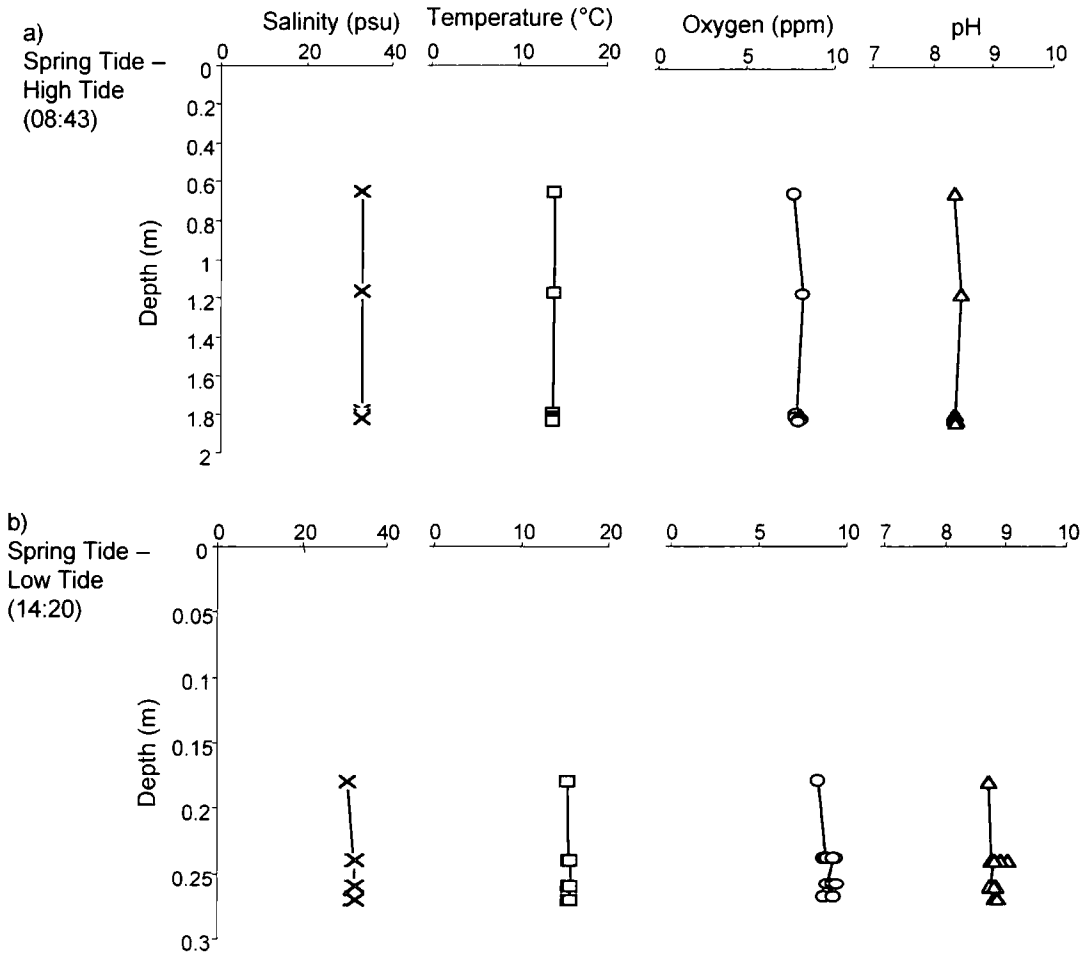


Figure 3.20b: Rumach Tidal Pond water column profiles at station 1 during mid-cycle tide tide LT and HT (7/8/02).

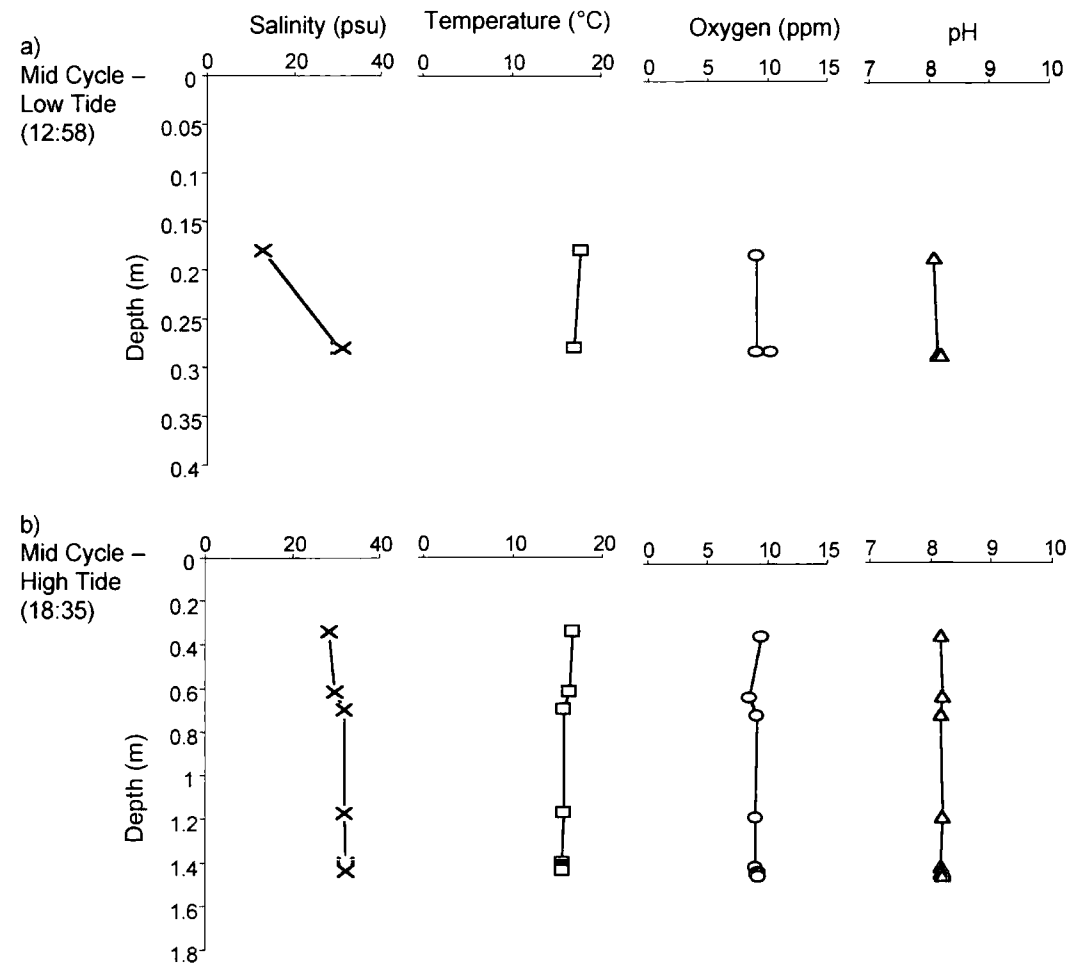
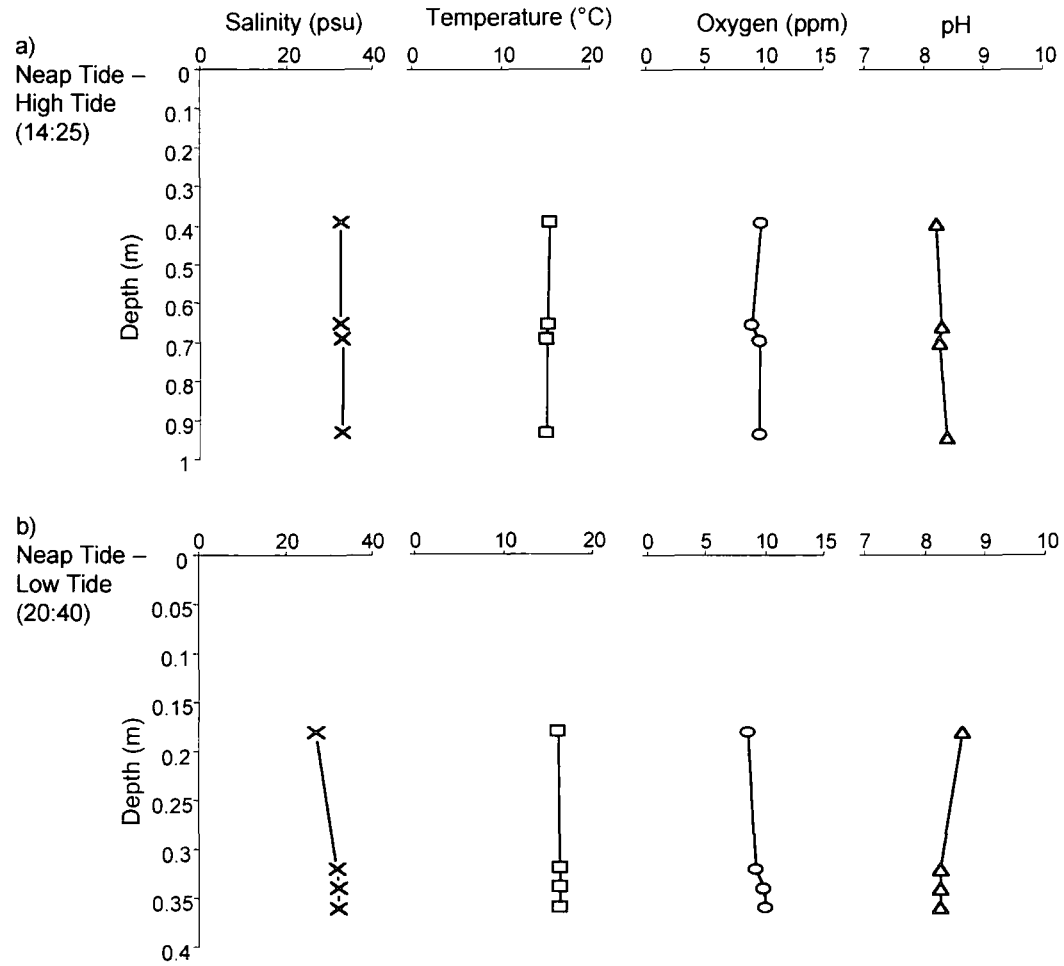


Figure 3.20c: Rumach Tidal Pond water column profiles at station 1 during neap-tide HT and LT (4/8/02).



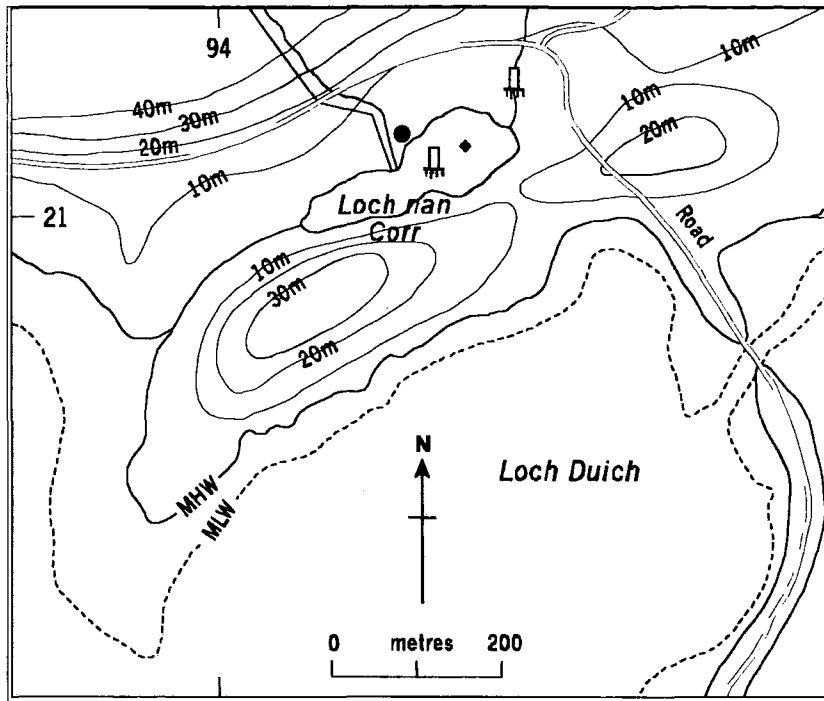


Figure 3.21: Loch nan Corr, Kintail site map - showing details of Loch nan Core site, including surface sediment sampling location (diamond) and core location (circle).



Figure 3.22a: Overview of Loch Nan Corr, the remaining shallow is marked with a arrow



Figure 3.22b: New piston core from Loch nan Corr. View of the shallow freshwater loch and the aquatic vegetation (arrow)

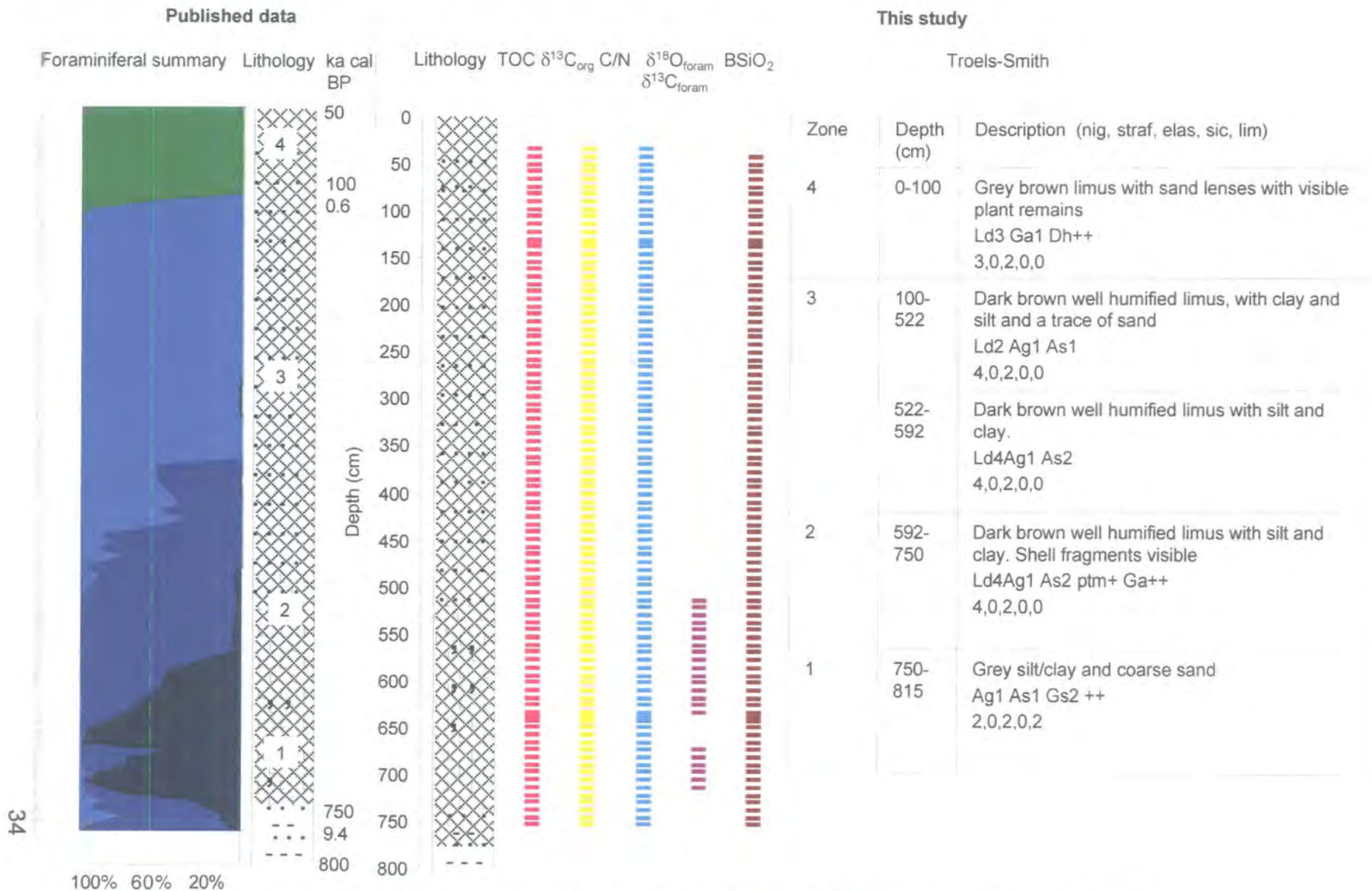


Figure 3.23: Loch nan Corr - overview of the lithostratigraphy and measurements down core. Published data Lloyd (2000).

Key organic limus clay silt, sand, shells. Foraminiferal classes: Marine Brackish lagoon Saltmarsh Fresh

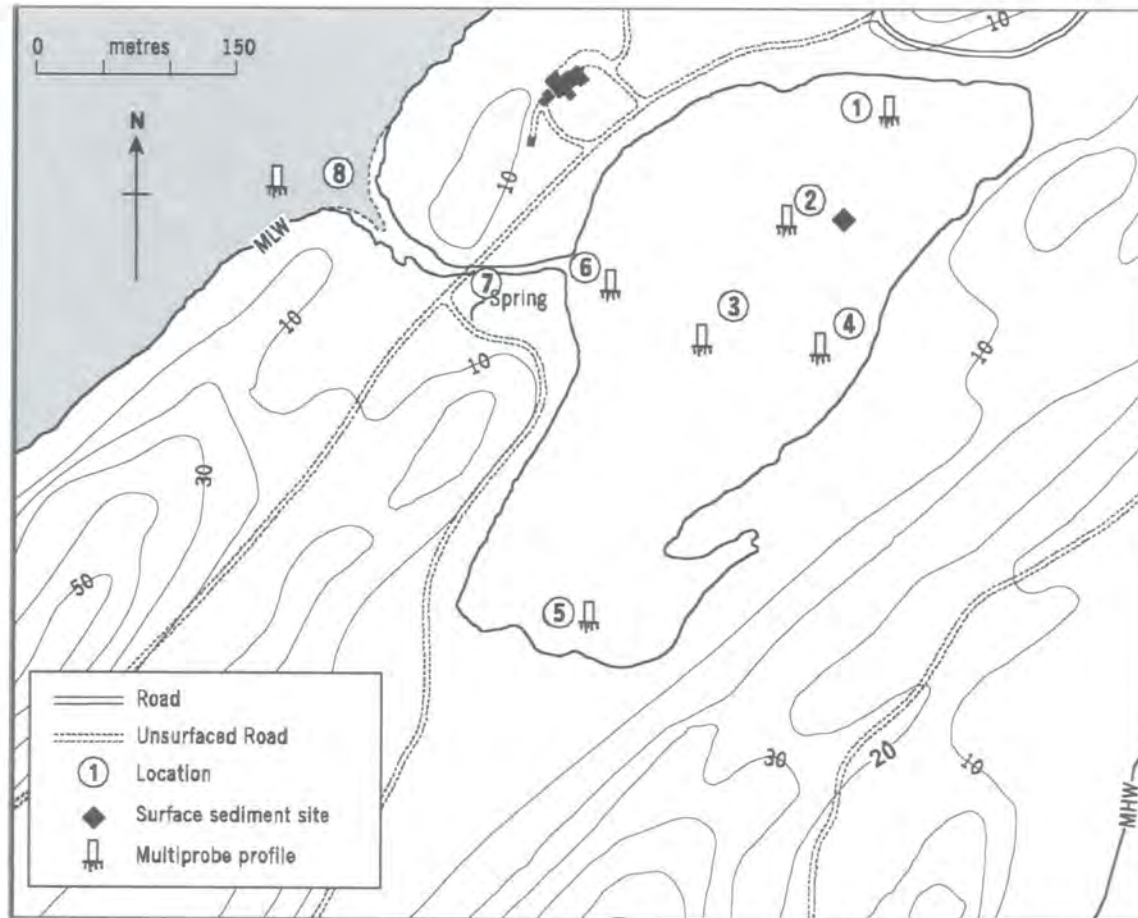


Figure 3.24: Craiglin site map - showing details for the site. Sampling stations (1-8) and type of sample or data obtained at each station is indicated. The locations of MHW, MLW and a freshwater spring input is also illustrated.



Figure 3.25a: View of Craiglin Lagoon (arrow) showing the culvert and the sill from Loch Sween



Figure 3.25b: View of sill waters entering the culvert. Sill marked with the arrow



Figure 3.25c: View of Loch Sween (arrow) and the inlet stream to the basin at high tide

Figure 3.26a: Craiglin Lagoon water column profiles at station 2 during spring-tide LT and HT (11/8/02). Note The well developed halocline at 0.5 m

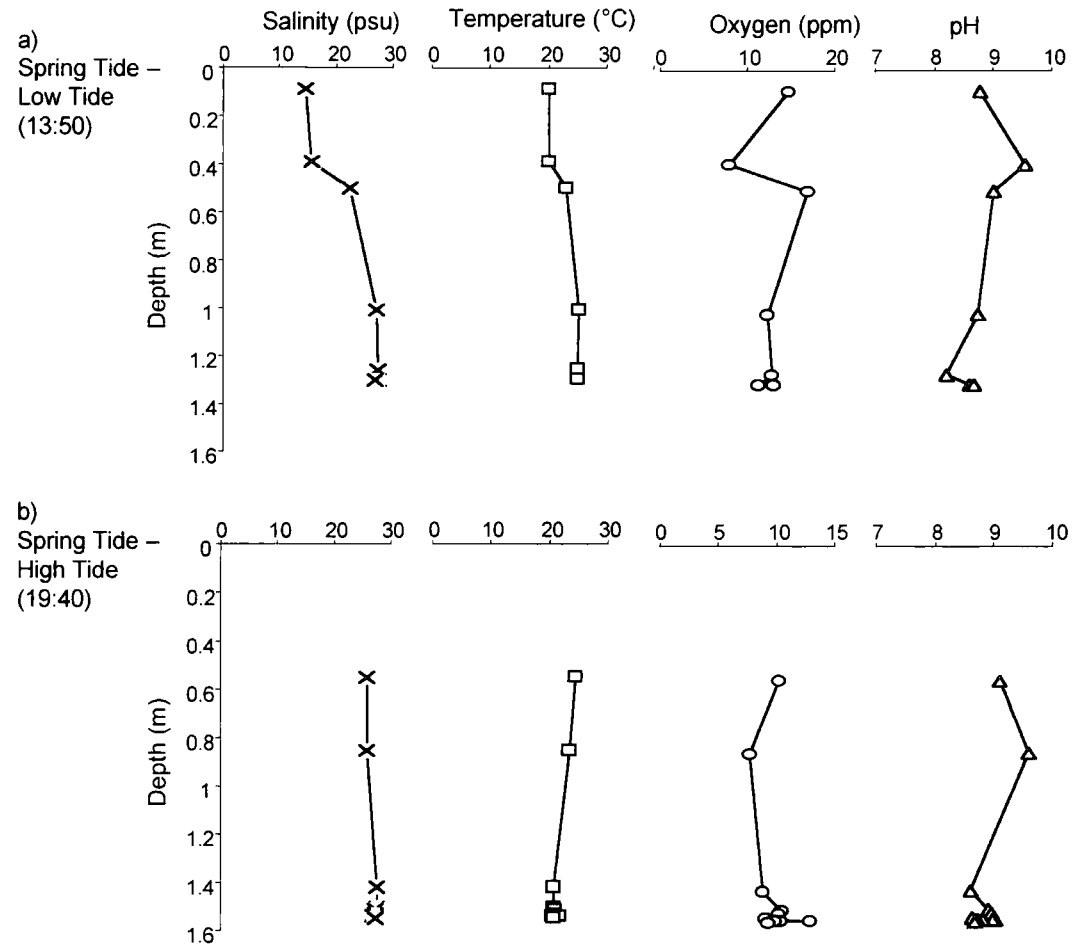


Figure 3.26b: Craiglin Lagoon water column profiles at station 2 during spring-tide LT and HT (7/10/02). Note the weaker haoline at 0.8m compared to Figure 3.25a.

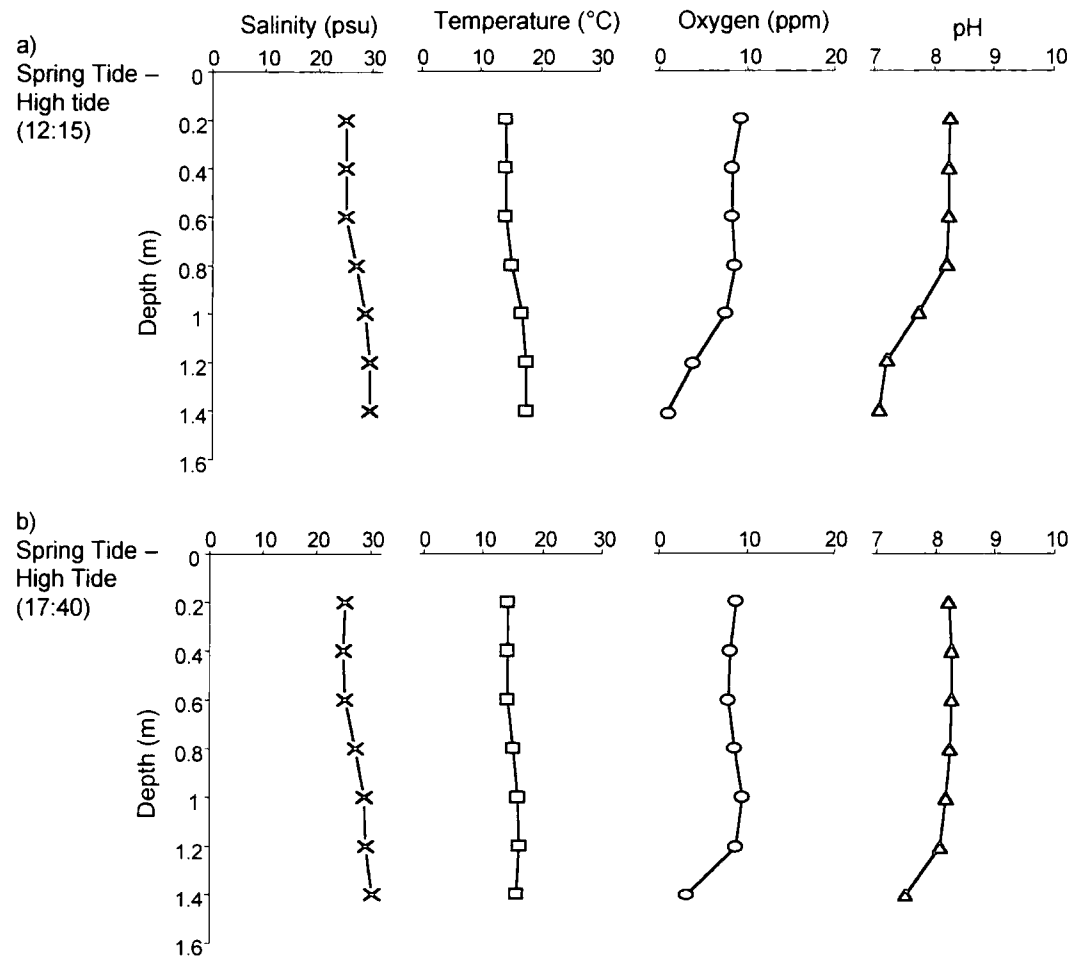


Table 3.3: Summary of geochemical and isotope proxies tested at each field site

Basin \ Proxy	TOC	C/N ratio	$\delta^{13}\text{C}_{\text{org}}$	$\delta^{18}\text{O}_{\text{foram}}$ $\delta^{13}\text{C}_{\text{foram}}$	$\delta^{13}\text{C}_{\text{diatom}}$	$^{87}\text{Sr}/^{86}\text{Sr}$	BSiO_2	Tephra
Arisaig								
Upper Loch Nan Eala	✓	✓	✓	X	✓	X	✓	✓
Main Loch Nan Eala	✓	✓	✓	X	X	X	X	✓
Rumach VI	✓	✓	✓	X	X	✓	X	X
Upper Allt Dail An Dubh-Asaid	✓	✓	✓	X	X	X	X	X
Torr a' Bheithe	✓	✓	✓	X	X	X	X	✓
Loch Torr a' Bheithe	✓	✓	✓	X	X	X	X	✓
Loch a' Mhuilinn	✓	✓	✓	X	X	X	X	✓
Rumach Tidal Pond	✓	✓	✓	✓	✓	X	X	X
Kintail								
Loch NanCorr sediment core	✓	✓	✓	✓	X	X	✓	X
Loch Nan Corr freshwater loch	✓	✓	✓	✓	✓	X	X	X
Knapdale								
Craiglin Lagoon	✓	✓	✓	✓	✓	X	X	X

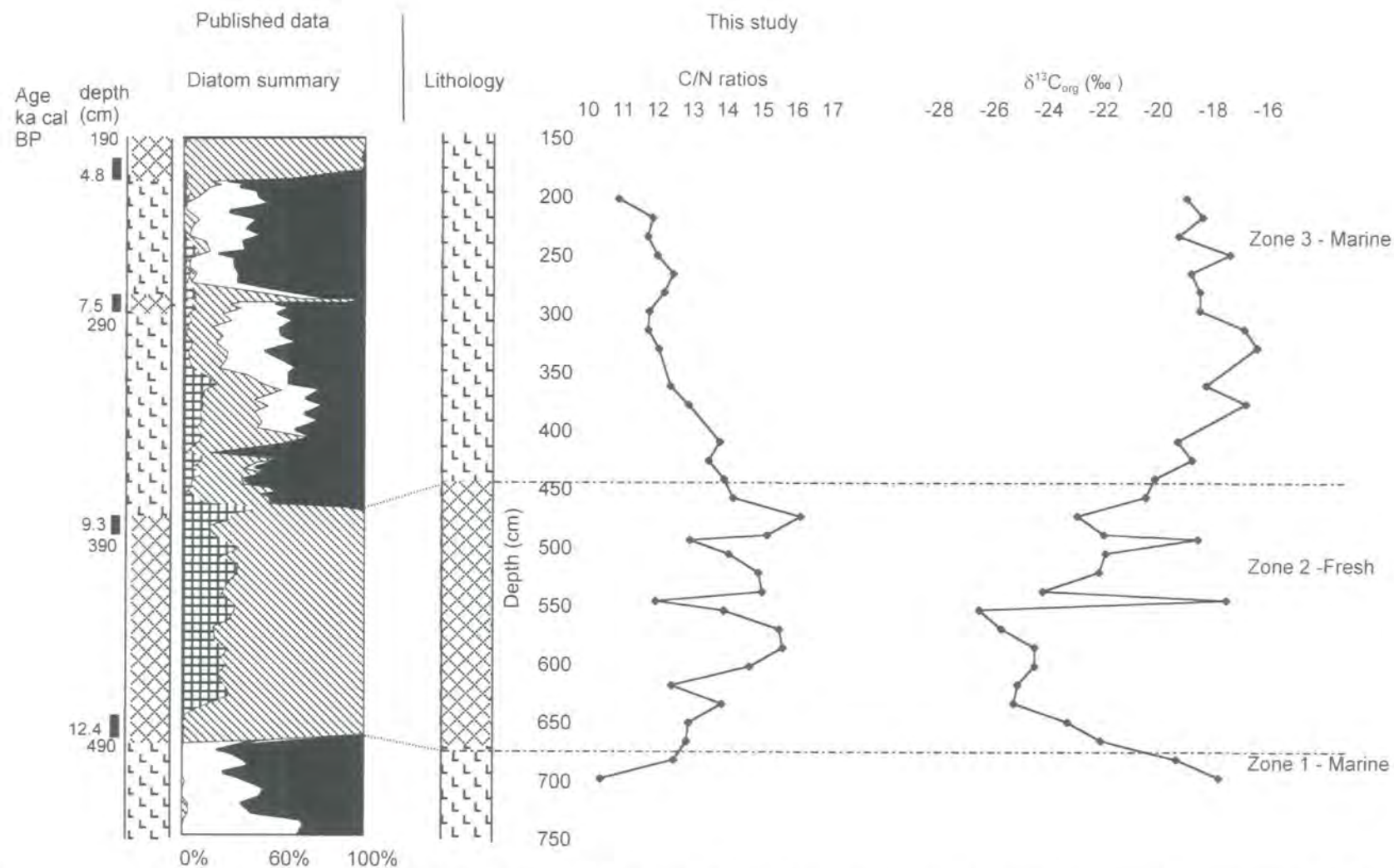


Figure 5.1: Upper Locha nan Eala (ULNE) - summary of $\delta^{13}C_{org}$ and C/N ratios data compared to the diatom palaeosalinity reconstruction by Shennan et al. (1994). Key for diatom summary and sediment lithology see as on Figure 3.6. Analysis conducted on a Russian core, the Holocene freshwater zone was not sampled in this core.

Depth (cm)	ULNE	Rumach VI	LNC
200	-	-	-
250	-	-	-
300	-	-	-
350	-	-	-
400	-	*	-
450	-	-	-
500	-	-	*
550	-	-	*
600	-	-	*
650	-	-	*
700	-	-	*
750	-	*	-
800	-	-	-
850	-	-	-
900	-	*	-
950	-	-	-
1000	-	-	-

Table 5.1: Summary table of the abundance of *H.germanica* foraminiferal in ULNE, Rumach VI and LNC. The * = *H.germanica*, - = no foraminiferal present at the depth in the core

Depth (cm)	No. diatoms per slide
100	>2000
200	>2000
300	>2000
400	>2000
500	>2000
600	>2000
700	>2000

Table 5.2: Summary table of the abundance of diatoms in ULNE (>2000 = so many diatoms the slide could not be properly counted)

Depth (cm)	No. diatoms per slide
380	669
476	130
572	158
668	783
764	775
860	18

Table 5.3: Summary table of the abundance of diatoms in MLNE

Depth (cm)	No. diatoms per slide
160	1093
170	1283
200	1338
250	1492
300	728
370	2529
390	>2000
410	4505
425	175
460	2223
480	135

Table 5.4: Summary table of the abundance of Rumach VI (Holocene core)

Sample	Salinity (psu)	$^{87}\text{Sr}/^{86}\text{Sr}$	$\delta^{87}\text{Sr}$
Waters			
Stream 1	0	0.713602948	335.4
Stream 2	0	0.714570933	432.2
HT basin	33	0.709191016	-105.7
HT sill	33	0.709172017	-107.6
LT basin	32.7	0.709175017	-107.3
LT sill	33	0.709163017	-108.5
Foraminifera			
412	-	0.709223	-102.5
764	-	0.709181	-106.7
892	-	0.709156	-109.2
Seawater standard			
		0.709171	
		0.709155	
		0.709164	
Dilute seawater std			
mean		0.709180	

Table 5.5: Summary of contemporary water samples from RTP and foraminifera from Rumach VI. HT = High tide, LT = Low tide. LT sill = water collected seaward of the sill at low tide.

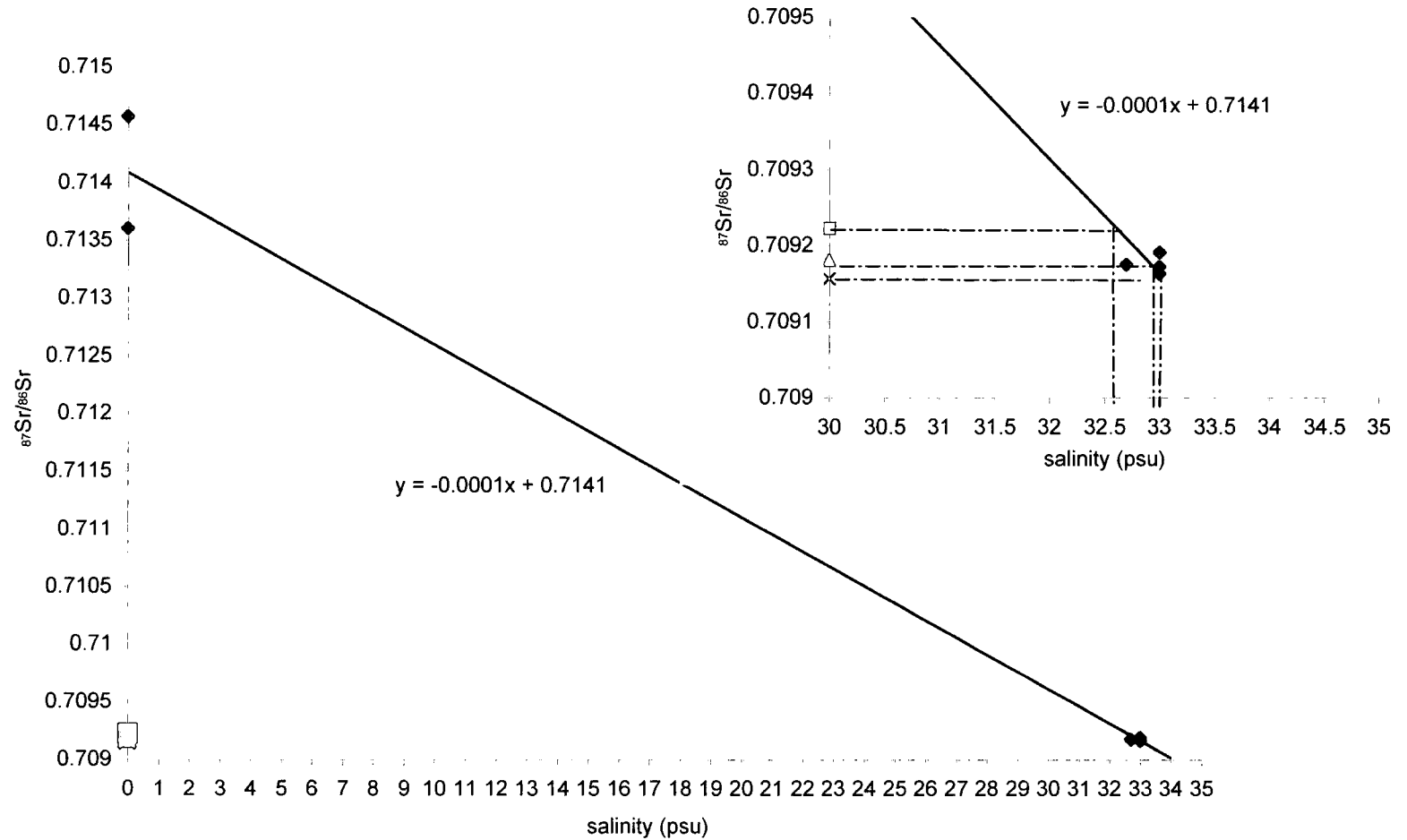


Figure 5.2: $^{87}\text{Sr}/^{86}\text{Sr}$ vs. salinity for water and foraminiferal samples from Rumach VI (Holocene core). Blue diamonds = water samples. Pink square = sample 412 cm, Orange triangle = 764 cm, Blue cross = sample 892 cm. Sample 412 cm has a predicted salinity of 32.5 psu, while samples 764 and 892 cm have a predicted salinity of 33 psu. Insert graph is an enlargement of the predicted salinity of the three foraminiferal samples.

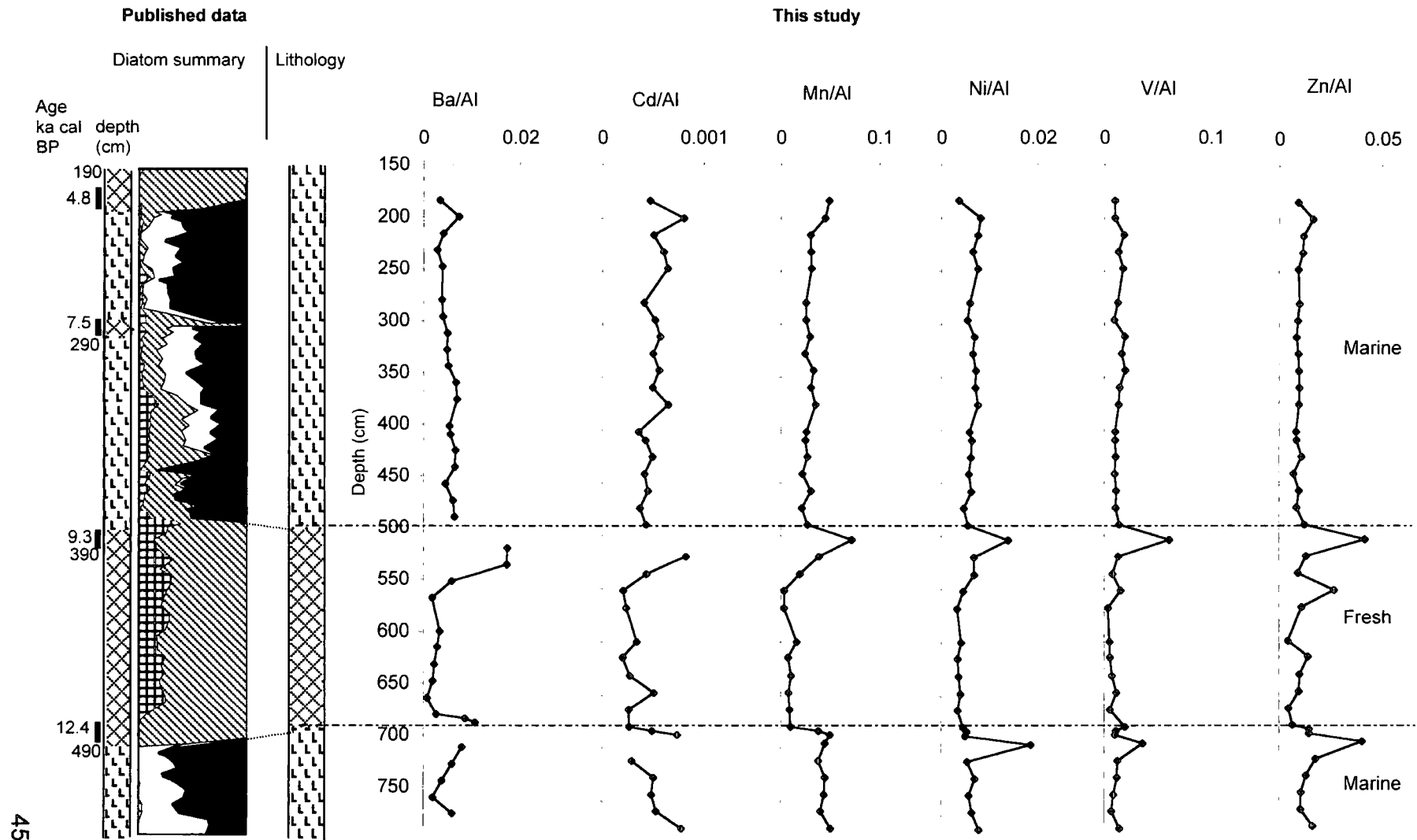


Figure 5.3: Elemental /Al ratios from ULNE compared against the diatom reconstruction (Shennan *et al.*, 1994). For lithological and diatom key see Figure 3.6. Analysis was conducted upon a test Russian core from ULNE

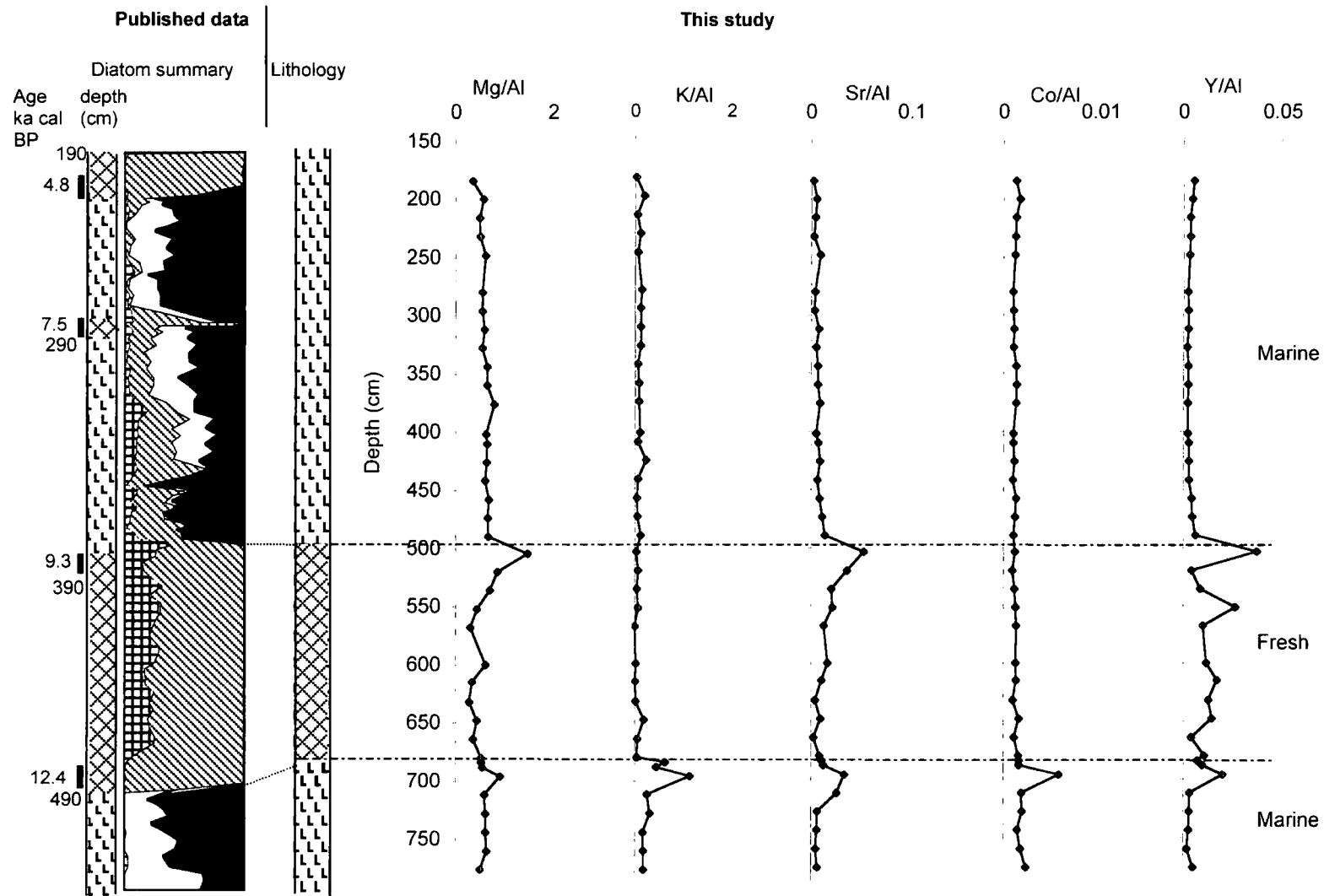


Figure 5.3 continued: Elemental/Al ratios compared against the diatom reconstruction (Shennan *et al.*, 1994). For lithological and diatom key see Figure 3.6.

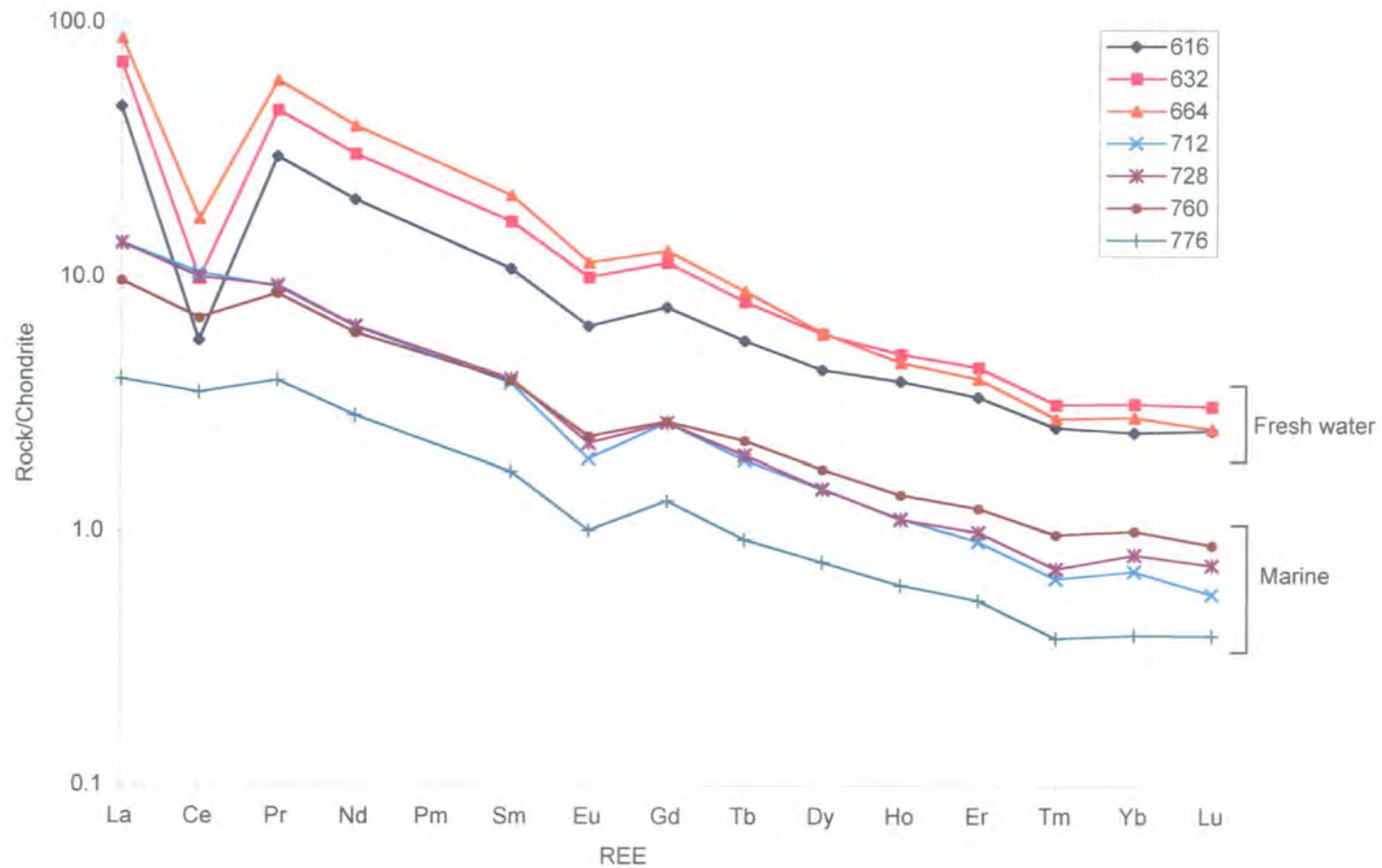


Figure 5.4: REE elements plotted from Upper Loch nan Eala.

Table 6.1: Values of contemporary data collected from NW Scotland

Terrestrial plants	$\delta^{13}\text{C}$ (‰)	C/N ratio
<i>Juncus</i> sp.	-27.6	29.4
<i>Cratageus monogyna</i>	-30.2	22.6
<i>Acer pseudoplatanus</i>	-30.2	15.5
<i>Quercus</i> sp.	-29.0	15.7
<i>Larix eurolepis</i> Henry	-27.7	53.4
<i>Pteridium aquilinum</i>	-25.1	10.2
<i>Iris pseudacorus</i>	-27.3	17.7
<i>Juncus</i> sp.	-27.9	27.0
<i>Juncus</i> sp.	-28.2	30.3
<i>Equisetum</i>	-25.7	10.7
<i>Caltha palustris</i>	-29.3	13.3
<i>Sphagnum</i> sp.	-29.6	57.3
<i>Alnus glutinosa</i>	-28.1	17.1
<i>Polytrichum commune</i>	-25.6	97.2
<i>Epilobium palustra</i>	-29.9	16.0
<i>Poteuntilla reptans</i>	-26.4	11.5
<i>Juncus</i> sp.	-28.2	25.4
<i>Calluna vulgaris</i>	-29.4	51.0
<i>Sphagnum</i> sp.	-26.7	24.8
<i>Blechnum spicant</i>	-29.9	28.9
<i>Myrica gale</i>	-27.6	16.0
<i>Primula veris</i>	-29.2	15.3
<i>Acer pseudoplatanus</i>	-29.0	12.2
<i>Caltha palustris</i>	-30.2	11.4
<i>Iris pseudacorus</i>	-27.9	17.1
<i>Pteridium aquilinum</i>	-25.5	12.0
<i>Gramineae</i>	-28.6	34.9
<i>Endymion non-scripta</i>	-28.5	19.6
Freshwater aquatics		
<i>Equisetum fluviatile</i>	-24.9	14.1
<i>Nymphaea alba</i>	-26.4	17.8
<i>Ranunculus repens</i>	-26.8	13.9
<i>Phragmites australis</i>	-25.0	12.1
<i>Potamogeton</i> sp.	-32.5	16.1
Marine plants		
<i>Ulva lactuca</i>	-18.3	23.2
<i>Fucus</i> sp.	-20.0	25.7
<i>Dictyota dichotoma</i>	-17.3	40.5
<i>Cladophora rupestris</i>	-21.7	8.2
<i>Fucus vesiculosus</i>	-19.0	27.0
Surface sediment samples		
LNC basin sediment (freshwater)	-28.4	14.6
RTP stream sediment (freshwater)	-29.3	14.4
Craiglin Lagoon stream sediment	-29.4	16.6
RTP basin sediment (marine)	-20.8	7.7
Craiglin Lagoon (marine /brackish)	-18.5	9.3

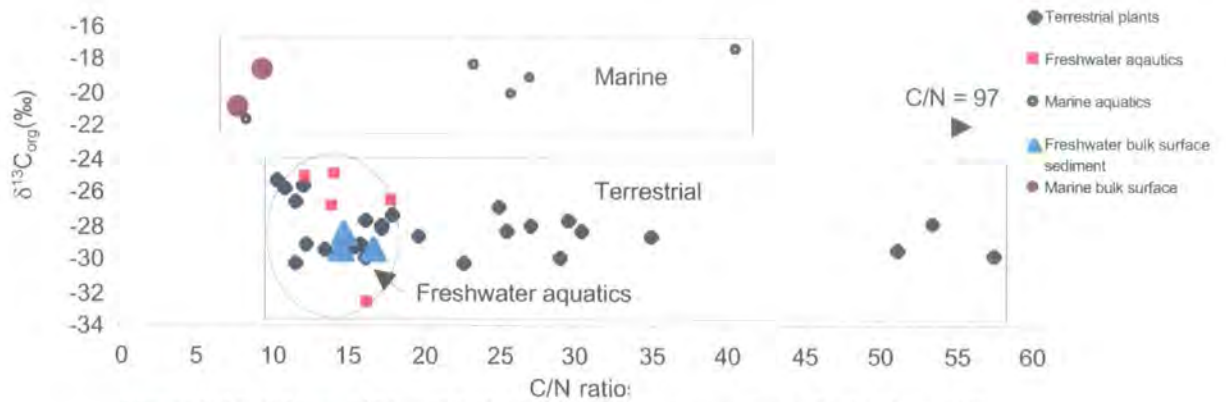


Figure 6.1a: C/N vs. $\delta^{13}\text{C}_{\text{org}}$ plot of the contemporary samples collected from NW Scotland. See Table 6.1 for data

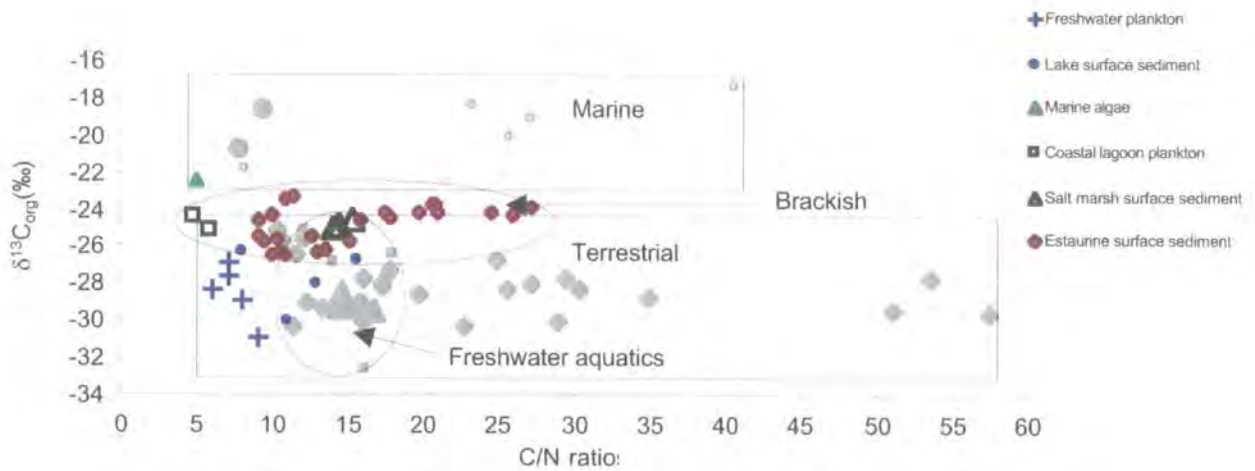


Figure 6.1b: C/N vs. $\delta^{13}\text{C}_{\text{org}}$ plot of contemporary data from this study (Table 6.1) and values from the published literature (Table 6.2). The contemporary data is in grey. Marine, brackish, terrestrial and freshwater aquatic fields are based on contemporary data from this study and published literature. These fields will be used in all subsequent C/N vs. $\delta^{13}\text{C}_{\text{org}}$ plots from sediment cores.

Organic matter source	Location	C/N ratio	$\delta^{13}\text{C}$ (‰)	Reference
C3 Vascular plants				
Peat	Shores of southern Baltic Sea.	16	-29.2	Müller & Voss, 1999
woody peat oak/hazel	Humber Estuary	17- 23	-28	Andrews <i>et al.</i> , 2000
	Shores of southern Baltic sea	10 to 85	n/a	Müller & Mathesius, 1999
	Russia	>12	n/a	Bordovskiy, 1965
	Dobob Bay Wasinghton	>12	n/a	Pharl <i>et al.</i> , 1980
	Catchment of Greifswalder	10 to 85	n/a	Müller & Mathesius, 1999
	Bodden, southern Baltic sea	20 to 200	n/a	Hedges <i>et al.</i> , 1986
	Amazon basin	n/a	-28 to -29	Emerson & Hedges, 1988
Lake plankton				
Mixed plankton	Lake Baikal, Russia.	9	-30.9	Prokopenko <i>et al.</i> , 1993
	Lake Michigan, Ammmerica	7	-26.8	Meyers, 1994
	Pyramid Lake, Nevada.	6	-28.3	Meyers, 1994
	Lake Biwa, Japan	7	-27.5	Nakai & Koyama 1987
	Walker Lake, Nevada	8	-28.8	Meyers, 1994
	America	n/a	-30 to -20	Galimov, 1985
Lake surface sediment				
	Loch Tay, Scotland	16	-26.6	Thornton & McManus 1994
	Loch Tummel, Scotland	13	-27.9	Thornton & McManus 1994
	Lake Baikal, Russia	11	-29.9	Qiu <i>et al.</i> , 1993
Marine algae				
Mixed plankton	Rhode Island, U.S.A	na	-20.3	Gearing <i>et al.</i> 1984
Nanoplankton	Rhode Island, U.S.A	n/a	-22.2	Gearing <i>et al.</i> 1984
Mixed plankton	Dabob Bay, Washington	5	-22.4	Prahl <i>et al.</i> 1980
Mixed plankton		n/a	-22 to -17	Galimov, 1985
Marine surface sediment				
	Gironde system, France	n/a	-19 to -22	Fontugne & Joanneau, 1987
	Washington continental shelf	15	n/a	Ertel & Hedges, 1985
	Russia	8 to 12	n/a	Bordovskiy, 1965
	Offshore Baltic Sea	na	-23	Voss & Sruck, 1997
	Gulf of St. Lawrence	n/a	-22.4	Tan & Strain, 1979
	Rhode Island, U.S.A	n/a	-21.8	Gearing <i>et al.</i> 1984
Intermediate group				
Estuary surface sediment (salinity unknown)				
Intermediate Mud Flat	Humber Estuary.	15.25	-24.49	Andrews unpublished
Lower Salt Marsh	Humber Estuary.	14.35	-24.82	Andrews unpublished
Salt Marsh	Humber Estuary.	14.02	-24.9	Andrews unpublished
	Tay Estuary	13	-26.2	Thornton & McManus 1994
		10.5	-26.2	Thornton & McManus 1994

Organic matter source	Location	C/N ratio	$\delta^{13}\text{C}$ (‰)	Reference
		9.3	-25.7	Thornton & McManus 1994
		9.9	-26.4	Thornton & McManus 1994
		12.6	-25.4	Thornton & McManus 1994
		15.1	-25.6	Thornton & McManus 1994
		10.2	-25.5	Thornton & McManus 1994
		9.1	-25.3	Thornton & McManus 1994
		13.5	-26.1	Thornton & McManus 1994
		15.7	-24.5	Thornton & McManus 1994
		10	-24.2	Thornton & McManus 1994
		9	-24.5	Thornton & McManus 1994
		10.1	-23.3	Thornton & McManus 1994
		11.3	-23.2	Thornton & McManus 1994
	Forth Estuary, Scotland	20.8	-24	Graham <i>et al.</i> , 2001
		27.1	-23.8	Graham <i>et al.</i> , 2001
		25.9	-24.2	Graham <i>et al.</i> , 2001
		19.6	-24.1	Graham <i>et al.</i> , 2001
		17.7	-24.4	Graham <i>et al.</i> , 2001
		24.4	-24	Graham <i>et al.</i> , 2001
		17.3	-24	Graham <i>et al.</i> , 2001
		20.7	-23.6	Graham <i>et al.</i> , 2001
		20.5	-23.6	Graham <i>et al.</i> , 2001
Coastal lagoons				
Aquatic macrophytes	Baltic Sea, Greifswalder,			
salinity <12 psu	Bodden	6 to 44	n/a	Müller & Mathesius, 1999
Plankton	Oder Estuary, Baltic Sea	5	-24.4	Müller & Voss, 1999
Plankton	Greifswalder, Bodden	6	-25.1	Müller & Voss, 1999
Baltic sea sub basins	Mecklenburg Bight	n/a	-22.5	Emeis <i>et al.</i> , 2003
Surface sediment salinity	Arkona Basin	n/a	-22.7	Emeis <i>et al.</i> , 2003
between 12 to 3.6psu	Bornholm Basin	n/a	-22.5	Emeis <i>et al.</i> , 2003
	Gotland Deep	n/a	-23.8	Emeis <i>et al.</i> , 2003
	Pomeranian Bight	n/a	-24.5	Emeis <i>et al.</i> , 2003
	North Gotland Basin	n/a	-23.6	Emeis <i>et al.</i> , 2003
	Bothnian Sea	n/a	-24.3	Emeis <i>et al.</i> , 2003
	Bothnian Bay	n/a	-25.7	Emeis <i>et al.</i> , 2003

Table 6.2: Published contemporary $\delta^{13}\text{C}_{\text{org}}$ and C/N ratios from a range of sedimentary and aquatic environments. Only where the reference gives pairs of $\delta^{13}\text{C}_{\text{org}}$ and C/N ratio are they plotted on Figure 6.1b.

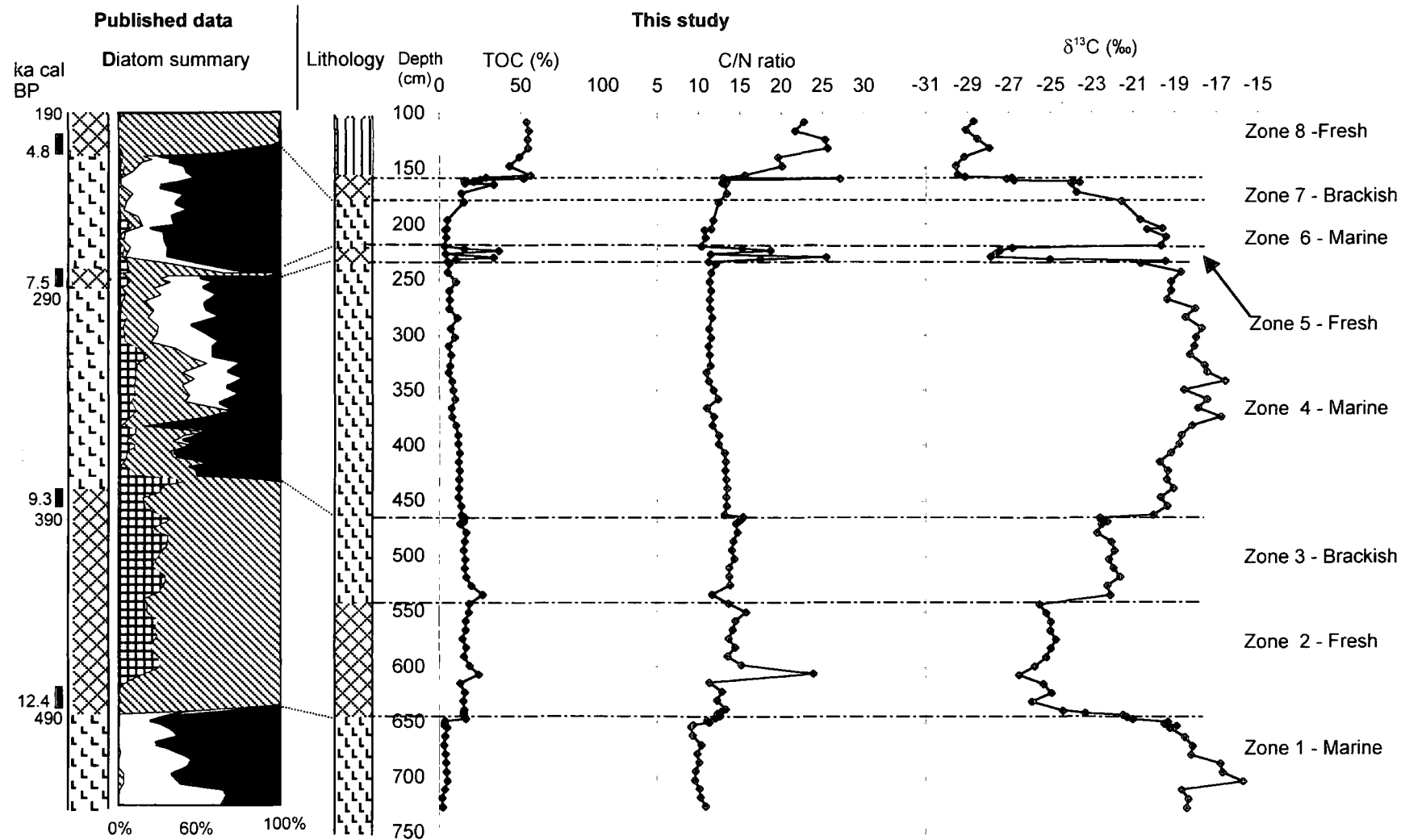


Figure 6.2: Upper Loch nan Eala - profiles of TOC, C/N ratios and $\delta^{13}\text{C}_{\text{org}}$ against the biological salinity reconstruction. Published data from Shennan *et al.* (1994). Lithological and diatom key as on Figure 3.6.

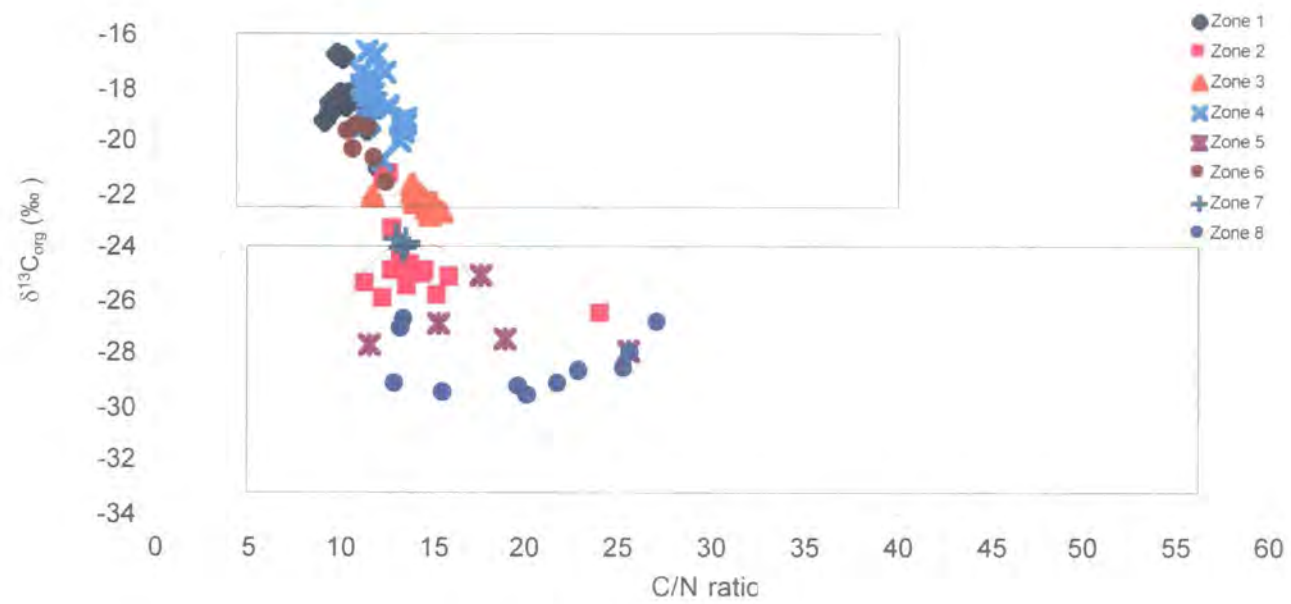


Figure 6.3: Upper Loch nan Eala C/N vs. $\delta^{13}C_{org}$

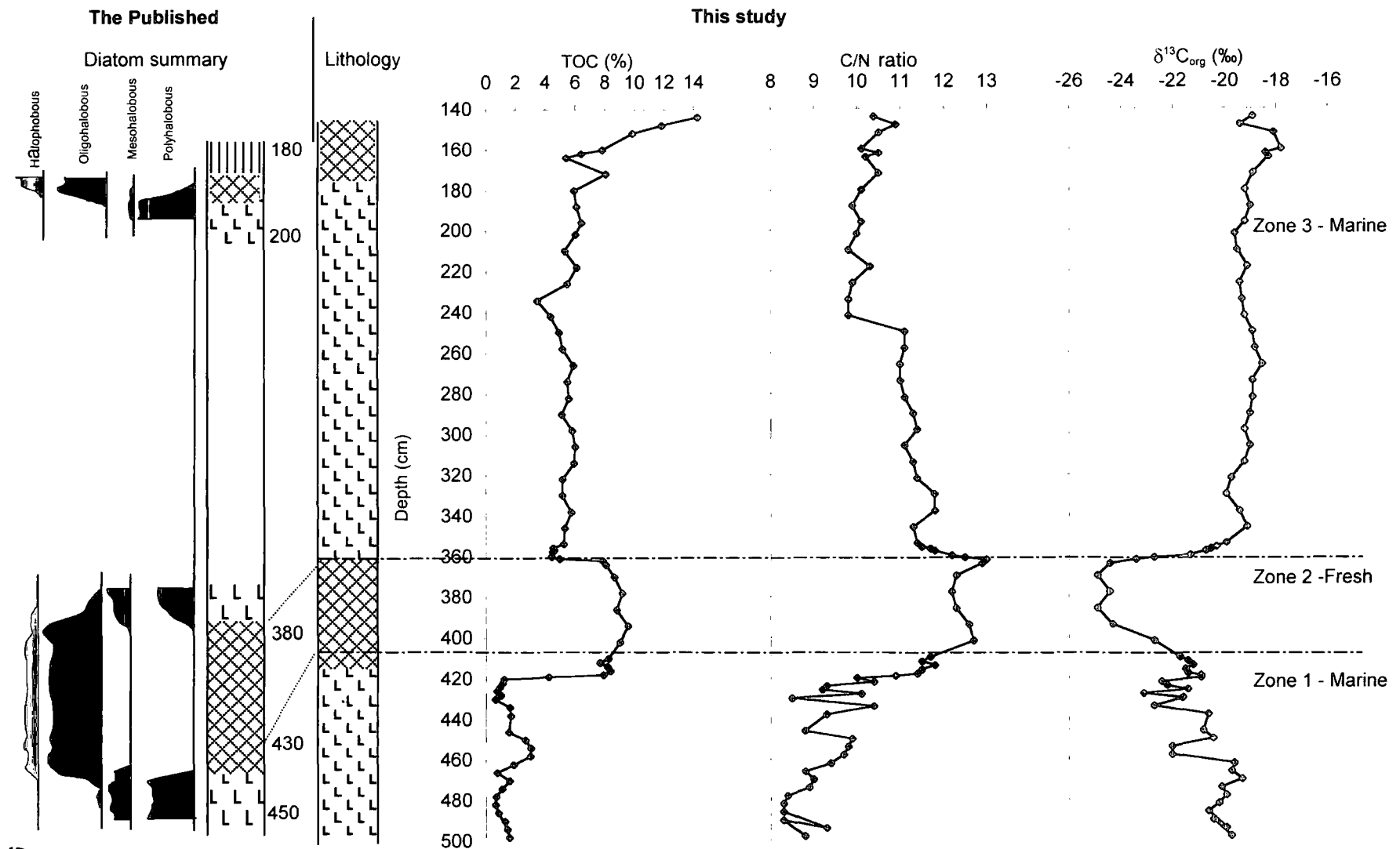


Figure 6.4: Main Loch nan Eala - profiles of TOC, C/N ratios and $\delta^{13}C_{org}$ compared to the diatom summary. Published data Shennan *et al.* (1994). Lithology and diatoms key as on Figure 3.6

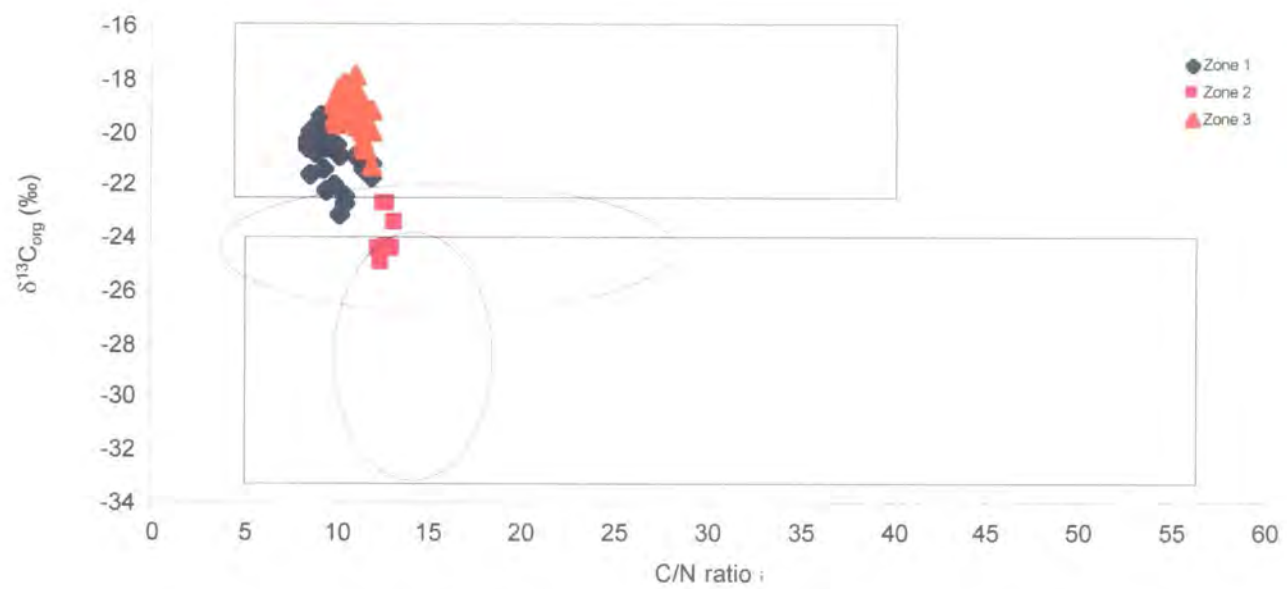


Figure 6.5: Main Loch nan Eala C/N vs. $\delta^{13}C_{org}$

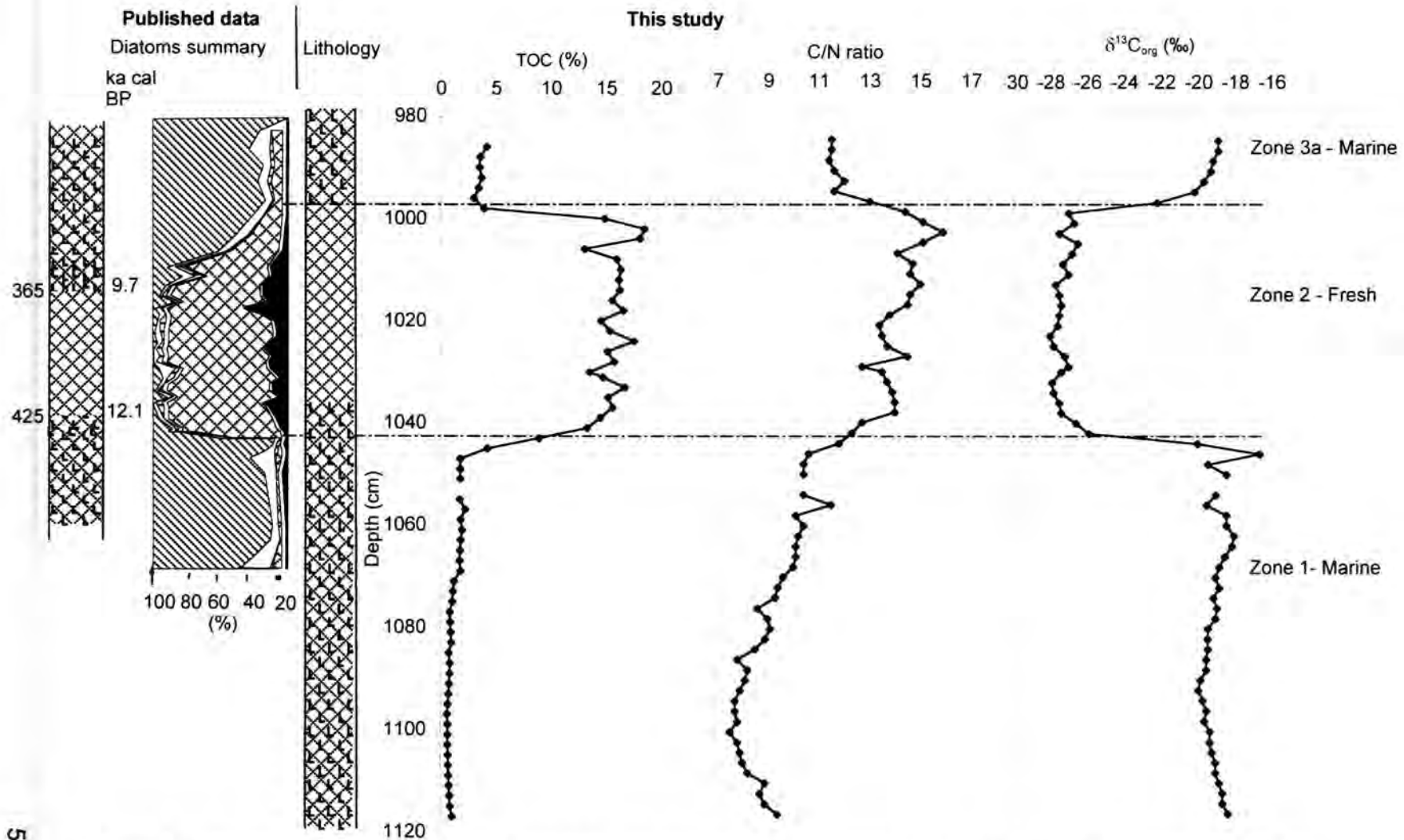


Figure 6.6a: Rumach VI - Lateglacial core- Profiles of TOC, C/N ratios and $\delta^{13}C_{org}$ compared to the diatom summary (Shennan *et al.*, 1999). Lithology and diatoms key as on Figure 3.6.

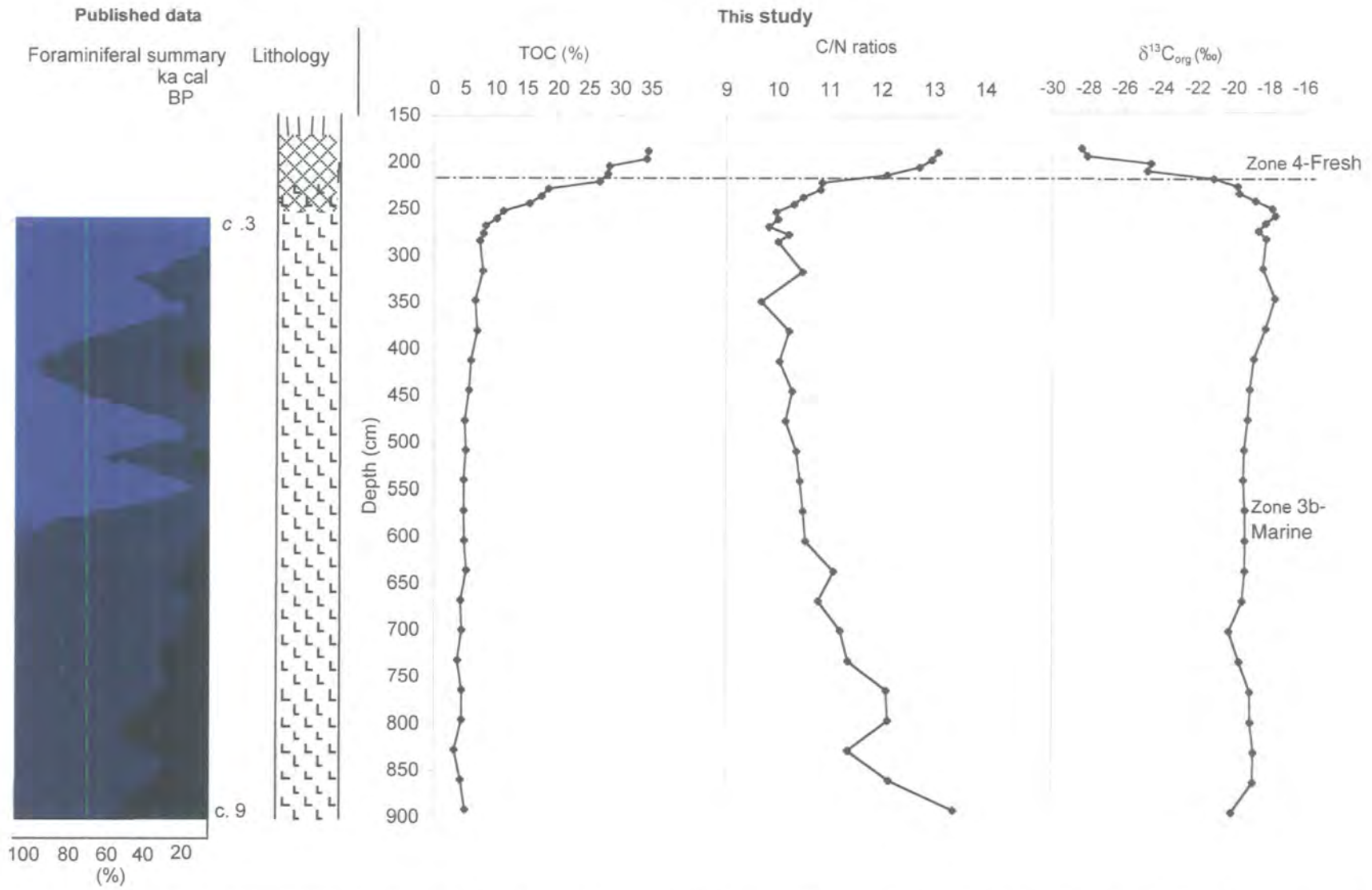


Figure 6.6b: Rumch VI (Holocene section) Summary of TOC, C/N and $\delta^{13}C_{org}$ against the foraminiferal salinity reconstruction (Lloyd and Evans, 2002). The foraminiferal reconstruction and the isotope data have been taken from the same core. Lithology and foraminiferal key as on Figure 3.21.

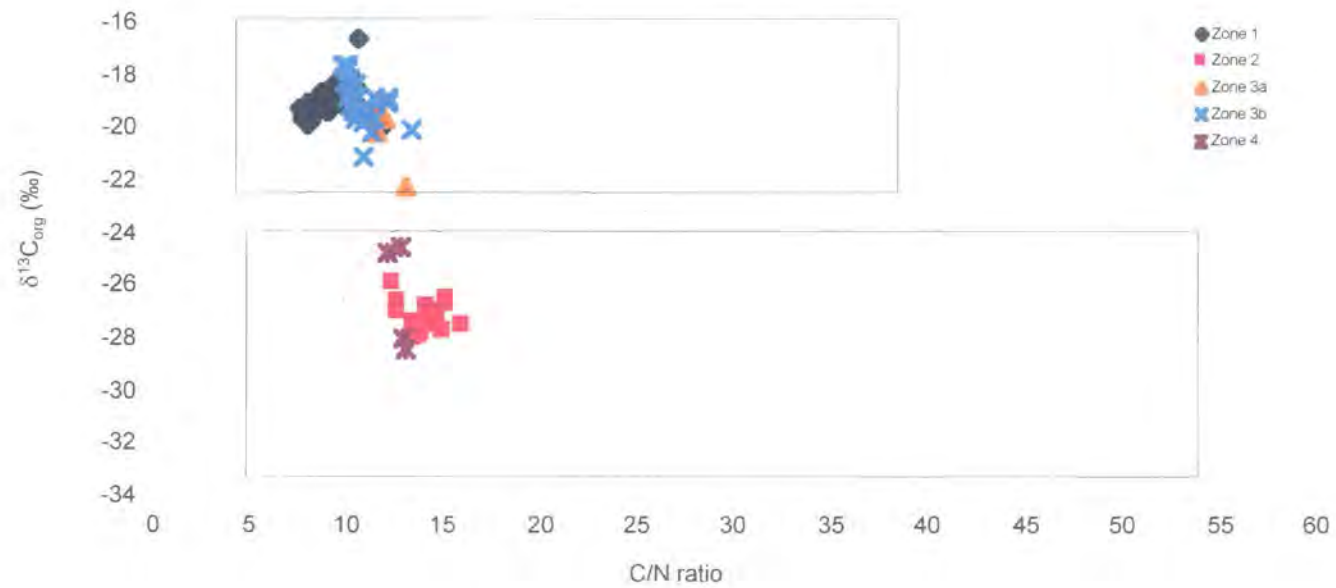


Figure 6.7: Rumach VI C/N vs. $\delta^{13}C_{org}$

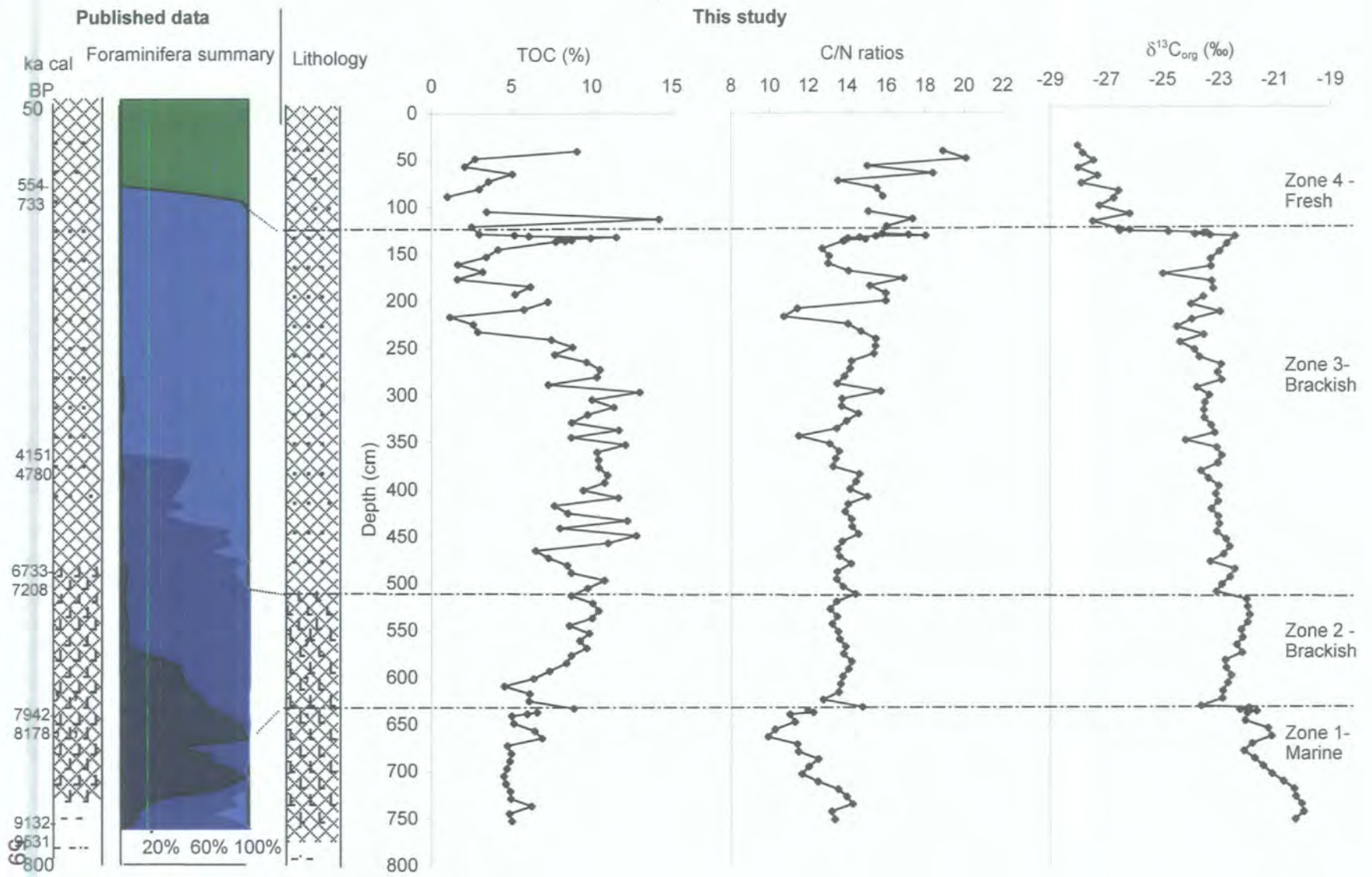


Figure 6.8: Loch nan Corr - profiles of TOC, C/N ratios and $\delta^{13}C_{org}$ compared to the foraminifera summary. Published data from Lloyd (2000). Key Figure 3.23

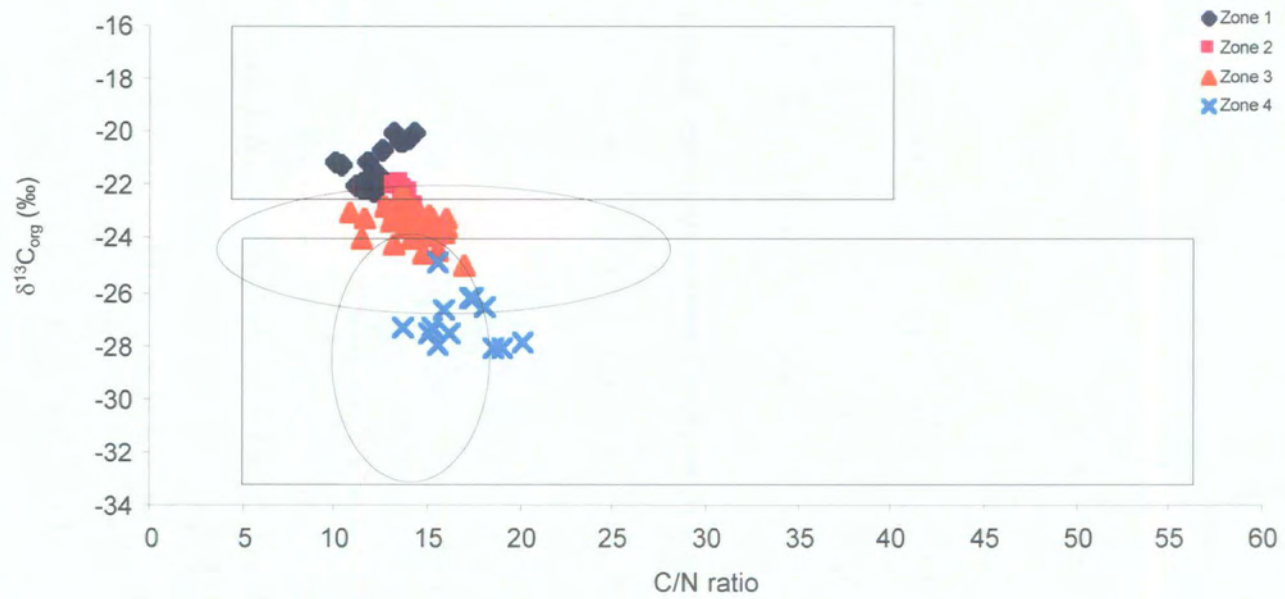


Figure 6.9: Loch nan Corr C/N vs. δ¹³C_{org}

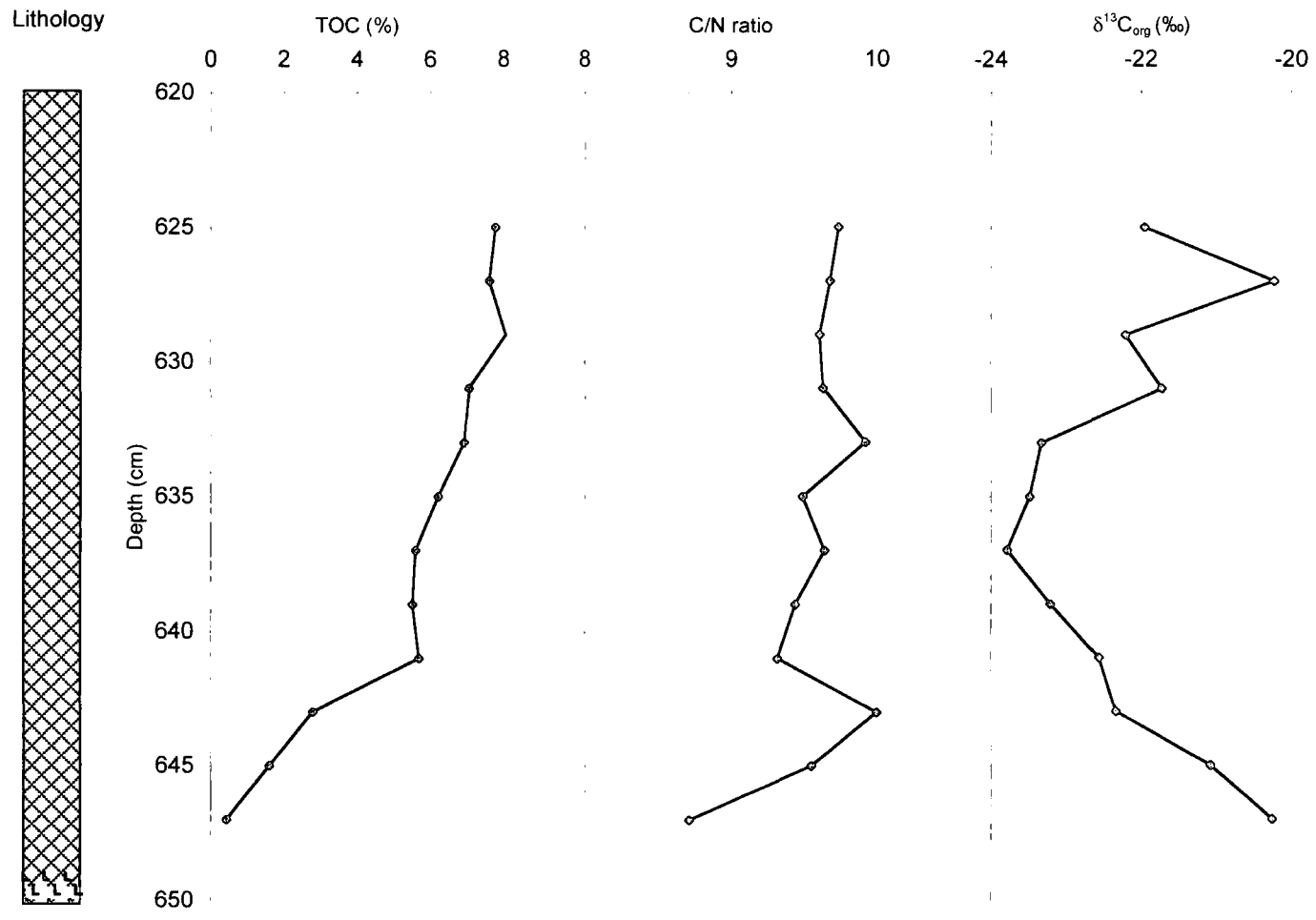


Figure 6.10: Upper Allt Dail An Dubh-Asaid - profiles of TOC, C/N ratios and $\delta^{13}C_{org}$

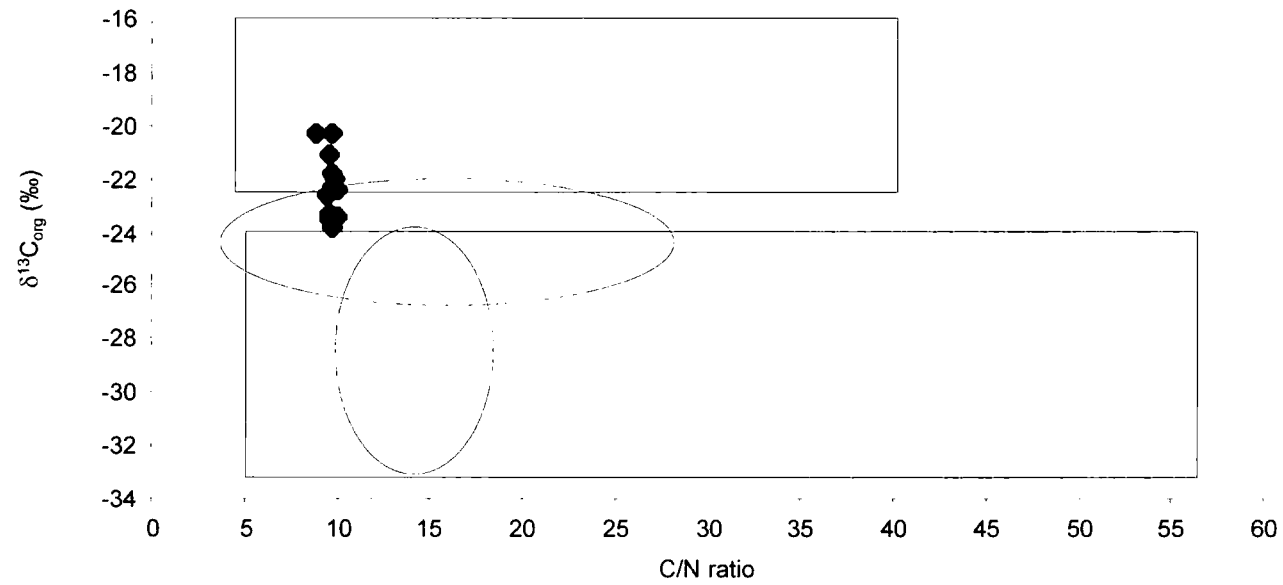


Figure 6.11: Upper Allt Dail Dubh-Asaid - C/N vs. $\delta^{13}\text{C}_{\text{org}}$

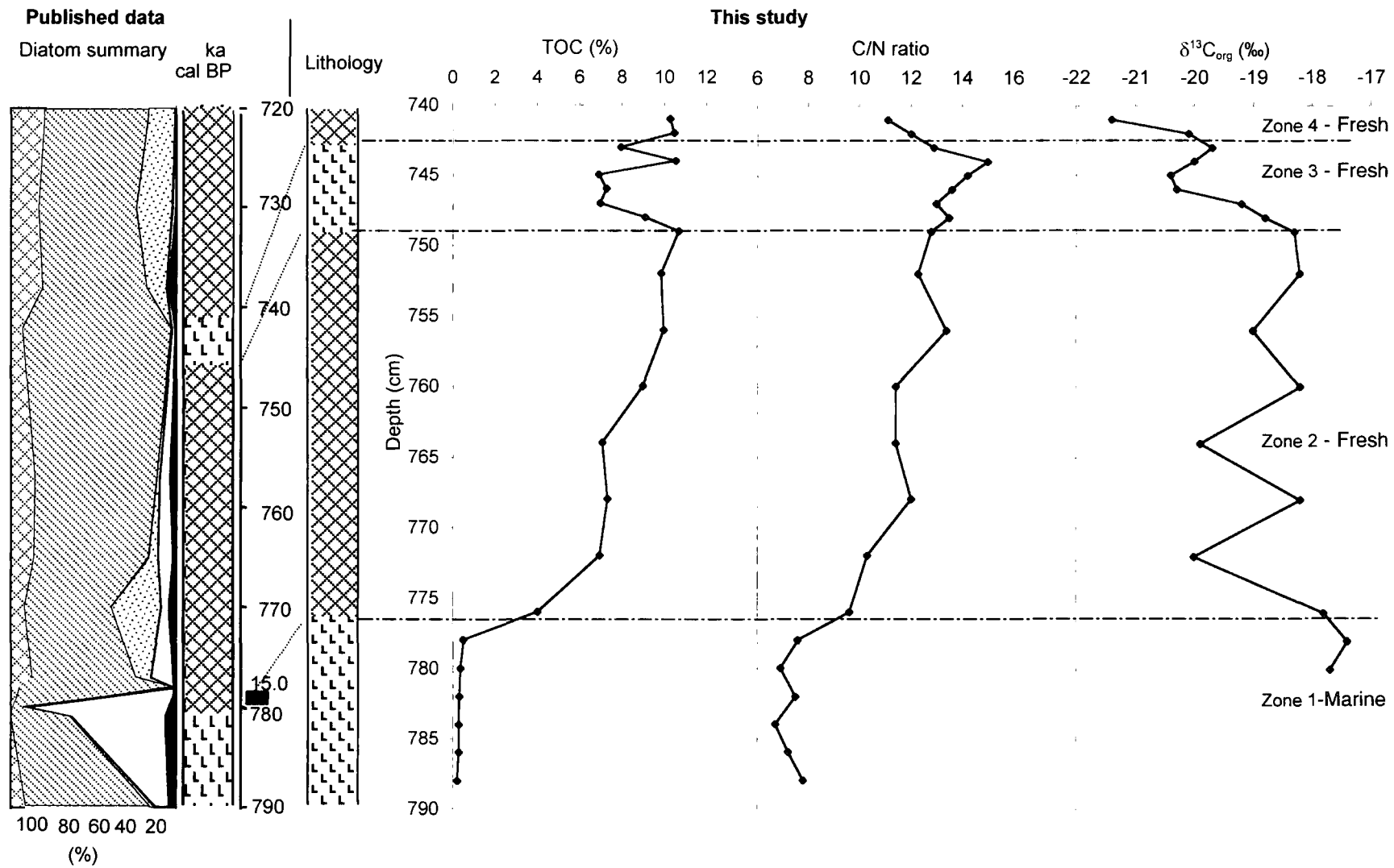


Figure 6.12: Torr a' Bheithe -profiles of TOC, C/N ratios and $\delta^{13}C_{org}$ against the diatom palaeosalinity reconstruction. Published data from Shennan *et al.*, 2000. Lithology and diatom key as on Figure 3.6.

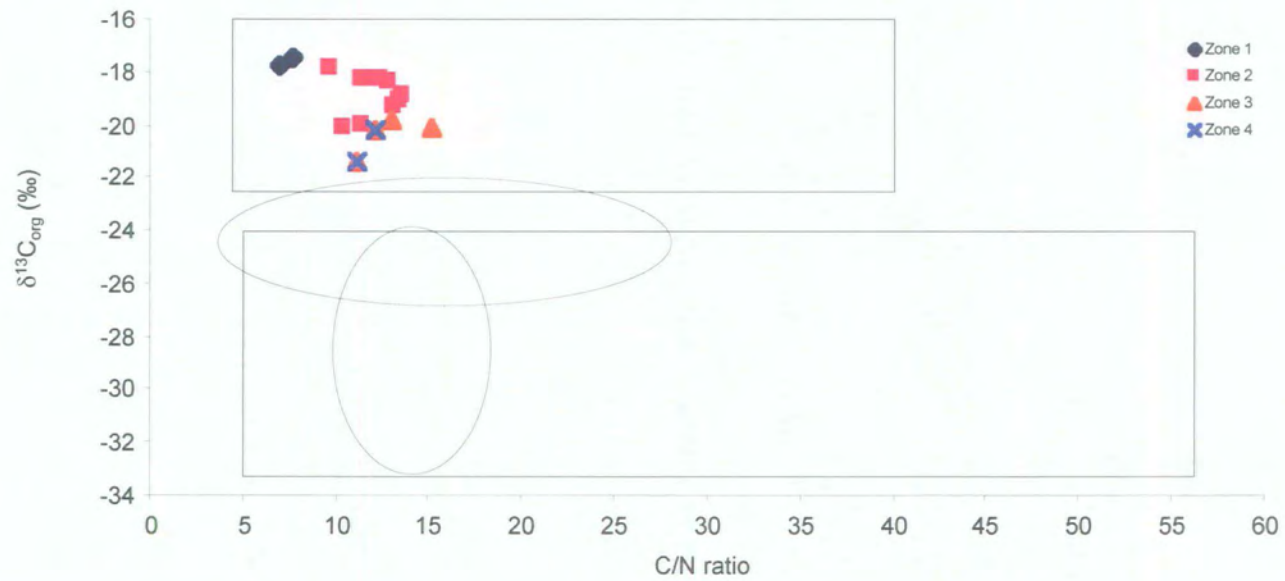


Figure 6.13: Torr a' Bheithe C/N vs. $\delta^{13}\text{C}_{\text{org}}$

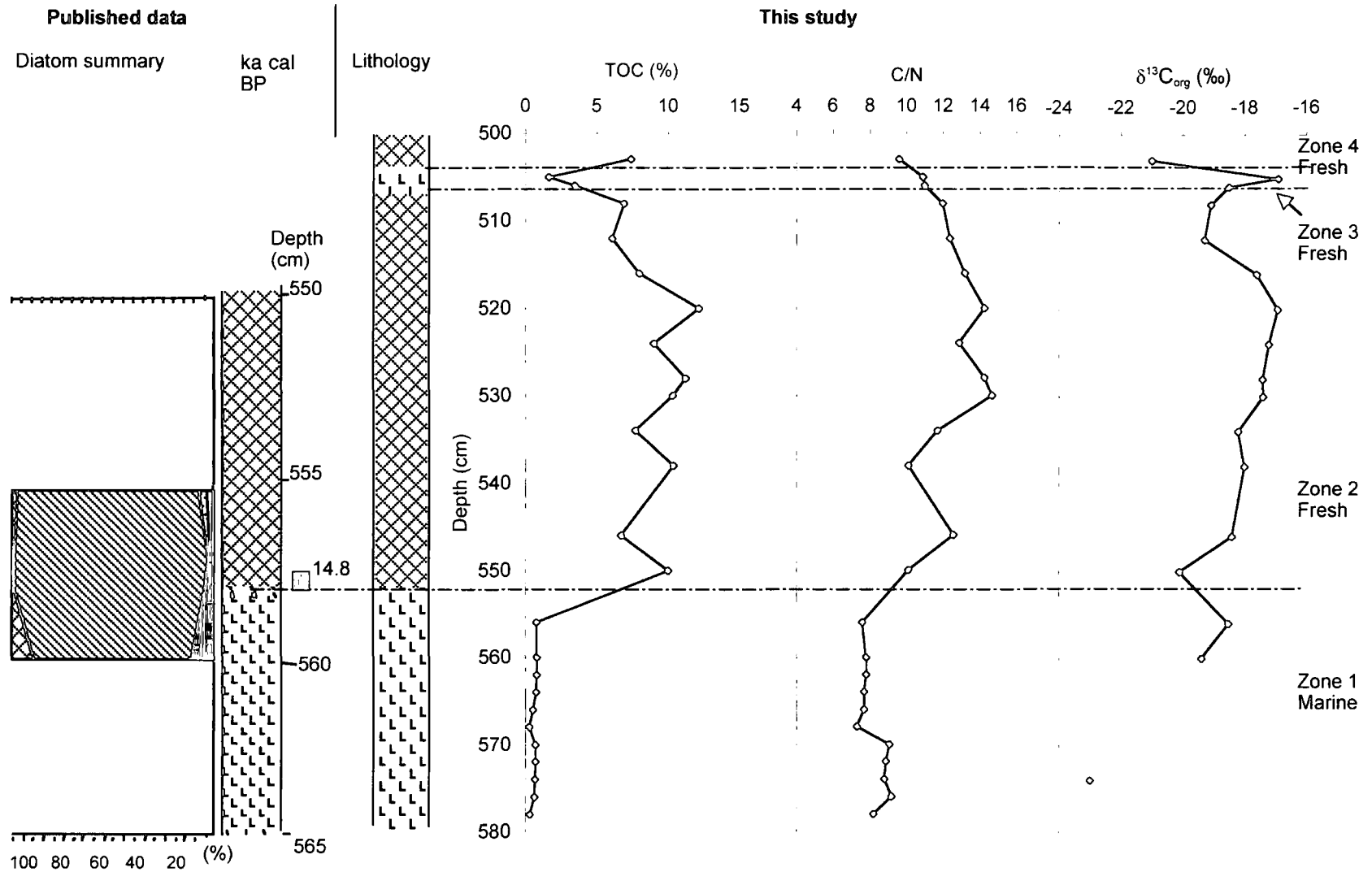


Figure 6.14: Loch Torr a' Bheithe -profiles of TOC, C/N ratios and $\delta^{13}C_{org}$ against the diatom summary. Published data from Shennan *et al.* (2000). Lithology and diatom key as on Figure 3.6.

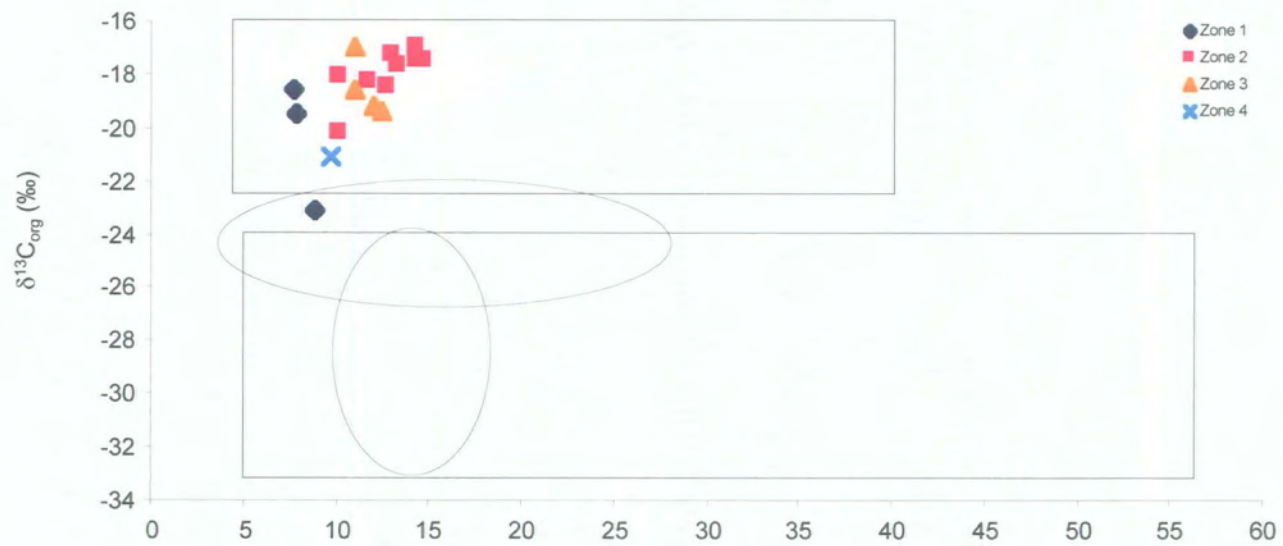


Figure 6.15: Loch Torr a' Bheith C/N vs. $\delta^{13}C_{org}$

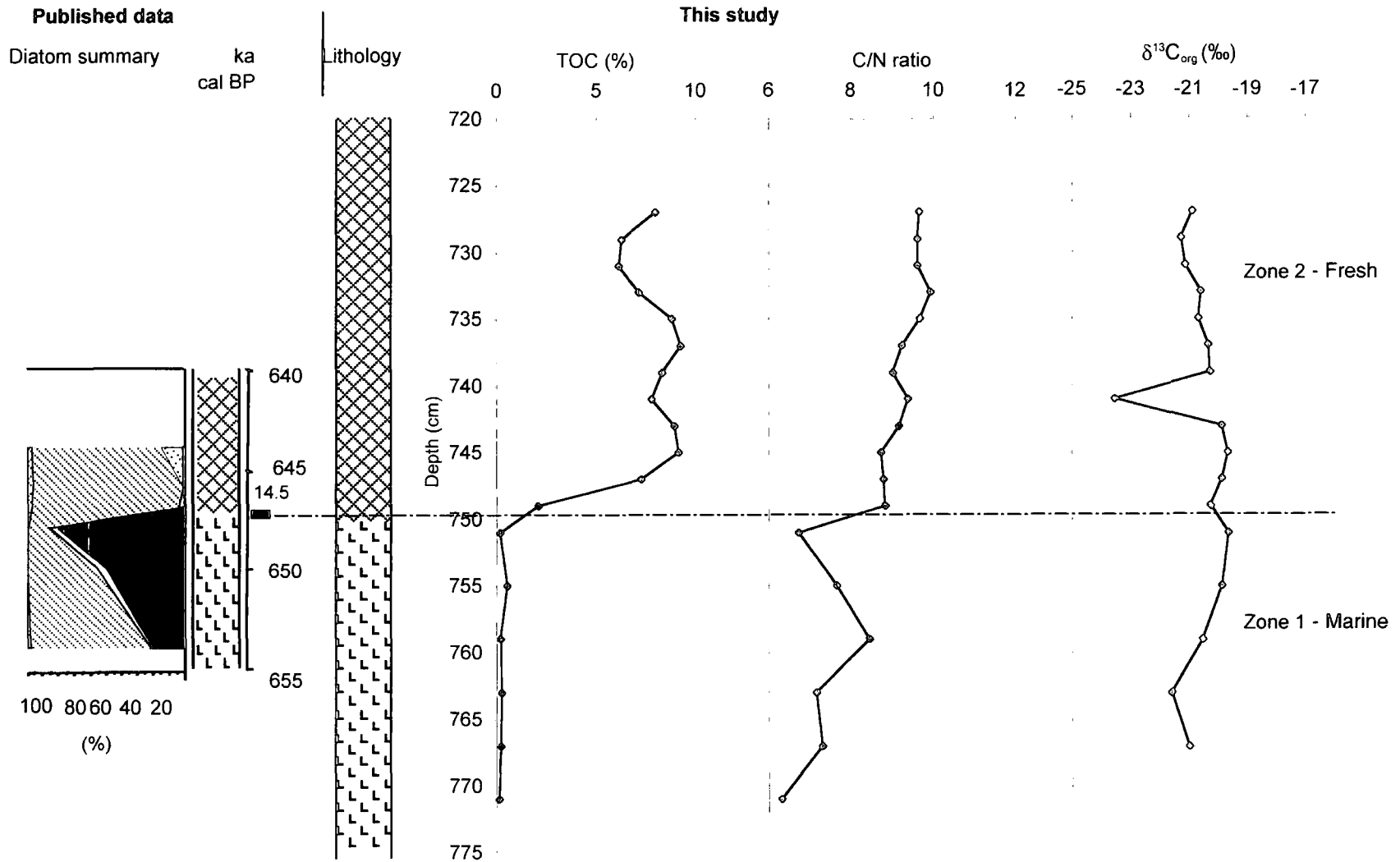


Figure 6.16: Loch a' Muihinn - profiles of TOC, C/N ratios and $\delta^{13}C_{org}$ against the diatom palaeosalinity reconstruction. Published data from Shennan *et al.* (2000). Lithology and diatoms key as on Figure 3.6.

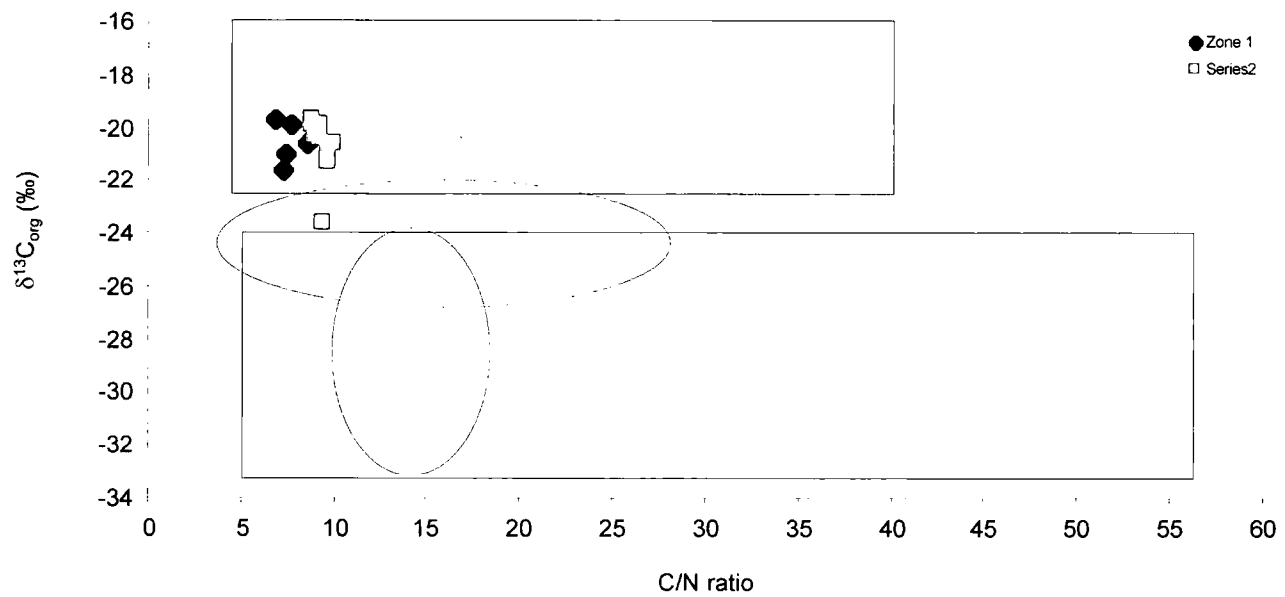


Figure 6.17: Loch a' Mhulinn C/N vs. $\delta^{13}\text{C}_{\text{org}}$

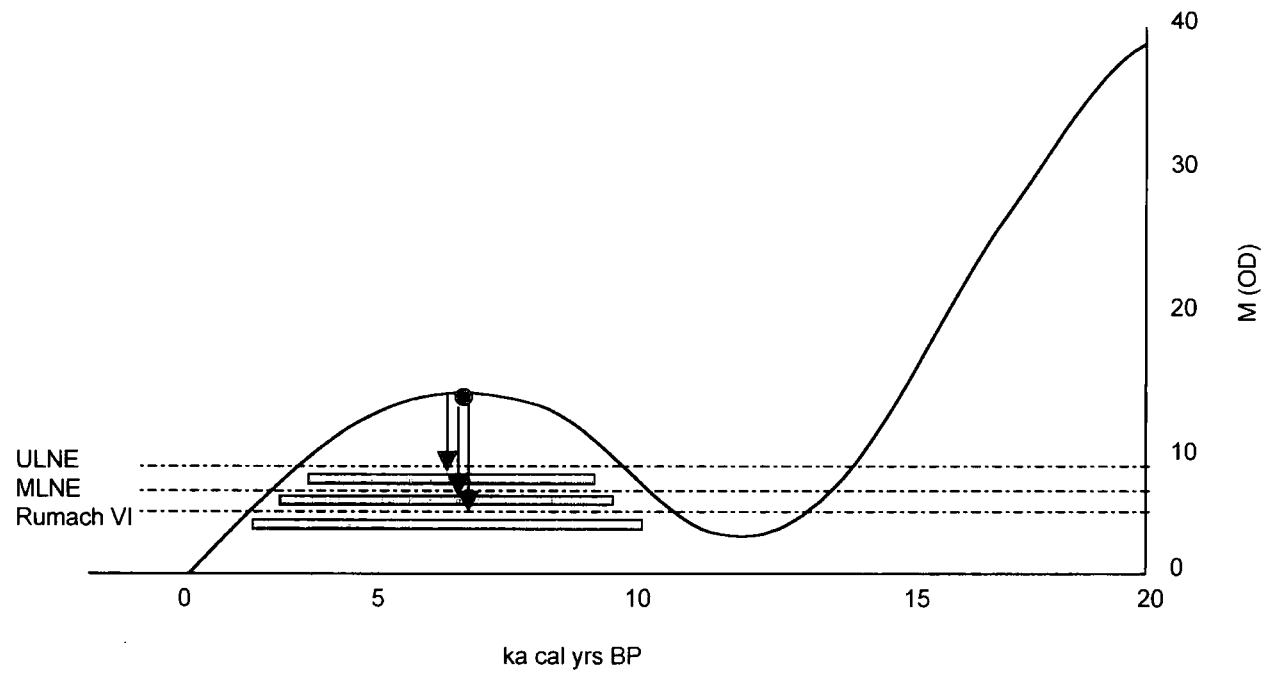


Figure 6.18: Regional RSL curve (adapted from Shennan *et al.*, 2000) showing altitude of Rumach VI, MLNE and ULNE. For a given marine interval Rumach VI will have deeper water (indicated by arrows) and will be marine for longer (indicated by green bar) than MLNE or ULNE

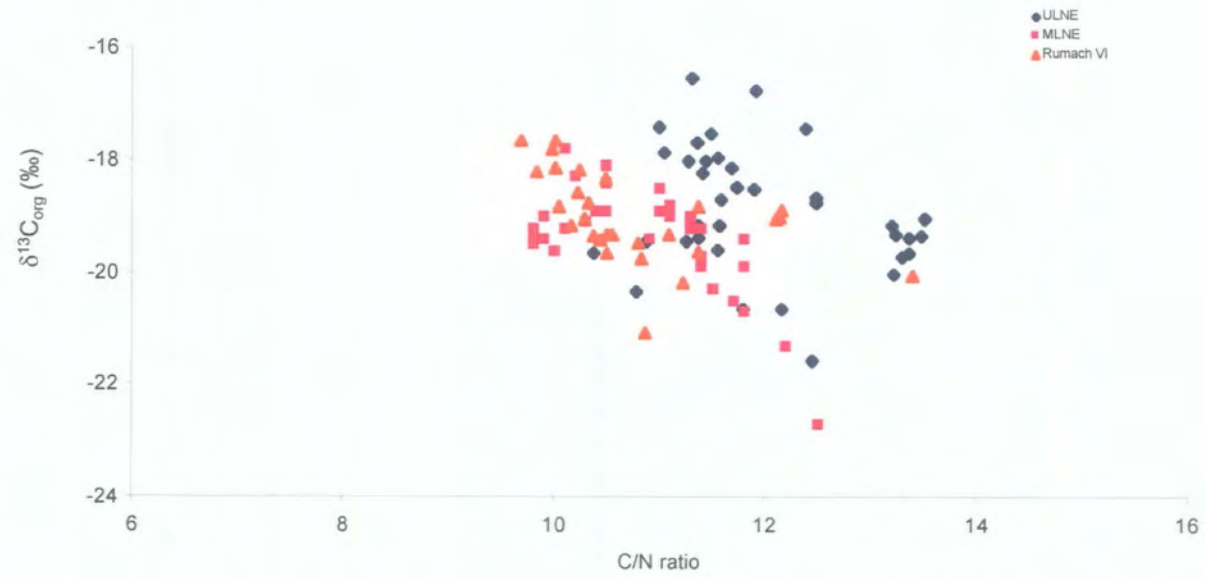


Figure 6.19: Biplot of $\delta^{13}\text{C}_{\text{org}}$ vs. C/N ratio from Holocene marine samples from ULNE, MLNE and Rumach VI

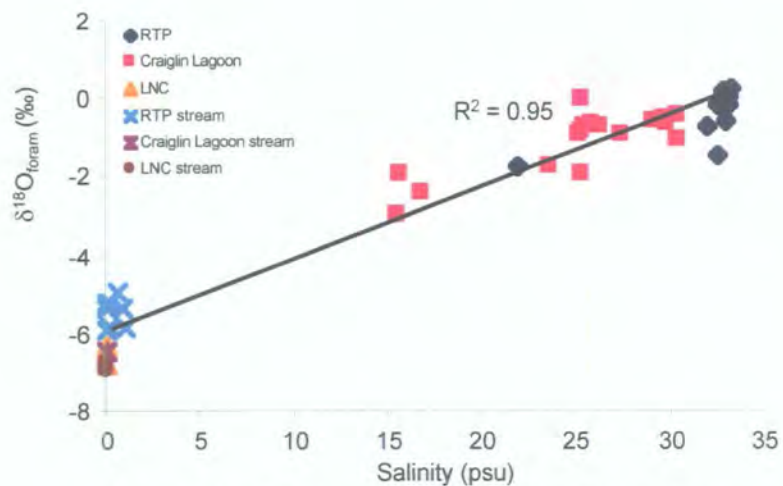


Figure 7.1a: Relationship between contemporary $\delta^{18}\text{O}_w$ vs. salinity for all samples taken from RTP, Craigin Lagoon and LNC. Errors are within (0.2(‰)) within the size of the symbol in all cases

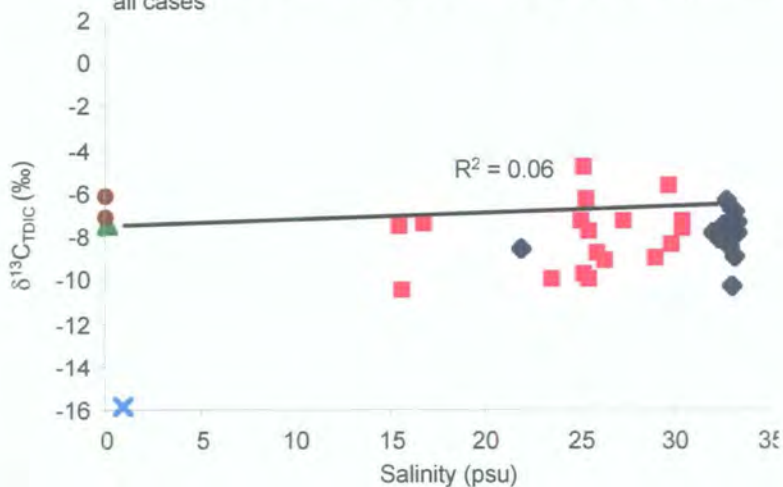


Figure 7.1b: Relationship between contemporary $\delta^{13}\text{C}_{\text{TDIC}}$ vs. salinity for all samples taken from RTP, Craigin Lagoon and LNC

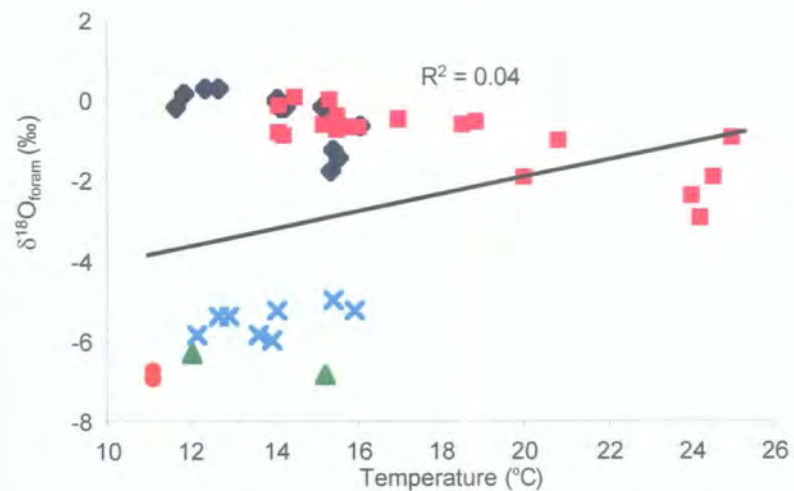


Figure 7.2a: Relationship between contemporary $\delta^{18}\text{O}_w$ vs. temperature for all samples taken from RTP, Craigin Lagoon and LNC

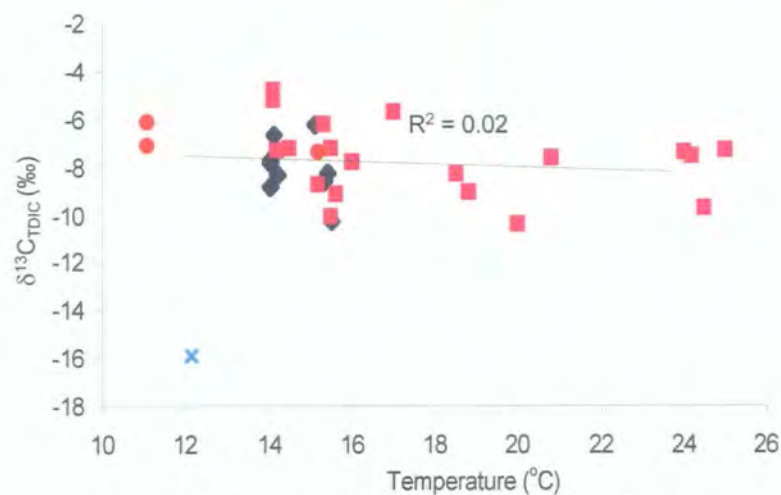


Figure 7.2b: Relationship between contemporary $\delta^{13}\text{C}_{\text{TDIC}}$ vs. temperature for all samples taken from RTP, Craigin Lagoon and LNC

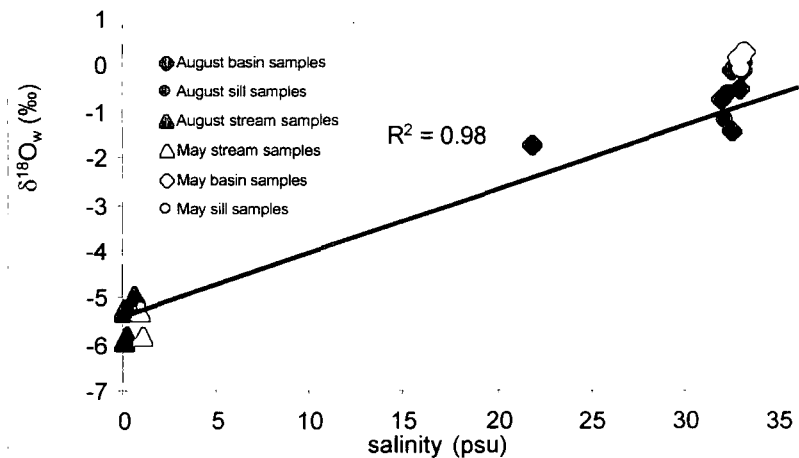


Figure 7.3a: Relationship between contemporary RTP $\delta^{18}\text{O}_w$ vs. salinity for basin, sill and stream waters

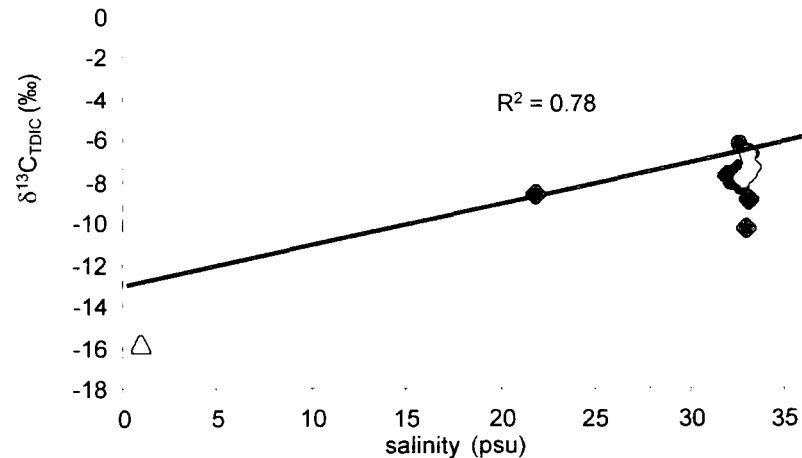


Figure 7.4a: Relationship between contemporary RTP $\delta^{13}\text{C}_{\text{TDIC}}$ vs. salinity for basin, sill and stream waters

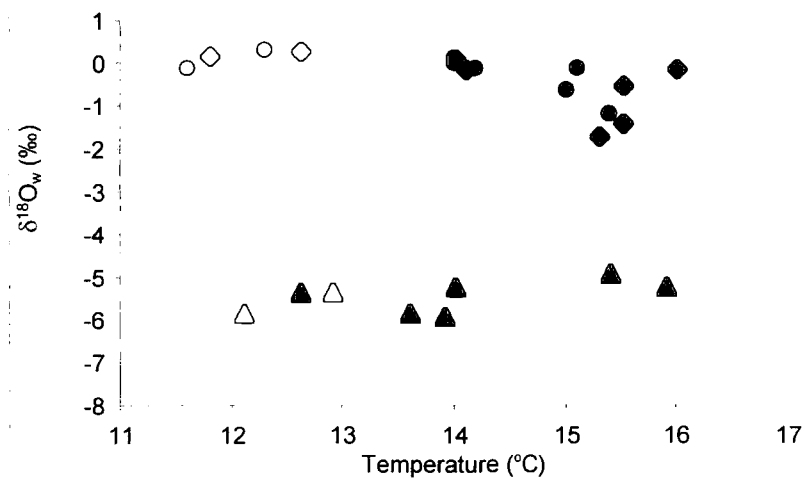


Figure 7.3b: Relationship between contemporary RTP $\delta^{18}\text{O}_w$ vs. temperature for basin, sill and stream waters

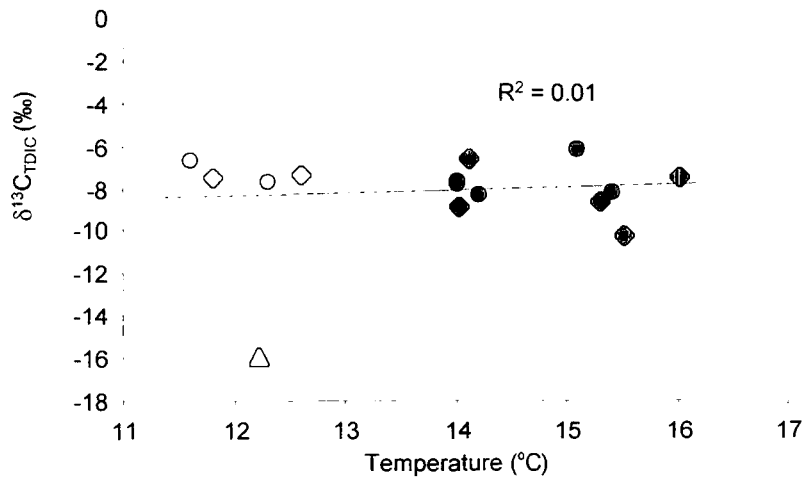


Figure 7.4b: Relationship between contemporary RTP $\delta^{13}\text{C}_{\text{TDIC}}$ vs. temperature for basin, sill and stream waters

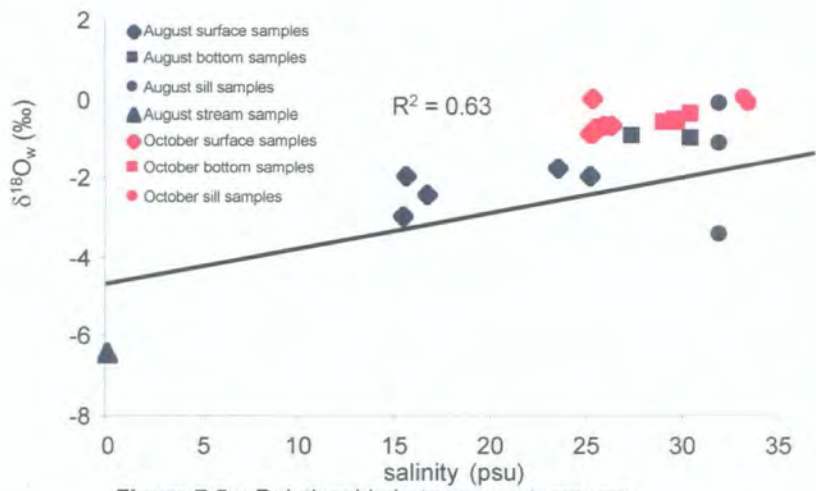


Figure 7.5a: Relationship between contemporary Craiglin Lagoon $\delta^{18}\text{O}_w$ vs. salinity for basin, stream and sill water samples

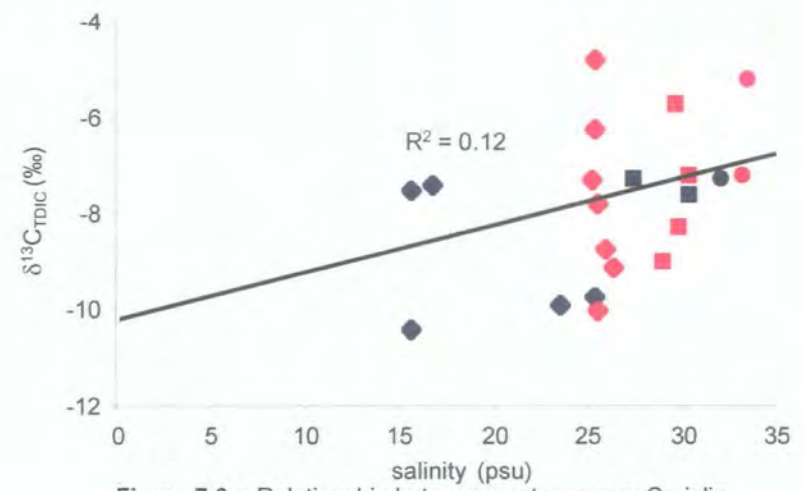


Figure 7.6a: Relationship between contemporary Craiglin Lagoon $\delta^{13}\text{C}_{\text{TDIC}}$ vs. salinity for basin, stream and sill water

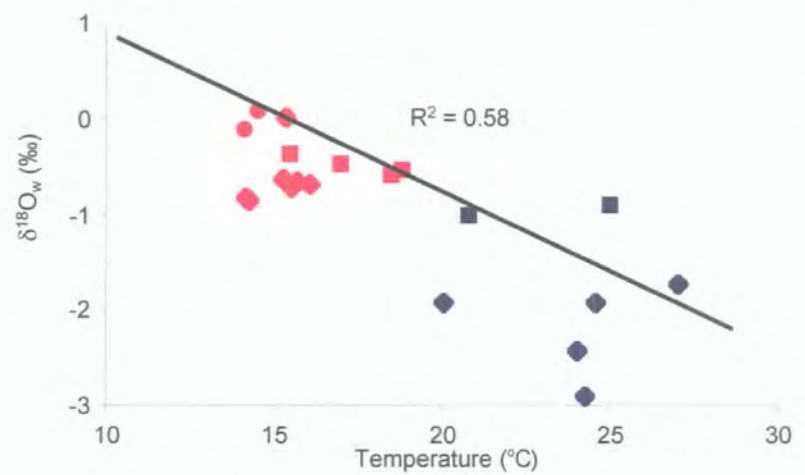


Figure 7.5b: Relationship between contemporary Craiglin Lagoon $\delta^{18}\text{O}_w$ vs. temperature for basin, stream and sill samples

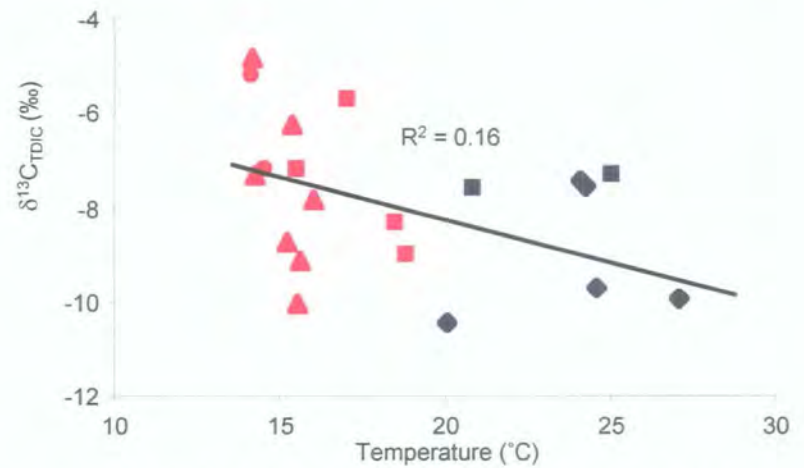


Figure 7.6b: Relationship between contemporary Craiglin Lagoon $\delta^{13}\text{C}_{\text{TDIC}}$ vs. temperature for basin, stream and sill samples

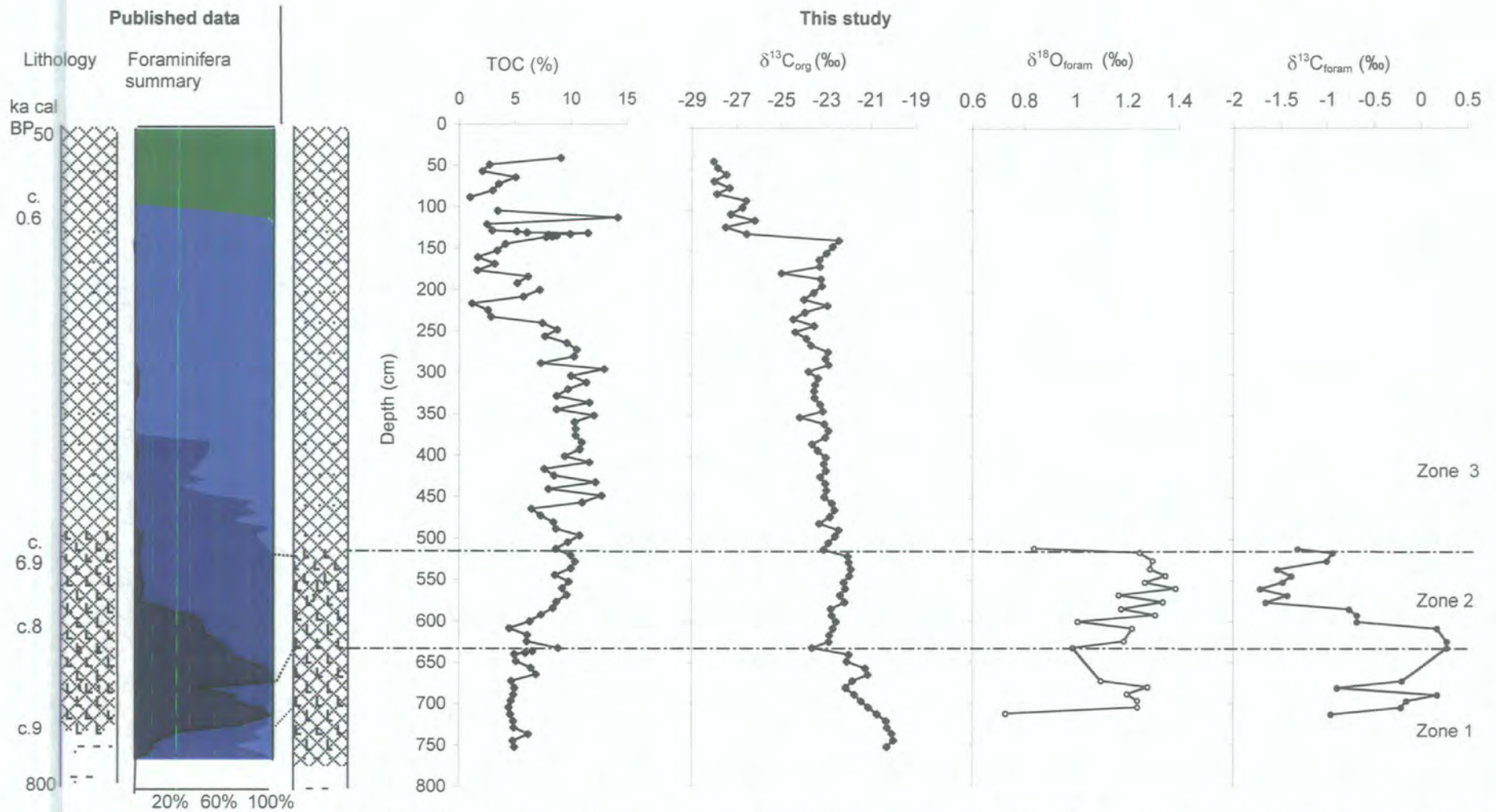


Figure 7.7: Loch nan Corr Profiles of TOC, $\delta^{13}C_{org}$, $\delta^{18}O_{foram}$, $\delta^{13}C_{foram}$ results against foraminiferal summary (Lloyd, 2000). Dotted lines indicate the correlation between the two cores. Sedimentology key and foraminifera classes are found in Figure 3.23

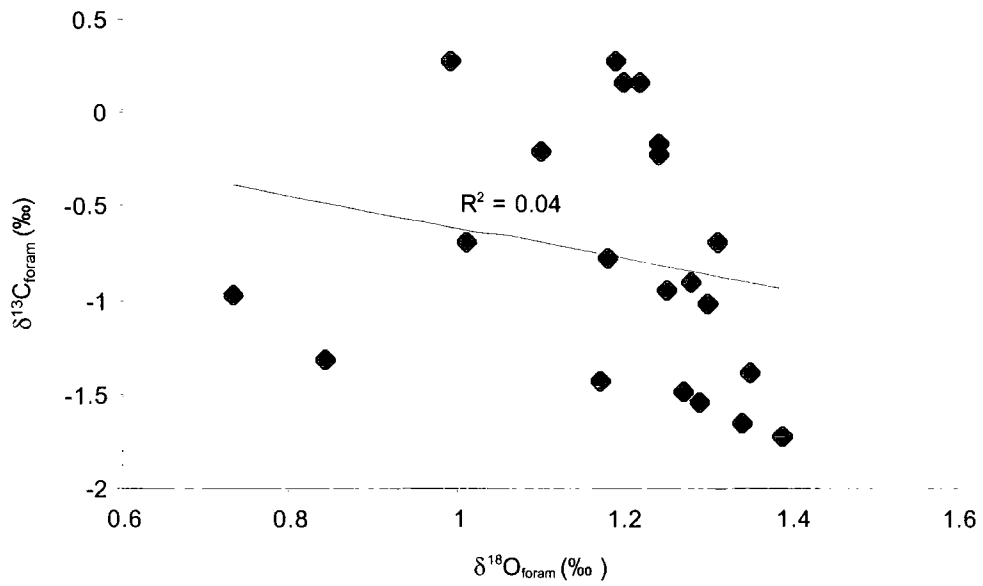


Figure 7.8: Relationship between $\delta^{13}\text{C}_{\text{foram}}$ and $\delta^{18}\text{O}_{\text{foram}}$ from sediment core LNC

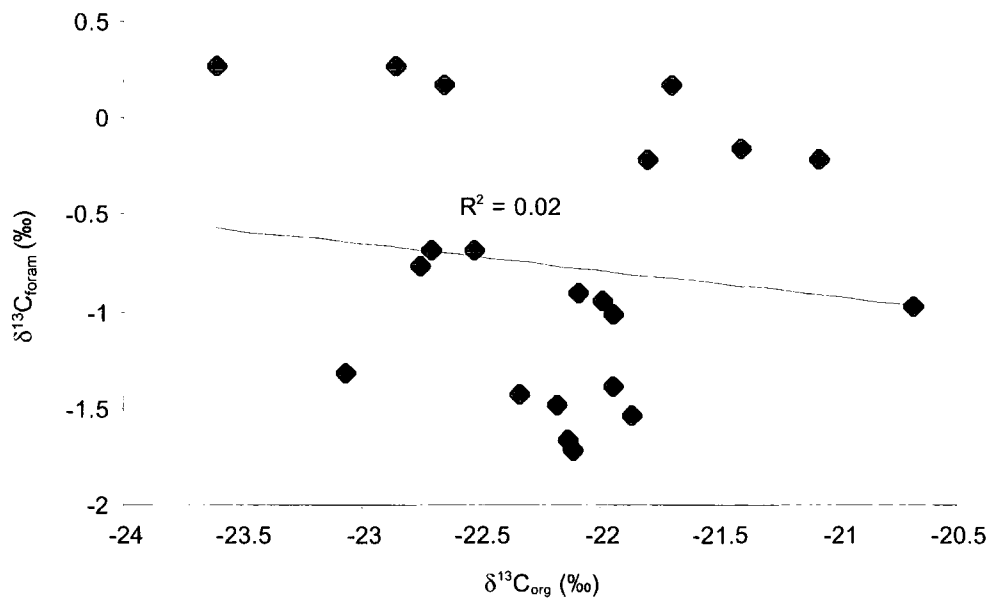


Figure 7.9: Relationship between $\delta^{13}\text{C}_{\text{org}}$ and $\delta^{13}\text{C}_{\text{foram}}$ from sediment core LNC



Figure 8.1a: Brackish water diatoms separated using an STP density of 2.2gcm^3 . Not the difference in species type between slides



Figure 8.1b: Marine diatoms separated using an STP density of 2.2gcm^3



Figure 8.1c: Marine diatoms separated using an STP density of 2.3gcm^3

Environment	Location	Type of material	$\delta^{18}\text{O}_{\text{diatom}}$ (‰)	Reference
Contemporary marine diatom				
Southern Ocean	51°59'S04°31'E	surface sediment	43	Juilett-Leclerc and Labeyrie, 1987
Antarctic Ocean	S59°53'W43°05'	surface sediment	40 to 43	Schmidt <i>et al.</i> , 2001
<i>living marine</i>				
Norwegian-Greenland sea	N53°32'W20°17' – N74°58'E14°44'	phytoplankton	29 to 35	Schmidt <i>et al.</i> , 2001
Antarctic Ocean	S56°40'W25°20'	phytoplankton	31	Schmidt <i>et al.</i> , 2001
Weddell sea	S54°20'W03°22'	sediment trap	34 to 38	Schmidt <i>et al.</i> , 2001
Fossil marine diatoms				
Equatorial Pacific	01°08'N;109°15'6"W	20 ka to present	45 to 46.5	Mikkelsen <i>et al.</i> , 1978
Southern Ocean	51°59'S04°31'E	80 ka to present	40 to 41	Shemesh <i>et al.</i> , 1992
<i>Sponges(spicules)</i>				
Indian Ocean	Kerguelen	surface sediment	40	Leclerc 1974
Mediterranean Sea	Banyuls	surface sediment	39	Leclerc 1974
Atlantic Ocean	37°48'N 25°53'W	surface sediment	39	Leclerc 1974
Atlantic Ocean	36°48'N 33°13'W	surface sediment	40	Leclerc 1974
Bahamas	-	surface sediment	36	Leclerc 1974
English Channel	Roscoff	surface sediment	38	Leclerc 1974
Contemporary lacustrine samples				
Freshwater diatoms	Gulf of California	Top core samples	30	Juilett-Leclerc and Labeyrie, 1987
Lake Pavin	France	contemporary	32	Leclerc 1974
Lake Myvatn	Iceland	contemporary	32	Leclerc 1974
Fossil lacustrine				
Simba Tarn	Mt. Kenya	8.3 to 1.2 ka BP	19 to 33	Barker <i>et al.</i> , 2001
Grandfather Lake	SW Alaska	13.5 to 7.5 ka BP	19 to 24	Hu and Shemesh 2003
Linsley Pond	Connecticut	Younger Dryas	25 to 33	Shemesh and Peteet, 1998
Chuna Lake	Kola Peninsula, NW Russia	last 9000 yrs BP	19 to 27	Jones <i>et al.</i> , 2004
Tonsberg peninsula	South Georgia	7.0 to ca. 15.7 ka BP	28 to 32	Rosqvist <i>et al.</i> , 1999
Lake Pinarbasi	Konya Basin, Turkey	58 to ca. 27 ka BP	16 to 32	Leng <i>et al.</i> , 2001
Lake 850	Abisko, Lapland, Sweden	Holocene	25 to 29	Shemesh <i>et al.</i> , 2001
Vuolep Allakasjaure	Abisko, Lapland, Sweden	last 5000 years	25 to 29	Rosqvist <i>et al.</i> , 2004

Table 8.1: Summary table of published $\delta^{18}\text{O}_{\text{diatom}}$ values from around the world

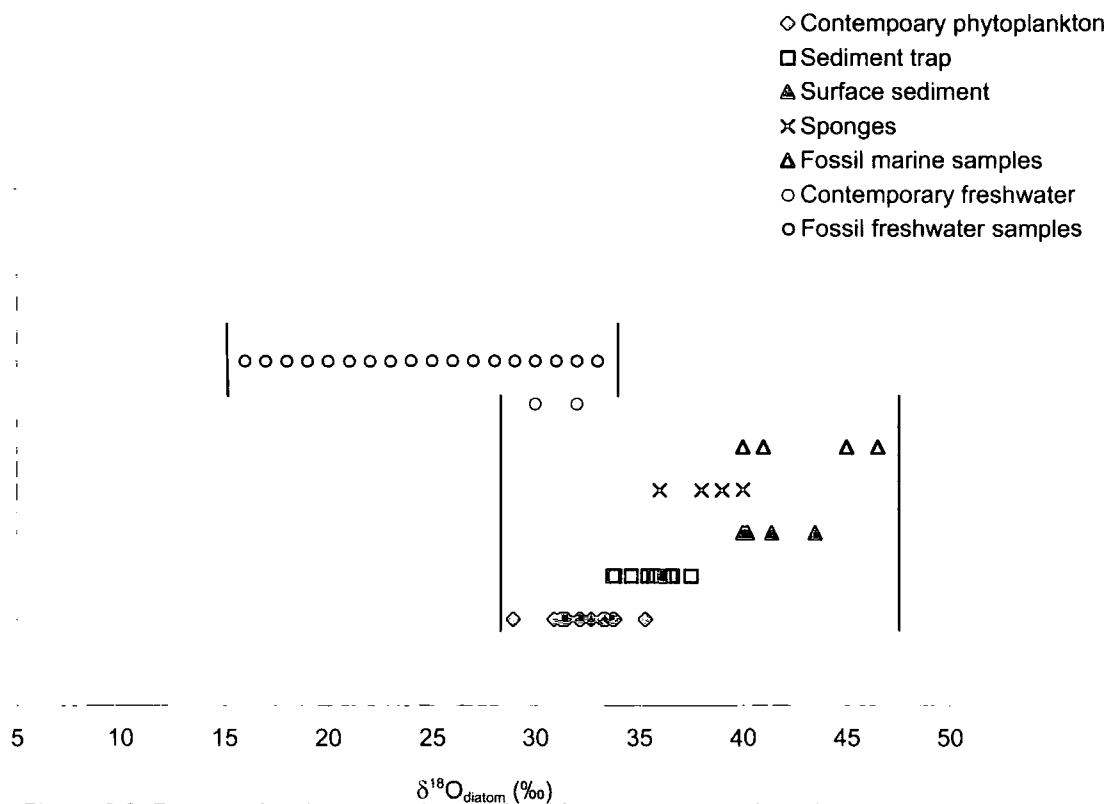


Figure 8.2: Ranges of end-member values defined from the published results (see Table 8.1)

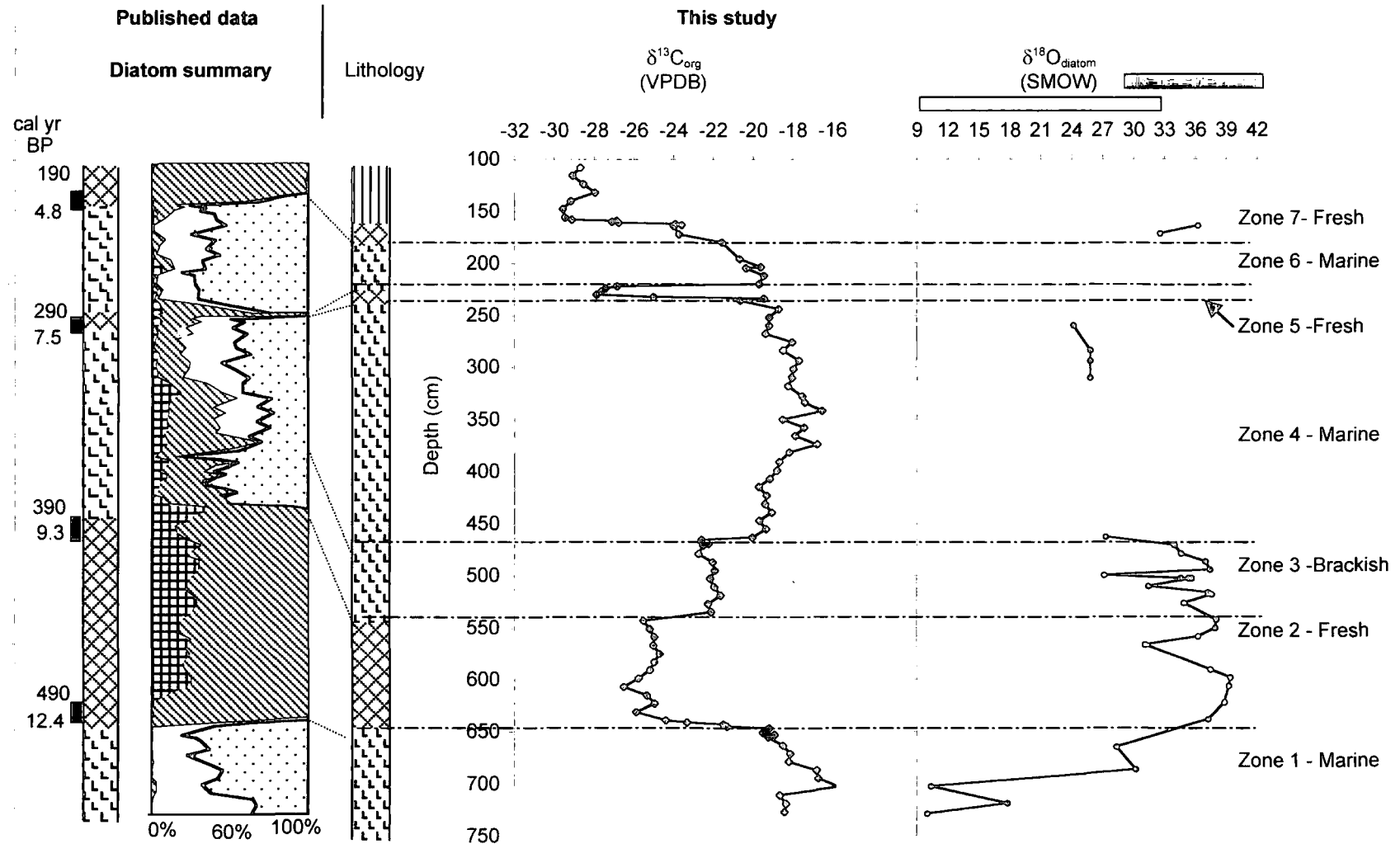


Figure 8.3: Summary of $\delta^{13}\text{C}_{\text{org}}$ and $\delta^{18}\text{O}_{\text{diatom}}$ data compared to the diatom salinity reconstruction from Shennan *et al.* (1994). Green box = typically range of freshwater $\delta^{18}\text{O}_{\text{diatom}}$ values, blue box = $\delta^{18}\text{O}_{\text{diatom}}$ values for marine samples. Ranges from Table 8.1. Key for lithology and diatom Figure 3.6.

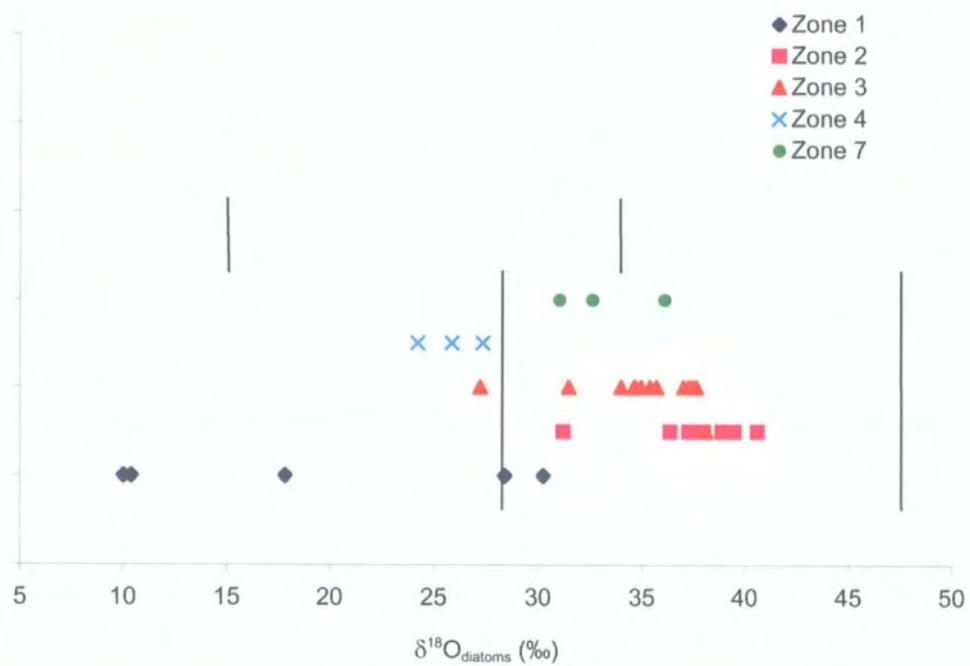


Figure 8.4: The $\delta^{18}\text{O}_{\text{diatom}}$ results from ULNE compared to the end-member ranges identified from the published literature (see Table 8.1 and Figure 8.2)

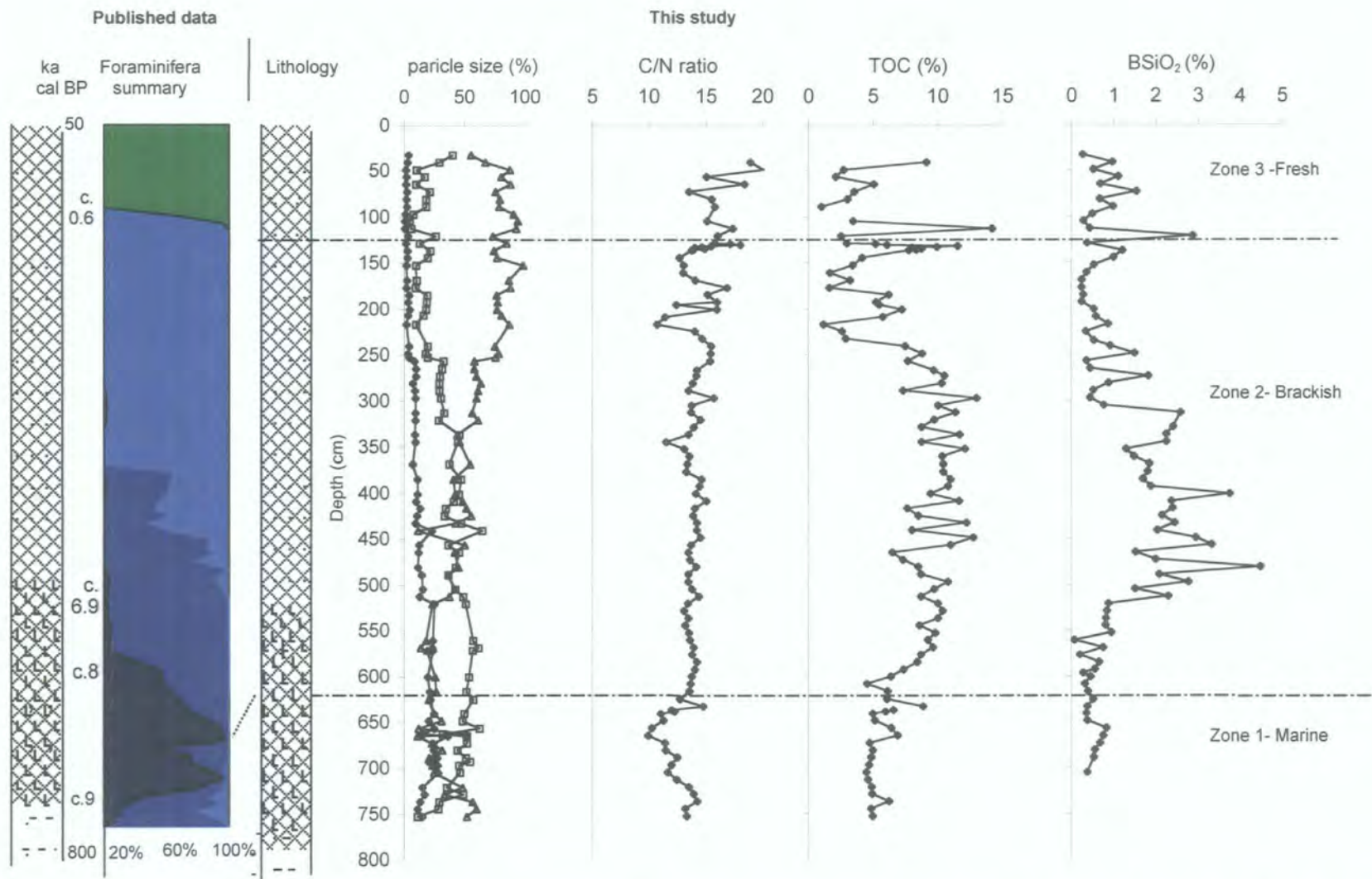


Figure 9.1: LNC- profiles of foraminiferal summary (Lloyd, 2000), particle size, TOC, BSiO₂, Key: foraminifera taxa Figure 3.23. Particle size: diamond = clay, square = silt, triangle = sand

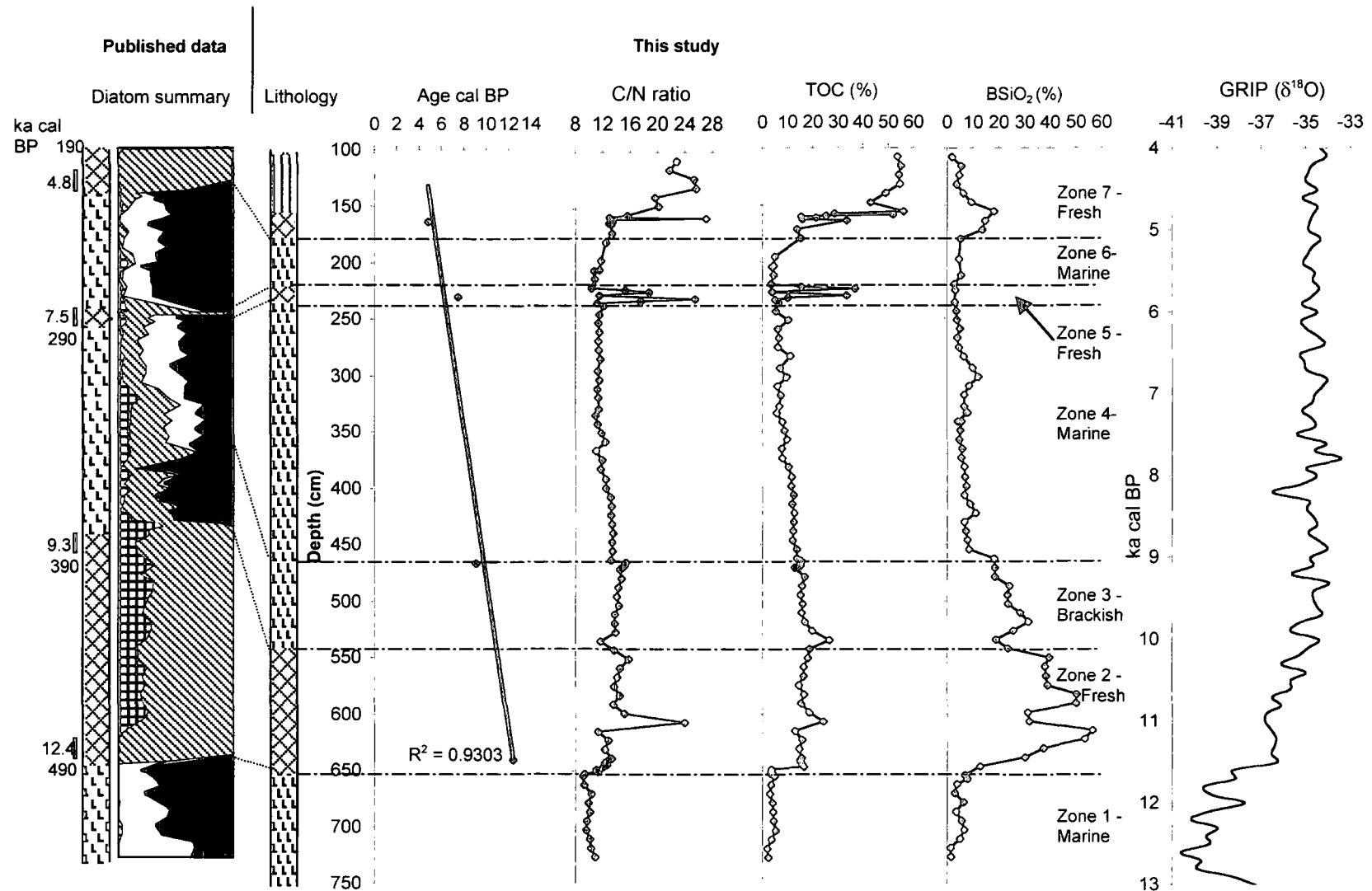


Figure 9.2: ULNE- Profiles of C/N ratios, TOC, BSiO₂ compared to the GRIP δ¹⁸O and diatom summary diagram (Shennan *et al.*, 1994). Key: as on Figure 3.6. δ¹⁸O data from www.ngdc.noaa.gov/paleo/icecore/greenland/summit/grip/isotopes/gripd18o.txt Johnsen *et al.*, 1997).

Environment	Location	Event	Date (ka cal BP)	Reference	
Peat bog	Bolton Fell Moss, UK	wet/cold	0.62	Barber <i>et al.</i> , 2003	
			0.72		
			1.4		
			2.2		
			2.35		
			2.44		
			2.58		
			2.9		
			3.02		
			3.2		
			3.6		
			3.75		
			4.02		
			4.28		
			4.42		
			4.62		
			5.25		
	5.42				
	5.7				
	6.2				
	7.5				
	7.8				
		Mongon Bog, UK	wet/cold	0.45	Barber <i>et al.</i> , 2003
	0.6				
	0.85				
	1.6				
	1.8				
	2.25				
	2.35				
	2.45				
	2.75				
	3.2				
		Abbeyknockmoy, UK	wet/cold	0.7	Barber <i>et al.</i> , 2003
	1.05				
	1.4				
	2.22				
	2.75				
	3.15				
	4				
	4.25				
		Walton Moss, UK	wet/cold	0.1	Hughes <i>et al.</i> , 2000
	1.45				
1.75					
2.32-2.04					
3.17 - 2.86					
3.5					
4.41-4.0					
5.3					
7.8					
	Talla Moss, UK	wet/cold	0.54	Chambers <i>et al.</i> , 1997	

Environment	Location	Event	Date (ka cal BP)	Reference
			1.7 1.93 2.27 2.6 3460	
	Kentra Moss, UK		0.325 0.6 1.15 1.4 2.15 2.55 3250	Ellis and Tallis, 2000
	Border mires, UK		0.55 0.85 1.03 1.4 1.74 1.98 2.13 2.54	Mauquoy and Barber 1999a,b
<i>Lake sediment</i>	Lake Holzmaar Germany	climate deterioration	varve yrs BP 900 1700 2700 5500 9600	Lüke <i>et al.</i> , 2003
	Lakes in Netherlands	climate deterioration	2750-2500	van Geel <i>et al.</i> , 1996
<i>Speleothem</i>	Ireland		1.4 2.8 4.2 5.9 8.1	McDermott <i>et al.</i> , 1999
<i>Marine cores</i>	North Atlantic	IRD events	1.4 2.8 4.2 5.9 8.1	Bond <i>et al.</i> , 1997

Table 9.1: A summary of climate events across Europe recorded in peat, lake, speleothem and marine records. Peat data modified from Barber *et al.* (2003).

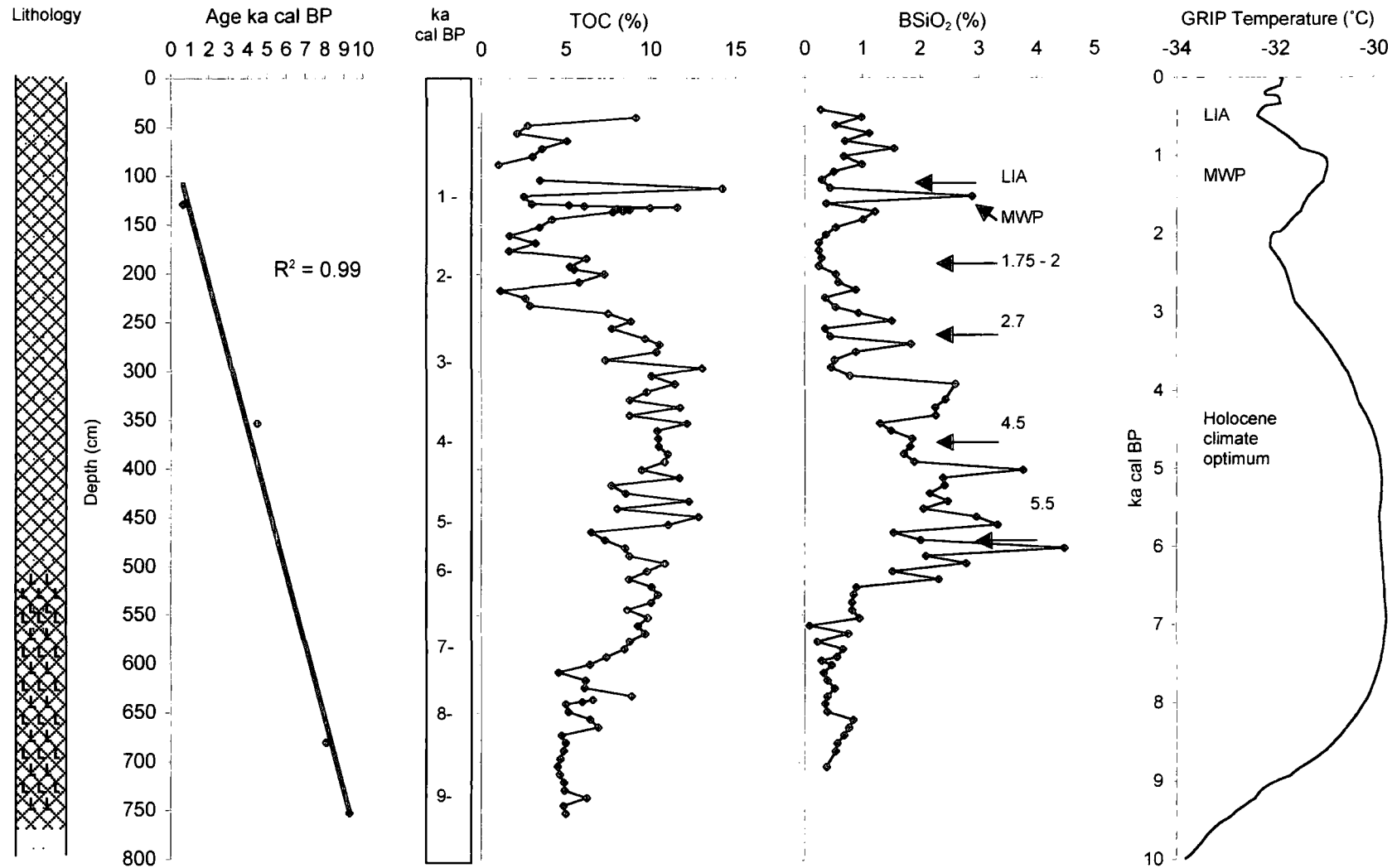


Figure 9.3: TOC, BSiO₂, and Age/depth model for the new core from LNC and the GRIP temperature record (after Dahl-Jensen *et al.*, 1998). LIA = Little Ice Age, MWP = Medieval War Period. Arrows on the BSiO₂ indicate possible climate events (ka cal BP) related to Table 9.1.

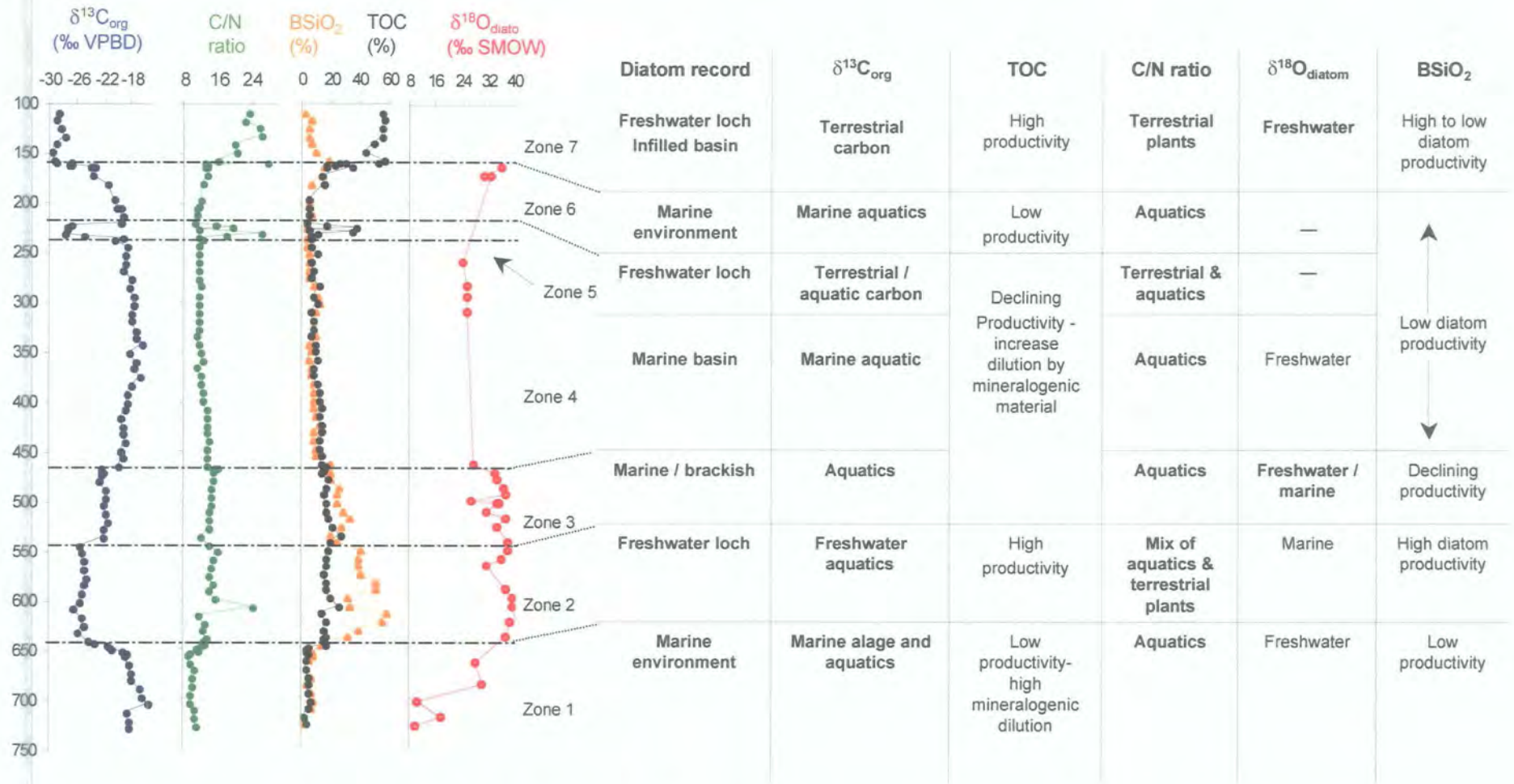


Figure 10.1: Environmental synthesis for Upper Loch nan Eala (ULNE) - comparing all geochemical proxies as palaeosalinity indicators against the published diatom summary (Shennan *et al.*, 1994). Proxies that correspond with the diatom palaeosalinity reconstruction are highlighted in bold.

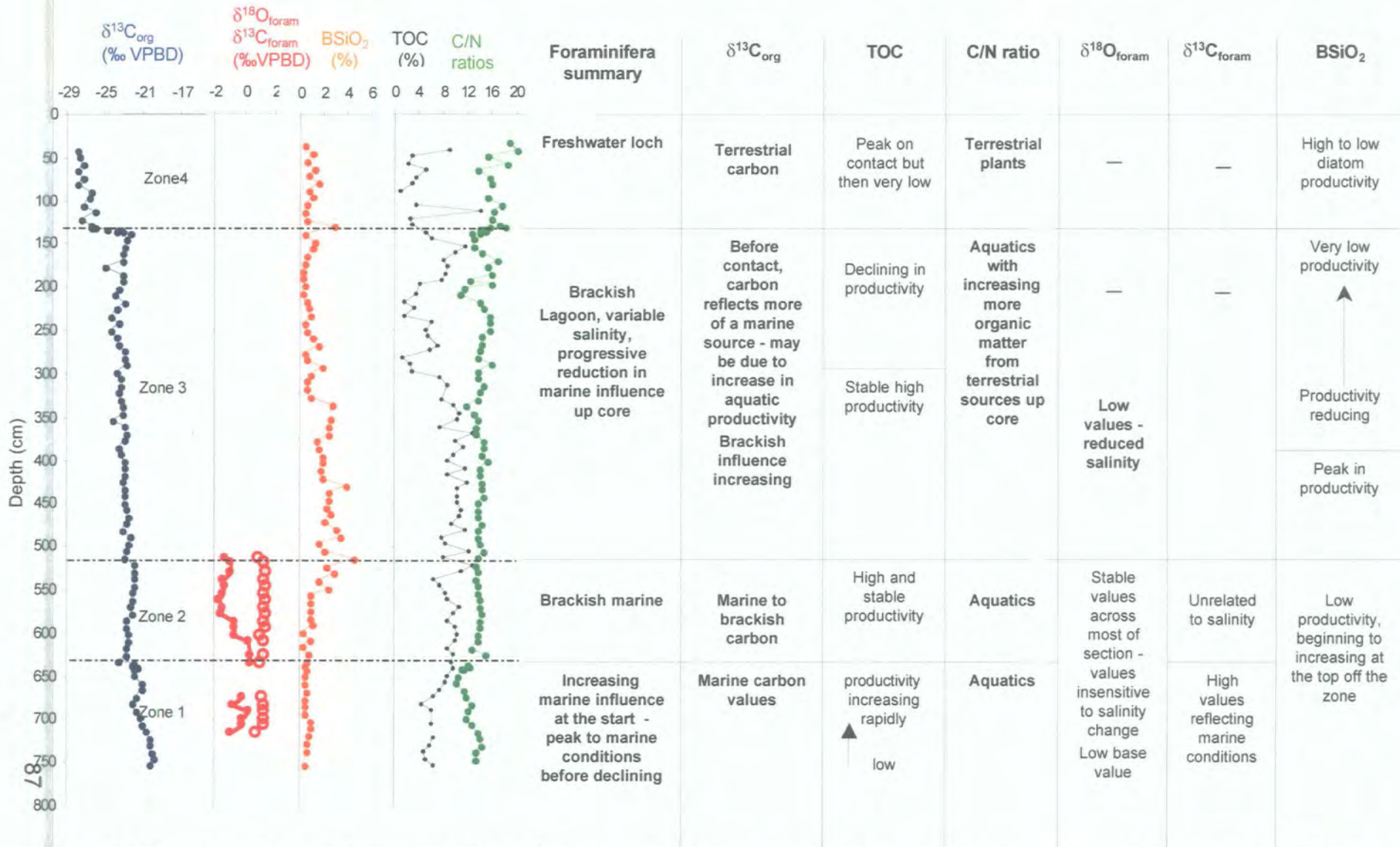


Figure 10.2: Environmental synthesis from Loch nan Corr (LNC) - comparing all geochemical proxies as palaeosalinity indicators. Proxies that correspond with the diatom palaeosalinity reconstruction are highlighted in bold. Open red circles = $\delta^{13}\text{C}_{\text{foram}}$ solid red circle = $\delta^{18}\text{O}_{\text{foram}}$